UNICA

UNIVERSITÀ
DEGLI STUDI
DI CAGLIARI

Ph.D. DEGREE IN

Innovation Sciences and Technologies

Cycle XXXV

TITLE OF THE Ph.D. THESIS

Study of metabolic changes in human erythrocytes and plasma under simulated microgravity conditions

Scientific Disciplinary Sector(s)

ING-IND/24 CHIM/10 CHIM/01

Ph.D. Student:	Cristina Manis
Supervisor:	Prof. Giacomo Cao
Supervisor:	Prof. Pierluigi Caboni

Final exam. Academic Year 2021/2022
Thesis defense: April 2023 Session

INDEX

PREFACE

This dissertation entitled “Study of metabolic changes in human erythrocytes and plasma under simulated microgravity conditions” is a result of the work of three academic years (from 2019 to 2022) in the Doctorate school entitled “Innovation Sciences and Technologies” at the University of Cagliari (Italy). The aim of this project was to investigate the metabolomic profiles of human plasma and erythrocyte samples trying to identify possible alterations identifiable as effect of the microgravity environment. During my PhD work, I studied the metabolomics analysis of human erythrocyte and plasma samples developing new analytical methods for the extraction and mass spectrometry analysis of biological sources. I also learnt advanced multivariate and univariate chemometric techniques to be applied to the acquired spectrometric data. The first and the second year were spent in Cagliari, Italy, at the Department of Life and Environmental Science and at the Department of Mechanical, Chemical and Materials Engineering where I analysed the lipid profile of human erythrocytes samples by using Ion Mobility Spectrometry/Quadrupole-Time-of-Flight Mass Spectrometry (UHPLC-IM-QTOF-MS) combined. In January 2022, I started an internship at The Centre of Metabolomics and Bioanalysis (CEMBIO) at the Faculty of Pharmacy (CEU-San Pablo University), Madrid, where I performed the analysis of polar profile of human plasma samples using capillary electrophoresis coupled to mass spectrometry (CE-MS). The research was complex and challenging but conducting in-depth investigations using different techniques allowed me to identify metabolic pathways involved in the haematological alterations caused by microgravity. Although these results need further investigation to better elucidate how microgravity induces these alterations, this PhD project, as it stands, can be considered valuable for in vivo aerospace biology investigations.

I would like to thank my supervisors Professor Pierluigi Caboni and Professor Giacomo Cao for their excellent guidance and support during this process.

Cristina Manis

Cagliari, December 15, 2022

ABBREVIATIONS

CCS: collisional cross section

CE: capillary electrophoresis

Cer: Ceramides

DT: drift time

EtherOxPC: ether-linked oxidized phosphatidylcholine

FA: fatty acid

IM-QTOF-LC/ MS: ion mobility coupled with a time-of-flight quadrupole and a liquid chromatograph

LC/MS: liquid-chromatography/mass spectrometry

MS: mass spectrometry

MS/MS: tandem mass spectrometry analysis

NIA: negative ion acquisition

OPLS-DA: orthogonal partial least square analysis

PA: phosphatidic acid

PC: phosphatidylcholines

pc: principal component

PCA: principal components analysis

PE: phosphatidylethanolamines

PIA: positive ion acquisition

PLS-DA: partial least square discriminant analysis

PS: phosphatidylserine

QC: quality control

Q-TOF: quadrupole time-of-flight

RBC: red blood cells

RPM: random positioning machines

SM: sphingomyelin

TG: triacylglycerols

VIP: variable importance in the project

CONTENTS

The PhD project described in this thesis work consists of seven chapters.

The first chapter contains a general introduction describing the history of space voyages from 1957 to the present with a look to the future missions. In the same chapter, the effects that space travel causes on the human body are reported, focusing on the space anaemia experienced by astronauts, as well as a summary of the scientific discoveries, divided by body district, concerning the cellular and molecular effects of microgravity.

The second chapter, on the other hand, explains the motivations and objectives proposed in this project.

The third chapter explains the techniques and methods used to achieve the aims. In particular, standard protocols of sample preparation, and analytical platforms used for metabolomic and lipidomic analyses are reported.

The next three chapters, contain the results obtained during the project and reported in three different scientific articles. In detail, the fourth chapter contains the article describing the lipidomic analysis using ion mobility carried out on samples of human erythrocytes under simulated gravity conditions, published in the International Journal of Molecular Sciences - MDPI. Instead, Chapter five contains the article published in the International Journal of Molecular Sciences - MDPI which reports the modifications observed in the plasma membranes of erythrocytes following exposure to microgravity. While the results obtained from the metabolomic analysis using capillary electrophoresis on human plasma under microgravity are reported in chapter six.

Finally, the chapter seven contains the conclusions elaborated considering the results obtained through the various analytical techniques applied to the study.

ABSTRACT

The absence of gravity is considered as an extreme biological stressor and the human body's adaptive response to microgravity conditions triggers a series of metabolic changes that are often associated with bone density loss, skeletal muscle atrophy, nervous system dysfunction, and anaemia. To understand the biological mechanisms underlying aerospace anaemia we investigated the structural and/or metabolic changes that occur in the erythrocytes under low gravity, as well as we compared the profile of human plasma polar metabolite under normal- and micro-g conditions.

Erythrocytes exposed to simulated microgravity showed morphological changes, a constant increase in reactive oxygen species (ROS), a significant reduction in total antioxidant capacity (TAC), a remarkable and constant decrease in total glutathione (GSH) concentration, and an increase of malondialdehyde (MDA) levels.

In this PhD work, experiments were also performed to evaluate the lipid profile of erythrocyte membranes changes under microgravity conditions. Lipidomics results showed an upregulation of the levels of complex lipids such as phosphocholines and sphingomyelins. Alterations in the lipid composition of the membrane determine membrane rigidity and fluidity, and plays a crucial role in membrane organization, dynamics, and function. No less important is the role that lipids have in the signalling of programmed cell death.

In conjunction with these results, the metabolomics analysis revealed that microgravity in human plasma induced an increase of glycolysis, Krebs cycle and fatty acids β-oxidation perturbations, and lactic acid production. These findings indicate an evident damage of circulating mitochondria causing a defective respiratory chain, oxidative environment, and incomplete β-oxidation of fatty acids with consequent accumulation of carnitines, in particular propionyl carnitine.

INTRODUCTION

1.1. Historical background

Humans have always looked up into the night sky and dreamed about exploring space. In the second half of the 20th century, rockets were developed that were powerful enough to overcome the force of gravity to reach orbital velocities, paving the way for space exploration to become a reality. The development of intermediate-range and intercontinental missiles provided, not only the critical electronic technologies, but also the rockets necessary to boost small payloads into orbit. On October 4th, 1957, the Soviets launched the first artificial satellite, Sputnik 1, into space. The launch of Sputnik indicated not only the Soviet technical leadership in a new field but also the capability and extent of Soviet large-missile development and production. Indeed, soviet leader Nikita Khrushchev used the fact that his country had been first to launch a satellite as evidence of the technological power of the Soviet Union and of the superiority of communism.

Following the Soviet launch of the world's first artificial satellite (Sputnik 1), the United States of America's attention turned to its budding space efforts. The U.S. response came a year later when, on January 31, 1958, the first U.S. satellite, Explorer 1, went into orbit. But during this year the United States Congress, alarmed by the perceived threat to the Soviet Union's national security and technological leadership (known as the "Sputnik crisis"), called for immediate and swift action; President Dwight D. Eisenhower and his advisers suggested more deliberate measures. On January 12, 1958, NACA [1] organized a "Special Committee on Space Technology," headed by Guyford Steer. On July 29, 1958, Eisenhower signed the National Aeronautics and Space Act, establishing NASA [2].

Four years after the launch of Sputnik, on April 12, 1961, Russian Lt. Yuri Gagarin became the first human to orbit Earth in Vostok 1. His flight lasted 108 minutes, and Gagarin reached an altitude of 327 kilometres. Although, the U.S. President Dwight David Eisenhower had decided not to compete for prestige with the Soviet Union in a space race, but his successor, John Fitzgerald Kennedy, had

a different view. “Landing a man on the moon and returning him safely to Earth within a decade” was a national goal set by President John F. Kennedy on May 25, 1961, and on February 20, 1962, John Glenn’s historic flight made him the first American to orbit Earth as part of ‘‘Project Mercury’. On July 20, 1969, the Apollo 11 crew successfully completed the national goal set by President John F. Kennedy eight years prior: to perform a crewed lunar landing and return to Earth [1], ending the space race between the United States and the Soviet Union in the broader scenario of the Cold War. Six Apollo missions were made to explore the moon between 1969 and 1972.

Immediately following the success of Apollo 11, NASA planned even more ambitious activities that should have led to a manned mission to Mars, but the reduction of the perceived threat and the change in political priorities almost immediately caused the conclusion of most of these plans. NASA turned its attention to a temporary space laboratory and a semi-reusable Earth orbital shuttle. In the 1990s, funding was approved for NASA to develop a permanent Earth orbital space station in partnership with the international community, which now included former rival, post-Soviet Russia (Roscosmos) with Japan (JAXA), Europe (ESA), and Canada (CSA) [3]. In September 1993, American Vice-President Al Gore and Russian Prime Minister Viktor Chernomyrdin announced plans for a new space station, which eventually became the International Space Station (ISS) [4]. The ISS was originally intended to be a laboratory, observatory, and factory while providing transportation, maintenance, and a low Earth orbit staging base for possible future missions to the Moon, Mars, and asteroids. However, not all the uses envisioned in the initial memorandum of understanding between NASA and Roscosmos have been realized [5]. In the 2010 United States National Space Policy, the ISS was given additional roles of serving commercial, diplomatic [6], and educational purposes [7]. Currently, the station serves as a microgravity and space environment research laboratory where scientific research is conducted in astrobiology, astronomy, meteorology, physics, and other fields [8]. The ISS is suitable for testing spacecraft systems and equipment needed for possible future long-duration missions to the Moon and Mars.

The International Space Station was the first laboratory for carrying out investigations concerning human health both in space and on Earth. Several human biological and physiological investigations have yielded important results,

including a better understanding of basic physiological processes normally masked by gravity and the development of new medical technologies and protocols driven by the need to support astronaut health. Advances in telemedicine, disease models, psychological stress response systems, nutrition, cellular behavior, and environmental health are just a few examples of the benefits that have been gained from the space station's unique microgravity environment [8].

Modern space exploration is reaching areas once only dreamed about. Mars is focal point of modern space exploration, and manned Mars exploration is a long-term goal of the United States. NASA is on a journey to Mars, with a goal of sending humans to the Red Planet in the 2030s.

1.2. Risks and effects of spaceflight

To date, 594 humans, including astronauts and cosmonauts, have been flown into space, but only 8 long-duration missions (>300 days) have been concluded. During spaceflight, astronauts experience several hostile environments which affect several physiological systems in the human body [9].

NASA is continuously studying the risks associated with spaceflight which can be grouped into five classes of stressors for the human body. These can be summarized with the acronym "RIDGE", short for Space Radiation, Isolation and Confinement, Distance from Earth, Gravity fields and Hostile/Closed Environments [10].

Space Radiation. In space, astronauts are exposed to levels of radiation not normally experienced on earth because shielded by the planet's magnetic field and atmosphere. Three main sources contribute to the space radiation environment: particles trapped in the Earth's magnetic field, solar energetic particles from the Sun (SPEs), and galactic cosmic rays (GCR).

SPEs are predominantly low-low linear energy transfer (LET) protons with energies up to 1 GeV/n (energy per single nucleon) that can be shielded relatively easily by spacecraft hulls. Even so, there can be very high-density proton fluxes with energies above 30 MeV that can be of concern to astronauts in thinly shielded vehicles and habitats [11]. The frequency of SPEs is proportional to sunspot activity and depend on the solar cycle, peaking when equatorial sunspot activity is maximal.

GCR ions originate from outside our solar system and contain mostly highly energetic protons and alpha particles [12]. The GCR spectrum consists of approximately 87% hydrogen ions (protons) and 12% helium ions (alpha particles), with the remaining 1%–2% of particles being HZE nuclei with charges ranging from Z = 3 (lithium) to approximately Z = 28 (nickel) [13].

Outside of shielding vehicles, each astronaut's cell nucleus would be traversed, on average, by a hydrogen ion every few days and heavier high-energy nuclei (HZE nuclei) (e.g., ^{16}O, ^{28}Si, ^{56}Fe) every few months [14]. Thus, despite their low flux, HZE ions represent a deleterious biological threat and contribute significantly to the cumulative dose of GCR to which astronauts may be exposed. It is not yet

clear how moderate to large magnitude SPEs, when combined with continued exposure to GCRs, will affect the health and performance of astronaut crews during interplanetary transits. However, it is known that space radiation exposure affects multiple organs and physiological systems in complex and different ways, due to acute and chronic effects. The acute radiation effects include changes in peripheral leukocytes, changes in expression of genes associated with programmed cell death and extracellular matrix remodeling [15] oxidative stress, gastrointestinal tract bacterial translocation [16] and immune system activation [17], peripheral hematopoietic cell counts, emesis [18], blood coagulation [19], skin [20], heart functions [21]. While among the long-term effects, the most important are cancer [22] and cataract development [23]. These effects are usually dose-related. Therefore, since future missions to the Moon and Mars will be of longer duration than previous flights, the current strategy to reduce the health risks of space radiation exposure is to implement shielding, radiation monitoring and specific operating procedures.

Isolation and Confinement. There is no "standard" time for astronauts to stay in space. Space missions have a duration of few hours or even a few months.
During space missions, especially those of longer duration, changes in morale and motivation of crew members are possible. This may be due to reduced stimulation, longing for loved ones, interpersonal stressors, or homesickness. These feelings combined with more restricted the space, loneliness and less contact with people, can alter the astronauts behaviour and psychology [24]. Among the psychiatric trouble, astronauts can manifest anxiety, depression and psychosis, psychosomatic symptoms, emotional problems and postflight personality changes [25]. For this reason, before recruiting, NASA studies people in isolated and confined environments and has developed methods and technologies to counter possible problems [10].

Distance from Earth. The space station is kept in orbit at an altitude of between 330 and 410 km above the Earth. The Moon is 1,000 times farther from Earth than the space station, while the distance of Mars from the earth varies from a minimum of 55.7 million km to a maximum of about 401 million km. Due to these distance to Earth, communications may be delayed, up to 22 min, for example, in the case

of a mission to Mars, which will require crews to operate more autonomously, including in situations requiring to resolve conflicts. The delay may also increase conflict between the crew and ground-based mission control [26]. This may not only increase psychological risks related to the performance of the individual crew member but can give rise to new psychological challenges never lived before [27]. For this reason, NASA is using human spaceflight experiences on the space station to understand what medical events may occur in space and what kinds of skills, procedures, equipment, and supplies are needed for future missions to the Moon and Mars [10].

Gravity Fields. The term "gravity" refers to the acceleration we experience on Earth (~9.81 m/s^2), and according to the International System of Units (SI) it is expressed in g. "Hypergravity" means gravity levels greater than 1g. A gravity level of less than 1g is called "hypogravity" or "partial gravity", "reduced gravity", or "microgravity" [28]. Astronauts will encounter three different gravitational fields on a mission to Mars. During the six-month journey between planets, the crews will be weightless. While on Mars, they will experience about a third of Earth's gravity and eventually, upon returning to Earth, the crews will have to readjust to Earth's gravity [10]. The transition from one gravitational field to another is a major physiological stressor. In fact, since man is the result of an evolutionary process that took place in the presence of gravity, when the gravitational force no longer acts on the body, drastic biological changes occur. Astronauts returning from missions show several health problems [29] with main clinical disorders including orthostatic hypotension, caused by the persistent lowering of peripheral vascular resistance [30] bone and muscle mass loss [31], immune dysfunction [32], central nervous system [33] and cardiovascular disorders [34]. Additionally, astronauts develop several haematological abnormalities, anaemia [35], thrombocytopenia, and abnormalities in red blood cell structure [36;37;38], reduction of plasma volume by 10-17% and hemolysis [39].

Understanding how the body changes in weightlessness and after returning to Earth's gravity allows the development of protective measures against these changes for a mission to Mars. Progress has already made in this area. For example, Leblanc et al., report that alendronate (bisphosphonate) ingestion plus

physical exercise can prevent the decline in bone mass and strength and elevate levels of urinary calcium and bone resorption in astronauts during 5.5 months of spaceflight [30]. Furthermore, Krieger et al., show how citrate, metabolized to bicarbonate, should decrease calcium excretion by reducing bone resorption and increasing renal calcium reabsorption [40]. However, due to the unclear mechanisms, for most of the disorders caused by microgravity, no preventive solutions have been so far proposed.

Hostile/Closed Environments. During space travel, astronauts are forced to live in a hostile and highly confined environment. The closed environment in which the crew lives have significant impact on their well-being, such as CO_2 levels, toxic exposures from materials or leaking fluids, and possible changes in the microbes present in the environment [41]. NASA is using technology to monitor the air quality of the space station to ensure the atmosphere is safe to breathe and not contaminated with gases, such as formaldehyde, ammonia, and carbon monoxide, but the main hazard, in this case, is represented by microbes. The microbiome is increasingly recognized as having fundamental roles in human physiology [42] including its involvement in human health and disease [43]. Inside the spacecraft, of course the presence of humans also imposes the presence of their associated microorganisms which in this closed space can be transferred more easily from person to person. For this reason, during spaceflight blood and saliva samples of astronauts are analysed to identify changes in the immune system and the reactivation of latent viruses.

Despite recent advances in understanding the relationship between extracellular forces and cell behavior, very little is understood about cellular biology and mechanotransduction under microgravity conditions. Considering, all these risks and actual evidence, understanding the effects of spaceflight on humans is essential as astronauts move from the International Space Station in low-Earth orbit to deep space destinations on and around the Moon and Mars, and beyond. In order to increase the knowledge related to the mechanisms by which space travel affects human health, different scientific studies carried out using animal models and human cell lines.

1.3. State of art

As previously described, experiencing gravity conditions different from that of the earth, is not without effects for the human body. Indeed, during space flight, profound changes occur in human physiology. At the moment, these physiological changes present major obstacles to long-term space missions. However, the alterations at the cellular level that underlie the dysregulations manifested by astronauts are not yet fully understood. To clarify cellular mechanisms of different body districts, readjust when exposed to microgravity conditions, several cellular studies have been conducted including morphology, differentiation, proliferation, and adhesion.

Density bone loss. Spaceflight is an environmental condition where astronauts can lose up to 19% of bone density during long-duration missions [31]. At first, the researchers hypothesized that the reduction in bone density observed in astronauts could be explained by cephalic fluid shift, which affects bone blood flow [44]. In 2007 the authors provided a new insight: the main cause of this loss appears to be due to a reduction in osteoblast number, and an increase of apoptosis induced by microgravity. Indeed, microgravity environment inhibites osteoblastogenesis, increases adipocyte differentiation in human mesenchymal stem cells and stimulates Osteoclastogenesis [45]. Additionally, Bucaro et al., showed a low level of the antiapoptotic protein Bcl-2, as well as Akt protein, and the redox status of the cells was disturbed. All of these parameters indicated that vector-averaged gravity disrupts mitochondrial function, thereby sensitizing osteoblasts to apoptosis [46; 47]. Over the years, this hypothesis has been supported by several other authors such us Chatziravdeli et al. that highlighted how several apoptotic genes, including p53 and apoptosis regulator BAX, were upregulated in osteoblasts under microgravity conditions [48], as well as F-Box Protein 3 (Fbxo3), Death-Associated Protein Kinase 1 (DapK1), and Death domain-containing protein (Cradd) [49].

Furthermore, Nabavi et al., demonstrated that osteoblasts exposed to 5 days of microgravity exhibit shorter and wavy microtubules, smaller and fewer focal adhesions, and thinner actin and cortical stress fibers [50]. Finally, in 2017,

Michaletti et al., demonstrated the mitochondria role in the microgravity-induced stress in osteoblasts. In more detail, they showed a dysregulation of mitochondrion homeostasis, an interrupted Krebs cycle, and Complex II of the mitochondrial respiratory chain, which catalyses the biotransformation of this step, was under-represented by 50%, suggesting that microgravity may suppress bone cell functions, impairing mitochondrial energy potential and the energy state of the cell [51].

Immune system disfunction. Space flight have been shown to affect a variety of immunological responses in humans. Already in 1998, Lewis et al., reported an increase of programmed cell death in human T lymphoblastoid cells (Jurkat) under real microgravity conditions [52], and release of the soluble form of the cell death factor, Fas/APO-1 (sFas) [53]. Has been show that spaceflight, as well as altered gravity produced by clinostat rotation, affects microtubule and mitochondria organization and results in an increase of Jurkat cells apoptosis [54].

At the same time, intercellular adhesion molecule 3 may be an important adhesion molecule involved in the induction of leukocyte apoptosis [55]. The mechanism that induces apoptosis of lymphocytes appears to be based on calcium-dependent 5-LOX activation, damage of the mitochondrial membrane, the release of cytochrome c, and caspase activation [56]. While after 48 hours of real microgravity conditions, showed an increase of DNA fragmentation and cleaved–poly (ADP-ribose) polymerase (PARP) protein expression, as well as mRNA levels of apoptosis-related markers such as p53 and calpain, and an immediate increase of 5-LOX activity [57]. Furthermore, the microRNA (miRNA) and mRNA expression of human peripheral blood lymphocytes (PBLs) exposed to simulated gravity environment showed 42 miRNAs altered [58].

In summary, all altered pathways described so far seem to be the cause of the astronauts' immune system dysfunction of the which leads them to contract bacterial and viral infections more easily.

Brain and Eye Cells. Up to 60% of astronauts conducting long-term missions on the ISS and 29% of astronauts on short-duration space shuttle flights reported to have experienced a wide spectrum of ocular disfunctions, resulting in deprivation in near and distant view [59]. In the "Mader" study conducted on seven astronauts ophthalmic anomalies were highlighted such as disc edema, globe flattening, choroidal folds, cotton wool spots, and nerve fiber layer, leading the researchers to hypothesize that the optic nerve and ocular changes may result from cephalad fluid shifts due to prolonged microgravity exposure [59]. In according with Mader, other studies showed that microgravity induces an increase of intracranial pressure [60], and stimulates apoptosis in astrocytes [61] and photoreceptor cells [62]. However, the symptoms presented by the astronauts could also be due to the retina damage. Already in 2005, Tombran-Tink and Barnstable showed a microgravity-induced degeneration in the retina [63]. In fact, Cingolani et al., demonstrated how microgravity can cause retinal degeneration from oxidative damage [64], including cytoskeletal alterations and changes in gene expression, in human retina pigment epithelium [65]. Numerous genes involved in oxidative stress and in the regulation of the mitochondria-associated apoptotic pathway were affected by microgravity conditions [62], indicating an increase apoptosis in the inner nuclear layer and the ganglion cell layer of the retina.

The presence in the spectrum of symptoms manifested by astronauts of neurophysiological problems, suggesting that brain cells are also affected by the microgravity environment. Rat C6 glioma cells were studied at different duration of microgravity conditions. After 30 minutes of microgravity they revealed chromatin condensation, nuclear fragmentation and the precence of caspase-7 in the cytoplasm, while at 32-h incubation at simulated microgravity, the number of apoptotic cells declined significantly, suggesting that glial cells have the ability to acclimatise to reduced gravity [61]. Similarly, in primary neural cultures, was observed a a time-dependent reduction of neurite length and soma size undr microgravity environment. After 24 hours of simulated gravity, the return of the neurons to Earth's gravity allowed recovery of soma size, while neurite length was not readjusted [66].

These results, taken together, indicate that microgravity can induce temporary or permanent damage to both the eye and the nervous system of astronauts.

Pancreatic Cells. Despite what has been said for the body districts described so far, with regard to pancreatic cells it seems that microgravity have beneficial effects in terms of function and growth. Pancreatic islets cultured under simulated microgravity condition exhibited increased growth, higher survival rates, decreased apoptosis, and well-developed mitochondria compared with normal gravity control islets [67]. Moreover, pancreatic islets cultured under simulated microgravity conditions and in combination with a polyglycolic acid scaffold showed a prolonged survival time and increased insulin production and release [68].

Cardiovascular System. Side-products of normal mitochondrial metabolism and respiratory chain include the accumulation of potentially damaging levels of reactive oxygen species (ROS). The enzymes involved in these processes are nitric oxide oxidase (NOX), xanthine oxidase (XO), lipoxygenase, nitric oxide synthase (NOS), and myeloperoxidase. NOX proteins are widely expressed in the cardiovascular system—specifically NOX1 (vascular smooth muscle cells), NOX2 (endothelium, vascular smooth muscle cells, adventitia, and cardiomyocytes), NOX4 (endothelium, vascular smooth muscle cells, cardiomyocytes, and cardiac stem cells), and NOX5 (vascular smooth muscle cells) [69]. NOX is involved in several cardiovascular diseases such as hypertension, left ventricular hypertrophy, myocardial infarction [69], angiogenesis [70], and blood pressure regulation [71]. Increased oxidative stress induces monomerization of the endothelial isoform of NOS (eNOS), which in turn results in further production of superoxide anion instead of nitric oxide [72], contributeing to endothelial dysfunction and then to cardiovascular disorders, including hypertension [73].

In addition, it has been demonstrated that heart rate, diastolic pressure, variability of heart rate and diastolic pressure, and premature ventricular contractions all were significantly reduced in flight [74]. Finally, some astronauts experience cardiac dysrhythmias due to reduced aerobic capabilities [75].

1.4. The Spatial Anemia

In the framework of risky health status manifested by the astronauts, haematological alterations take up significant importance. Indeed, astronauts develop several haematological abnormalities, anaemia [35], thrombocytopenia, and abnormalities in red blood cell structure [36;37;38], reduction of plasma volume by 10-17% and hemolysis [39]. These symptoms represent what is commonly known as "space flight anemia' [76]. In recent years, concern about the effects of space flight on haematological processes has been increasing.

Anaemia in astronauts has been noted since the earliest space missions but contributing mechanisms during space flights remained unclear. In fact, until now it was thought that the condition of Pseudopolicythemia in astronauts occurred due to the rapid redistribution of blood and the increase in renal production.

Over the years, several scientific studies allowed to formulate various theories that could explain the alterations in the size and number of erythrocytes. In more detail, Erslev [77] proposed that erythropoietin controls the number of divisions of blast-forming units (BFU-e), which determine the number of proerythroblasts and, thus, the number of RBCs produced. On the other hand, Koury and Bondurant [78] assumed that the number of BFU-e is considerably higher than that required and that their survival depends on the presence of erythropoietin. In other words, they propose that erythropoietin modulates the degree of apoptosis. Upon returning to Earth, the astronauts' plasma volume increased, while the hemoglobin concentration and red blood cell count decreased. On the other hand, serum erythropoietin is increased [35]. The fact that serum erythropoietin has increased but that hemoglobin and red blood cells are decreased supports the hypothesis that there are other factors contributing to erythrocyte death. A recent study by the University of Ottawa showed, for astroanuts, a 54% reduction of red blood cells when compared to gravity experienced on Earth [79]. These results were also obtained by the research group of Leach and Johnson [80]. In their study, red cell mass, plasma volume, hematocrit, and reticulocyte number of were measured in both the American and Soviet manned programs. On their return the space travelers showed values of red cell mass, plasma volume, hematocrit, and reticulocyte number reduced and even two weeks after landing these values remained lower than the pre-flight value [80]. Therefore, the main cause of spatial

anemia is not to be found either in the production of red blood cells by the bone marrow or in an anomalous redistribution of body biofluids, but in an early and accelerated degradation of these cells which is reflected in a reduction of the red cell mass.

However, it is not known whether hemolysis occurs at an intravascular or extravascular level, in the spleen, liver or bone marrow [81].

On the contrary, it is well known that many factors can lead a human cell to programmed death. Among the various factors we certainly find the activity of specific lipid categories. Indeed, bioactive lipid molecules known as signaling molecules, such as fatty acid, eicosanoids, diacylglycerol, phosphatidic acid, lysophosphatidic acid, ceramide, sphingosine, sphingosine-1-phosphate, phosphatidylinositol-3 phosphate, and cholesterol, are involved in the activation or regulation of different signaling pathways leading the cell to death by apoptosis. Another important aspect that should not be underestimated is the fact that the plasma membrane of human cells, including erythrocytes, is made up of lipids. Alterations in the lipid composition of the membrane determine membrane rigidity and fluidity, and plays a crucial role in membrane organization, dynamics, and function [82]. Despite the great relevance of the topic, currently few studies have been carried out to investigate the behaviour of lipids in erythrocytes samples cultured under simulated gravity conditions. In 2009, Ivanova et al., investigated blood samples from Russian cosmonauts by observing significant changes in phospholipids class [83]. An increase in the percentage of phosphatidylcholine may be clearly associated with the increase in membrane rigidity. On the other hand, changes in physicochemical properties of the plasma membrane of erythrocytes (microviscosity and permeability) can influence the efficiency of oxygen transfer, the state of the haemoglobin and changes in the conformation of hematoporphyrin.

References

[1] Brooks, G. Courtney, Grimwood, M. James, Swenson, and L. S. Jr., *Chariots for Apollo: A History of Manned Lunar Spacecraft. NASA History Series*. Scientific and Technical Information Branch, NASA, 1979.

[2] United States Congress Senate Committee on Armed Services Subcommittee on Military Construction, *Fiscal Year 1958 Supplemental Military Construction Authorization (Air Force)*. U.S. Government Printing Office, 1958.

[3] Gary Kitmacher, *Reference Guide to the International Space Station (Apogee Books Space Series)*. 2006.

[4] D. Heivilin, *Space Station: Impact of the Expanded Russian Role on Funding and Research*. Government Accountability Office., 1994.

[5] NASA and CSA, "Memorandum of Understanding Between the National Aeronautics and Space Administration of the United States of America and the Canadian Space Agency Concerning Cooperation on the Civil International Space Station," 1998.

[6] J. Payette, "Research and Diplomacy 350 Kilometers above the Earth: Lessons from the International Space Station," *Sci. Dipl.*, vol. 1, no. 4, 2012.

[7] A. Schepard, *2011 U.S. Commercial Space Transportation Developments and Concepts: Vehicles, Technologies, and Spaceports*, vol. 49, no. 1. 2011.

[8] D. Thomas, J. Robinson, J. Tate, and Thumm T., "Inspiring the Next Generation: Student Experiments and Educational Activities on the International Space Station." NASA, pp. 1–108, 2006.

[9] G. C. Demontis, M. M. Germani, E. G. Caiani, I. Barravecchia, C. Passino, and D. Angeloni, "Human pathophysiological adaptations to the space environment," *Front. Physiol.*, vol. 8, no. AUG, pp. 1–17, 2017.

[10] J. A. Laurie, N. Cranford, C. W. Lloyd, M. J. Shelhamer, and J. L. Turner, "The Human Body in Space," *Kelli Mars*, vol. 184, no. 1, pp. 16–19, 2022.

[11] L. W. Townsend, F. A. Cucinotta, J. W. Wilson, and R. Bagga, "Estimates of HZE particle contributions to SPE radiation exposures on interplanetary missions," *Adv. Sp. Res.*, vol. 14, no. 10, pp. 671–674, 1994.

[12] J. C. Chancellor, G. B. I. Scott, and J. P. Sutton, "Space radiation: The number one risk to astronaut health beyond low earth orbit," *Life*, vol. 4, no. 3, pp. 491–510, 2014.

[13] G. D. Badhwar and P. M. O'Neill, "Long-term modulation of galactic cosmic radiation and its model for space exploration," *Adv. Sp. Res.*, vol. 14, no. 10, pp. 749–757, 1994.

[14] F. A. Cucinotta, H. Nikjoo, and D. T. Goodhead, "The effects of delta rays on the number of particle-track traversals per cell in laboratory and space exposures," *Radiat. Res.*, vol. 150, no. 1, pp. 115–119, 1998.

[15] J. K. Sanzaria *et al.*, "Acute Hematological Effects of Solar Particle Event Proton Radiation in the Porcine Model," *Radiat Res.*, vol. 180, no. 1, pp. 1–7, 2013.

[16] W. Jiang *et al.*, "Plasma levels of bacterial DNA correlate with immune activation and the magnitude of immune restoration in persons with antiretroviral-treated HIV infection," *J. Infect. Dis.*, vol. 199, no. 8, pp. 1177–1185, 2009.

[17] Y. Zhou *et al.*, "Effect of Solar Particle Event Radiation and Hindlimb Suspension on Gastrointestinal Tract Bacterial Translocation and Immune Activation," *PLoS One*, vol. 7, no. 9, pp. 1–9, 2012.

[18] R. L. Kohl, “Hormonal responses of metoclopramide-treated subjects experiencing nausea or emesis during parabolic flight,” *Aviat Sp. Env. Med*, vol. 58, no. 9, 1987.

[19] M. Hoffman and D. M. Monroe, “A cell-based model of hemostasis,” *Thromb. Haemost.*, vol. 85, no. 6, pp. 958–965, 2001.

[20] J. M. Wilson *et al.*, “Acute Biological Effects of Simulating the Whole-Body Radiation Dose Distribution from a Solar Particle Event Using a Porcine Model,” *Radiat. Res.*, vol. 176, no. 5, pp. 649–659, 2011.

[21] K. G. Soucy *et al.*, “Single exposure gamma-irradiation amplifies xanthine oxidase activity and induces endothelial dysfunction in rat aorta,” *Radiat. Environ. Biophys.*, vol. 46, no. 2, pp. 179–186, 2007.

[22] H. Bielefeldt-Ohmann, P. C. Genik, C. M. Fallgren, R. L. Ullrich, and M. M. Weil, “Animal studies of charged particle-induced carcinogenesis,” *Health Phys.*, vol. 103, no. 5, pp. 568–576, 2012.

[23] M. P. Little, “A review of non-cancer effects, especially circulatory and ocular diseases,” *Radiat. Environ. Biophys.*, vol. 52, no. 4, pp. 435–449, 2013.

[24] J. I. Pagel and A. Choukèr, “Effects of isolation and confinement on humans-implications for manned space explorations,” *J. Appl. Physiol.*, vol. 120, no. 12, pp. 1449–1457, 2016.

[25] N. Kanas, “Psychological, psychiatric, and interpersonal aspects of long-duration space missions,” *J. Spacecr. Rockets*, vol. 27, no. 5, pp. 457–463, 1990.

[26] N. Kanas *et al.*, “Psychology and culture during long-duration space missions,” *Acta Astronaut.*, vol. 64, no. 7–8, pp. 659–677, 2009.

[27] N. Kanas, “Space Psychology and Psychiatry,” *J. Chem. Inf. Model.*, vol. 53, no. 9, pp. 1689–1699, 2013.

[28] N. Goswami, O. White, A. Blaber, J. Evans, J. J. W. A. van Loon, and G. Clement, “Human physiology adaptation to altered gravity environments,” *Acta Astronaut.*, vol. 189, no. August, pp. 216–221, 2021.

[29] F. Strollo and J. Vernikos, “Aging-like metabolic and adrenal changes in microgravity: State of the art in preparation for Mars,” *Neurosci. Biobehav. Rev.*, vol. 126, no. January, pp. 236–242, 2021.

[30] W. Wieling, J. R. Halliwill, and J. M. Karemaker, “Orthostatic intolerance after space flight,” *J. Physiol.*, vol. 538, no. 1, p. 1, 2002.

[31] M. Hughes-Fulford, R. Tjandrawinata, J. Fitzgerald, K. Gasuad, and V. Gilbertson, “Effects of microgravity on osteoblast growth.,” *Gravit. Space Biol. Bull.*, vol. 11, no. 2, pp. 51–60, 1998.

[32] Y. Sun, Y. Kuang, and Z. Zuo, “The emerging role of macrophages in immune system dysfunction under real and simulated microgravity conditions,” *Int. J. Mol. Sci.*, vol. 22, no. 5, pp. 1–21, 2021.

[33] G. R. Clément *et al.*, “Challenges to the central nervous system during human spaceflight missions to Mars,” *J. Neurophysiol.*, vol. 123, no. 5, pp. 2037–2063, 2020.

[34] S. Patel, “The effects of microgravity and space radiation on cardiovascular health: From low-Earth orbit and beyond,” *IJC Hear. Vasc.*, vol. 30, p. 100595, 2020.

[35] C. P. Alfrey, M. M. Udden, C. Leach-Huntoon, T. Driscoll, and M. H. Pickett, “Control of red blood cell mass in spaceflight,” *J. Appl. Physiol.*, vol. 81, no. 1, pp. 98–

104, 1996.

[36] G. R. Taylor, “Advances in experimental medicine,” in *Advances in experimental medicine and biology*, vol. 225, no. 1, 1997, pp. 269–271.

[37] C. Manis *et al.*, “Understanding the Behaviour of Human Cell Types under Simulated Microgravity Conditions: The Case of Erythrocytes,” *International Journal of Molecular Sciences*, vol. 23, no. 12. 2022.

[38] R. T. Meehan *et al.*, “Alteration in human mononuclear leucocytes following space flight.,” *Immunology*, vol. 76, no. 3, pp. 491–497, 1992.

[39] A. Diedrich, S. Y. Paranjape, and D. Robertson, “Plasma and blood volume in space,” *Am. J. Med. Sci.*, vol. 334, no. 1, pp. 80–86, 2007.

[40] N. S. Krieger *et al.*, “Effect of potassium citrate on calcium phosphate stones in a model of hypercalciuria,” *J. Am. Soc. Nephrol.*, vol. 26, no. 12, pp. 3001–3008, 2015.

[41] J. A. Robinson, “International Astronautical Congress (IAC), Washington, DC, 21-25 October 2019. Copyright ©2019 by National Aeronautics and Space Administration in all jurisdictions outside the United States of America. Published by the International Astronautical Federa,” no. October, pp. 21–25, 2019.

[42] J. C. Clemente, L. K. Ursell, L. W. Parfrey, and R. Knight, “The impact of the gut microbiota on human health: An integrative view,” *Cell*, vol. 148, no. 6, pp. 1258–1270, 2012.

[43] M. H. Mohajeri *et al.*, “The role of the microbiome for human health: from basic science to clinical applications,” *Eur. J. Nutr.*, vol. 57, pp. 1–14, 2018.

[44] B. Prasad *et al.*, “Influence of microgravity on apoptosis in cells, tissues, and other systems in vivo and in vitro,” *Int. J. Mol. Sci.*, vol. 21, no. 24, pp. 1–32, 2020.

[45] R. Saxena, G. Pan, and J. M. McDonald, “Osteoblast and osteoclast differentiation in modeled microgravity,” *Ann. N. Y. Acad. Sci.*, vol. 1116, pp. 494–498, 2007.

[46] M. A. Bucaro *et al.*, “Bone cell survival in microgravity: Evidence that modeled microgravity increases osteoblast sensitivity to apoptogens,” *Ann. N. Y. Acad. Sci.*, vol. 1027, pp. 64–73, 2004.

[47] M. A. Bucaro *et al.*, “The effect of simulated microgravity on osteoblasts is independent of the induction of apoptosis,” *J. Cell. Biochem.*, vol. 102, no. 2, pp. 483–495, 2007.

[48] V. Chatziravdeli, G. N. Katsaras, and G. I. Lambrou, “Gene Expression in Osteoblasts and Osteoclasts Under Microgravity Conditions: A Systematic Review,” *Curr. Genomics*, vol. 20, no. 3, pp. 184–198, 2019.

[49] E. A. Blaber *et al.*, “Microgravity Induces Pelvic Bone Loss through Osteoclastic Activity, Osteocytic Osteolysis, and Osteoblastic Cell Cycle Inhibition by CDKN1a/p21,” *PLoS One*, vol. 8, no. 4, 2013.

[50] N. Nabavi, A. Khandani, A. Camirand, and R. E. Harrison, “Effects of microgravity on osteoclast bone resorption and osteoblast cytoskeletal organization and adhesion,” *Bone*, vol. 49, no. 5, pp. 965–974, 2011.

[51] A. Michaletti, M. Gioia, U. Tarantino, and L. Zolla, “Effects of microgravity on osteoblast mitochondria: A proteomic and metabolomics profile,” *Sci. Rep.*, vol. 7, no. 1, pp. 1–12, 2017.

[52] M. L. Lewis, J. L. Reynolds, L. A. Cubano, J. P. Hatton, B. D. Lawless, and E. H.

Piepmeier, “Spaceflight alters microtubules and increases apoptosis in human lymphocytes (Jurkat),” *FASEB J.*, vol. 12, no. 11, pp. 1007–1018, 1998.

[53] L. A. Cubano and M. L. Lewis, “Fas/APO-1 protein is increased in spaceflown lymphocytes (Jurkat),” *Exp. Gerontol.*, vol. 35, no. 3, pp. 389–400, 2000.

[54] H. Schatten, M. L. Lewis, and A. Chakrabarti, “Spaceflight and clinorotation cause cytoskeleton and mitochondria changes and increases in apoptosis in cultured cells,” *Acta Astronaut.*, vol. 49, no. 3–10, pp. 399–418, 2001.

[55] A. Sokolovskaya *et al.*, “Changes in the surface expression of intercellular adhesion molecule 3, the induction of apoptosis, and the inhibition of cell-cycle progression of human multidrug-resistant Jurkat/A4 cells exposed to a random positioning machine,” *Int. J. Mol. Sci.*, vol. 21, no. 3, pp. 1–16, 2020.

[56] M. Maccarrone *et al.*, “Creating conditions similar to those that occur during exposure of cells to microgravity induces apoptosis in human lymphocytes by 5-lipoxygenase-mediated mitochondrial uncoupling and cytochrome c release,” *J. Leukoc. Biol.*, vol. 73, no. 4, pp. 472–481, 2003.

[57] N. Battista *et al.*, “5-Lipoxygenase-dependent apoptosis of human lymphocytes in the International Space Station: data from the ROALD experiment,” *FASEB J.*, vol. 26, no. 5, pp. 1791–1798, 2012.

[58] C. Girardi *et al.*, “Integration analysis of MicroRNA and mRNA expression profiles in human peripheral blood lymphocytes cultured in modeled microgravity,” *Biomed Res. Int.*, vol. 2014, 2014.

[59] T. H. Mader *et al.*, “Optic disc edema, globe flattening, choroidal folds, and hyperopic shifts observed in astronauts after long-duration space flight,” *Ophthalmology*, vol. 118, no. 10, pp. 2058–2069, 2011.

[60] J. S. Lawley *et al.*, “Effect of gravity and microgravity on intracranial pressure,” *J. Physiol.*, vol. 595, no. 6, pp. 2115–2127, 2017.

[61] B. M. Uva *et al.*, “Microgravity-induced apoptosis in cultured glial cells,” *Eur. J. Histochem.*, vol. 46, no. 3, pp. 209–214, 2002.

[62] X. W. Mao, L. M. Green, T. Mekonnen, N. Lindsey, and D. S. Gridley, “Gene expression analysis of oxidative stress and apoptosis in proton-irradiated rat retina,” *In Vivo (Brooklyn).*, vol. 24, no. 4, pp. 425–430, 2010.

[63] J. Tombran-Tink and C. J. Barnstable, “Space flight environment induces degeneration in the retina of rat neonates,” *Adv. Exp. Med. Biol.*, vol. 572, pp. 417–424, 2005.

[64] C. Cingolani, B. Rogers, L. Lu, S. Kachi, J. K. Shen, and P. A. Campochiaro, “Retinal degeneration from oxidative damage,” *Free Radic. Biol. Med.*, vol. 40, no. 4, pp. 660–669, 2006.

[65] J. E. Roberts, B. Kukielczak, C. Chignell, B. Sik, D. N. Hu, and M. A. Principato, “Simulated microgravity induced damage in human retinal pigment epithelial cells,” *Mol. Vis.*, vol. 12, no. February, pp. 633–638, 2006.

[66] G. Pani *et al.*, “Combined Exposure to Simulated Microgravity and Acute or Chronic Radiation Reduces Neuronal Network Integrity and Survival,” *PLoS One*, vol. 11, no. 5, pp. 1–19, 2016.

[67] C. Song *et al.*, “Experimental study of rat beta islet cells cultured under simulated microgravity conditions,” *Acta Biochim. Biophys. Sin. (Shanghai).*, vol. 36, no. 1, pp. 47–50, 2004.

[68] Y. Song *et al.*, “Simulated microgravity combined with polyglycolic acid scaffold culture conditions improves the function of pancreatic islets,” *Biomed Res. Int.*, vol. 2013, 2013.

[69] J. D. Lambeth, “Nox enzymes, ROS, and chronic disease: An example of antagonistic pleiotropy,” *Free Radic. Biol. Med.*, vol. 43, no. 3, pp. 332–347, 2007.

[70] R. Prieto-Bermejo and A. Hernández-Hernández, “The importance of NADPH oxidases and redox signaling in angiogenesis,” *Antioxidants*, vol. 6, no. 2, 2017.

[71] G. Gavazzi *et al.*, “Decreased blood pressure in NOX1-deficient mice,” *FEBS Lett.*, vol. 580, no. 2, pp. 497–504, 2006.

[72] Q. Li, J. Yon, H. Cai, C. L. Angeles, and L. Angeles, “Mechanisms and Consequences of eNOS Dysfunction in Hypertension,” *J. Hypertens.*, vol. 33, no. 6, pp. 1128–1136, 2016.

[73] L. Rochette *et al.*, “Nitric oxide synthase inhibition and oxidative stress in cardiovascular diseases: Possible therapeutic targets?,” *Pharmacol. Ther.*, vol. 140, no. 3, pp. 239–257, 2013.

[74] J. M. Fritsch-Yelle, J. B. Charles, M. M. Jones, and M. L. Wood, “Microgravity decreases heart rate and arterial pressure in humans,” *J. Appl. Physiol.*, vol. 80, no. 3, pp. 910–914, 1996.

[75] D. R. Williams, “Bioastronautics: Optimizing human performance through research and medical innovations,” *Nutrition*, vol. 18, no. 10, pp. 794–796, 2002.

[76] S. M. Smith, “Red blood cell and iron metabolism during space flight,” *Nutrition*, vol. 18, no. 10, pp. 864–866, 2002.

[77] A. J. Erslev, “Erytropoietin,” *N. Engl. J. Med.*, vol. 325, no. 3, pp. 147–52, 1991.

[78] M. J. Koury and M. C. Bondurant, “Erythropoietin retards DNA breakdown and prevents programmed death in erythroid progenitor cells,” *Science (80-.).*, vol. 248, pp. 378–381, 1990.

[79] G. Trudel, N. Shahin, T. Ramsay, O. Laneuville, and H. Louati, “Hemolysis contributes to anemia during long-duration space flight,” *Nat. Med.*, vol. 28, no. 1, pp. 59–62, 2022.

[80] C. S. Leach and P. C. Johnson, “Influence of spaceflight on erythrokinetics in man,” *Science (80-.).*, vol. 225, no. 4658, pp. 216–218, 1984.

[81] G. Trudel, J. Shafer, O. Laneuville, and T. Ramsay, “Characterizing the effect of exposure to microgravity on anemia: more space is worse,” *American Journal of Hematology*, vol. 95, no. 3. pp. 267–273, 2020.

[82] F. R. Maxfield and I. Tabas, “Role of cholesterol and lipid organization in diseas,” *Nature*, vol. 438, pp. 612–621, 2005.

[83] S. M. Ivanovaa *et al.*, “Morphobiochemical assay of the red blood system in members of the prime crews of the International Space Station,” *Hum. Physiol.*, vol. 43, no. 1, pp. 43–47, 2009.

AIM OF THE WORK

My PhD study is part of a large project aiming to investigate haematological alterations caused by microgravity conditions using a metabolomics approach. A part of the analyses was performed at the Centre of Metabolomics and Bioanalysis (CEMBIO) at the Faculty of Pharmacy (CEU-San Pablo University) led by Prof. Coral Barbas, in Madrid (Spain).

As previously reported, the Spatial Anemia in astronauts has been noted since the earliest space missions, but the mechanisms that contribute to anemia during space flight remained unclear.

With the aim to understand which metabolic and/or structural changes occur in the erythrocytes subjected to low gravity, an experimental analysis of the erythrocyte's metabolomic profile and human plasma polar profile under normal- and micro-g conditions was carried out.

Due to their high sensitivity and to their strong reproducibility in metabolomics analysis, the main analytical techniques used for this project were liquid chromatography coupled with mass-spectrometry and ion mobility, and capillary electrophoresis coupled with mass-spectrometry. Datasets were processed using multivariate statistic packages to fully understand the most significant metabolites implicated in haematological alterations. While three-dimensional SEM was used for the imaging analysis and a fine resolution of erythrocytes structure.

MATERIALS AND METHODS

3.1.Samples

To a freshly drawn blood (Rh +) from nine healthy adult volunteers (men and women) heparin was added and preserved in citrate-phosphate-dextrose with adenine (CPDA-1). Red blood cells (RBCs) were separated from plasma and leukocytes by washing three times with phosphate-buffered saline (127 mM NaCl, 2.7 mM KCl, 8.1 mM Na_2HPO_4, 1.5 mM KH_2PO_4, 20 mM HEPES, 1 mM $MgCl_2$, and pH 7.4) supplemented with 5 mM glucose (PBS glucose) to obtain packed cells. This study was conducted in accordance with Good Clinical Practice guidelines and the Declaration of Helsinki. No ethical approval has been requested as Human blood samples were used only to sustain in vitro cultures and patients provided written, informed consent in ASL. 1-Sassari (Azienda Sanitaria Locale.1-Sassari) center before entering the study.

3.2. Materials

Methanol, chloroform, isopropanol, acetonitrile, water and formic acid were purchased from Sigma Aldrich (Milano, Italy and St. Louis, Missouri, United State). Bidistilled water was obtained from a MilliQ purification system (Millipore, Milan, Italy) before use.

Methionine sulfone as IS (99% purity), MES and paracetamol were acquired from Sigma (Steinheim, Germany); and sodium hydroxide was acquired from Panreac, (Barcelona, Spain).

A SPLASH® LIPIDOMIX® standard component mixture was purchased from Sigma Aldrich (Milan, Italy) PC (15:0-18:1) (d7), PE(15:0-18:1) (d7), PS (15:0-18:1)(d7), PG (15:0-18:1)(d7), PI (15:0-18:1) (d7), PA (15:0-18:1) (d7), LPC (18:1) (d7) LPC 25, LPE (18:1) (d7), Chol Ester (18:1)(d7), MG (18:1) (d7), DG (15:0-18:1) (d7), TG ((15:0-18:1)(d7)-15:0)), SM (18:1) (d9), Cholesterol (d7).

3.3. Sample preparation

In this project, human erythrocytes and plasma samples were analysed with the aim to study the metabolomics profile and to investigate their morphology performing imaging analysis (**Figure 1**).

Samples were prepared in different ways according to the analysis to be performed.

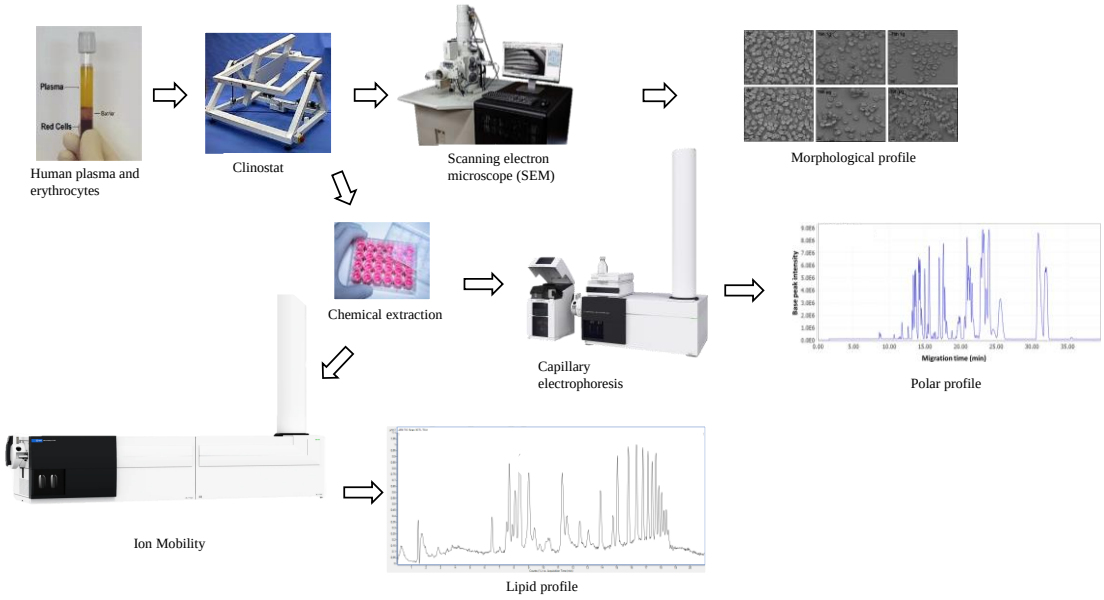

Figure 1. Experimental design of Phd project.

Sample preparation for lipidomics analysis. In order to investigate changes in the lipidome, 50 µL of human erythrocytes solution were subjected to the modify Folch procedure [1] to extract and separate hydrophilic and lipophilic metabolites. Briefly, 0.700 mL of a methanol and chloroform mixture (2/1, *v*/*v*). Samples were vortexed every 15 min up to 1 h, when 0.350 mL of chloroform and 0.150 mL of water were subsequently added. The solution thus obtained was centrifuged at 12,000 rpm for 10 min, and 0.600 mL of the organic layer was transferred into a glass vial and dried under a nitrogen stream. The dried chloroform phase was reconstituted with 50 µL of a methanol and chloroform mixture (1/1, *v/v*) and 75 µL isopropanol:acetonitrile:water mixture (2:1:1 *v*/*v*). Quality control (QC) samples were prepared taking an aliquot of 10 µL of each sample. All samples thus prepared were injected in UHPLC-IM-QTOF-MS/MS and acquired in negative ionization mode, while for positive ionization mode they were diluted in ratio 1:10.

Sample preparation for metabolomics analysis. Prior to the CE-MS analysis, 0.200 mL of the aqueous layer, derived from Folch extraction, was transferred into a glass vial and dried under a nitrogen stream. The dried aqueous phase was reconstituted with 75 µL of a standard mix solution consisting of formic acid (0.025M), methionine sulfone (0.2mM), 2-(N-morpholino) methanesulfonic acid (MES) (0.2mM) and paracetamol (1mM) and vortexed for 30 min. At this point, 0.175 mL of a methanol and water mixture (3:1, v/v) were added to each sample and vortexed again for 20 min. Then, 0.240 mL of the supernatant was taken from each sample, deposited in new eppendorf and placed in a desiccator (Hyper Vac) for 4 h at 40° C. Samples were reconstituted with 0.075 mL of an aqueous solution of 0.025 M formic acid and vortexed for 20 min. Subsequently, the samples were centrifuged for 10 min at 16000 rpm and at 4° C. Finally, the supernatant of each sample was collected and transferred to the respective vial for electrophoresis analysis. Quality control (QC) samples were prepared taking an aliquot of 5 µL of each sample. All samples thus prepared were injected in CE-MS and acquired in positive and negative ionization mode.

Sample preparation for the imaging analysis. For three-dimensional SEM imaging and a fine resolution of erythrocytes structure, samples were fixed with 1% paraformaldehyde in 0.1 M Na-cacodylate buffer (pH 7.4) for 1 h at room temperature.

After washing in Na-cacodylate buffer, samples have been left on microscope slides overnight. After numerous washes in PBS (Phosphate Buffered Saline), slides were dehydrated in ascending ethanol scales, dried at critical point in CO_2 and then mounted on aluminium support (stub) with double-sided tape. Finally, samples were covered with a gold conductive film and observed at SEM (ZEISS SIGMA 300).

3.4. Simulated gravity conditions.

By definition, the term “gravity” is specific to the acceleration we have on Earth (~9.81 m/s^2), and is expressed in the international system of units (SI) as g. “Hypergravity” includes the gravity levels above 1 g. A gravity level lower than 1 g is called “hypogravity” or “partial gravity” or “reduced gravity” or “microgravity”.

Scientific investigation in microgravity conditions is indispensable to disclose the impact of gravity on biological processes and organisms. One of the key challenges in using microgravity as an investigative tool is creating a microgravity condition that can be applied at a cellular level, on Earth. Starting from the classical clinostat introduced in 1879 by Julius Sachs, over the years were developed several ground-based microgravity simulators which are frequently used by gravitational biologists such as two-dimensional (2-D) clinostats, rotating wall vessels (RWVs), random positioning machines (RPMs), and diamagnetic levitation.

A clinostat is an instrument that allows a rotation of the samples such as to prevent the biological system from perceiving the gravitational acceleration vector. Clinostat with an axis of rotation, which run perpendicular to the direction of the gravity vector, are called 1-D (rarely) or 2-D clinostat, while those with two axes, also known as 3-D clinostats (most common), are represented by the random positioning machine (RPM) [2;3]. In this system, cells grow at low fluidity in a controlled environment, where the liquid counteracts slow sedimentation, creating a constant "free fall" of cells through the culture medium. Subsequently, NASA-designed rotating-wall vessels (RWVs), which are filled with culture medium and rotates around the Horizontal axis. The fluid medium within the RWV undergoes rotation of the solid body and eliminates the occurrence of the boundary layers, which is inherent in bioreactors in which the medium moves relative to the vessel wall. In this case, the cell undergoes rotation about its own axis as it moves around in the vessel [4]. The RWV is very suitable for the study of human tissues in microgravity conditions because the tissue structures grow often in form of

3D aggregates with many similarities to the native tissue and provide adequate and controlled supplies of oxygen and nutrients.

In our study, we used a 3D random positioning machine (RPM, Fokker Space, Netherlands) at the laboratory of the Department of Biomedical Sciences, University of Sassari, Sardinia, Italy. The 3D RPM is a micro-weight (microgravity) simulator based on the principle of 'gravity-vector-averaging', built by Dutch Space. The 3D RPM is constituted by two perpendicular frames that rotate independently (**Figure 2**). The direction of the gravity vector is constantly changed so that the average of the gravity vector simulates a microgravity environment. The 3D RPM provides a simulated microgravity less than 10^{-3} g. The dimensions of the 3D RPM are of 1000 × 800 × 1000 mm (length × width × height). The 3D RPM is connected to a computer and through a specific software the mode and speed of rotation were selected. Random Walk mode with an 80 degree/sec (rpm) was chosen. To simulate the effect of all the operating conditions, the following procedure was adopted.

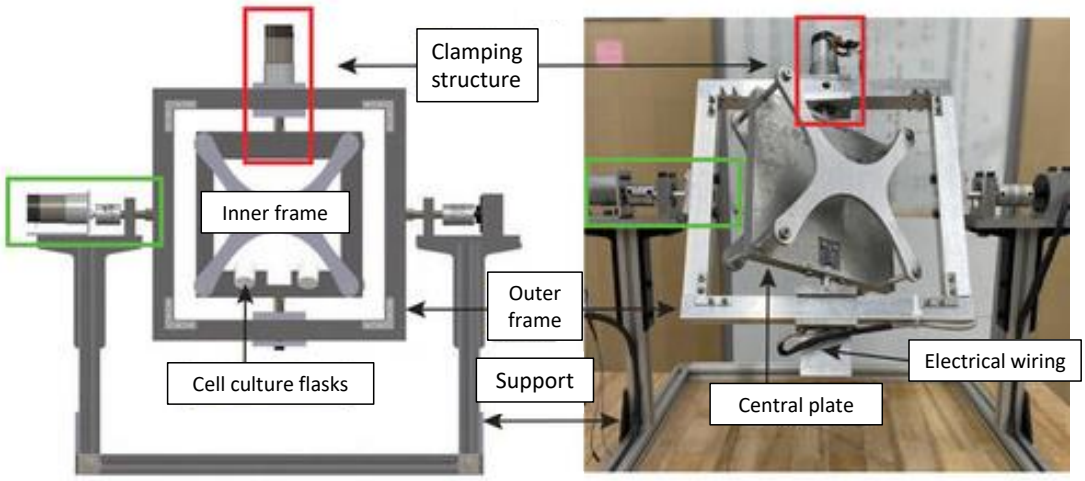

Figure 2. Random Positioning Machine (RPM).

3.5. Metabolomics

The metabolome is defined as the quantitative complement of low-molecular-weight metabolites present in a biological fluid, cell or organism under a given set of physiological conditions. Metabolites can be intermediates of biochemical reactions or the final products of cellular regulatory processes, and their levels have a crucial role in connecting the many different pathways that operate within a living cell responding to some genetic or environmental change. Adding further complexity is the fact that many intracellular metabolites participate in a large number of different biochemical reactions and, therefore, bind together many different parts of cellular metabolism as a tightly controlled metabolic network [5].

The set of metabolites synthetized by a biological system constitutes its metabolome [6]. Metabolome analyses are based on the identification and quantification of all intracellular and extracellular metabolites with molecular mass lower than 1500-2000 Da, using different analytical techniques [7]. In common with the genome and the proteome, the metabolome is associated with the physiological, developmental, and pathological state of a cell, tissue, or organism. Genome and proteome studies are based on target chemical analyses of biopolymers composed of nucleotides or amino acids, respectively. On the other hand, the metabolome consists of several different chemical compounds from ionic inorganic species to hydrophilic carbohydrates, volatile alcohols and ketones, amino and non-amino organic acids, hydrophobic lipids, and complex natural products. This complexity makes it difficult to simultaneously study the complete metabolome. For this reason, each metabolome study requires an evaluation of the sample preparation and the extraction procedure and a combination of different analytical tools in order to obtain as much information as possible [8]. The discipline that studies the metabolome is called “metabolomics” and it is generally defined as the analysis of intra and extra- cellular metabolites in simple biological systems. When the analysis is related to the quantitative measurement of the dynamic metabolic response of a living system to the physio-pathological stimuli or genetic modification it is called metabonomics [9]. Different metabolomics analyses were identified by Fiehn et al. with the most important being the untargeted and the target approaches [10]. Targeted analysis is useful for studying the primary effects due to genetic alteration. Metabolite identification and quantification are common methods used in this field. On the other

hand, untargeted analysis allows to achieve a larger number of metabolites with the objective to find a specific metabolic profile for a particular biological matrix [10].

The most common techniques used for metabolomics are nuclear magnetic resonance (NMR) spectroscopy, or chromatographic or electrophoretic separation methods combined with mass spectrometry (MS), such as gas chromatography (GC)-MS, liquid chromatography (LC)-MS and capillary electrophoresis (CE)-MS [11].

MS analysis is able to identify and characterize chemical compounds based on their masses or ion mass fragmentation. In order to identify multiple variables measured on multiple samples or at multiple time points, these techniques require the support of multivariate statistical data analysis. Multivariate data, contain much more information than univariate data. Multivariate data analysis techniques can be used to model factors and responses and find the relationships that exist between them. Information resulting from multivariate data is usually very helpful in order to understand the characteristics of metabolic systems and processes [12]. Initially used in chemistry to distinguish between useful and unusable chemical data, such as noise, repeated data and non-correlated data, these methods find several employments especially in clinical aspects. These studies allow for the consideration of all the variables and using those to exploit all the information inside of a complex data analysis. They can also be used to highlight their connection to a biological system. This is possible through different methods of modelling, classification, regression, and other analysis about the similarity of samples, optimization, and experimental design.

3.6. Lipidomics

Advances in mass spectrometry (MS) platforms, data processing tools, databases, knowledge of lipid diversity and the availability of high-quality standards allowed the systematic quantification of plasma lipids in various biological contexts [13]. In the last decade, lipidomics has emerged as a key useful approach to elucidate the lipid-related pathways and mechanisms underlying the cellular function. In fact, lipids are a class of molecules with central physiological roles, such as structural functions of cell membranes, energy storage sources and intermediates in cell-cell signalling pathways [14]. Lipids are very abundant in biological systems, approximately constituting 50% of the mass of most animal cell membranes approximately [15] with different degree of

complexity according to the body district or cellular compartment in which they are found [16]. Maintenance of an appropriate lipid composition is critical to ensure fluidity in cell membranes, the type and degree of exposure of surface proteins, and activity of membrane enzymes. Because of their central biological role, lipids have been an intense area of research since the 1960s, but which unfortunately could not emerge due to limiting instrument platforms. Nowadays lipidomics is considered an emerging science of fundamental importance for clarifying biochemical pathways involved in several pathologies or cellular stresses adaptation.

3.7. Scanning electron microscopy (SEM) analysis

Scanning electron microscopes (SEM) have high resolution for loose objects, large depth of field and shadow relief effect of electronic contrast. Also, their ability to examining objects at very low magnification represents a very useful tool both in the studies of the corpuscular part of the blood [17]. In the case of non-conductive samples, like non-dehydrated biological samples, it is necessary to coat them to make them conductive before an SEM analysis. Therefore, image formation becomes possible. Further technological developments led to environmental SEMs (ESEMs) (low vacuum), which allow the examination of uncoated samples making the technique widely suitable in case of biological samples [18]. SEM relies on the detection of high energy electrons emitted from the surface of a sample after being exposed to a highly focused beam of electrons from an electron gun. This beam of electrons is focussed to a small spot on the sample surface, using the SEM objective lens. Instrumental's variables such as the accelerating voltage used, size of aperture employed and the distance between the sample and electron gun (working distance) can be optimised to achieve the best quality images.

3.8. Analytical platforms

3.8.1. High-performance liquid chromatography (HPLC)

High-performance liquid chromatography is a commonly used technique for chemical analysis, and metabolomics, due to its ability to separate, analyse, and/or purify different samples [19]. This technique allows separation of eluted compounds quickly and with high efficiency by exploiting the different chemical affinity of the analysed compounds with solvents (mobile phase), silica particles (stationary phase) under a pressure which can achieve 1000 bar. Furthermore, with this technique for every analysis it is possible to use a small volume of sample that imply a smaller use of eluent [20] (**Figure 3**).

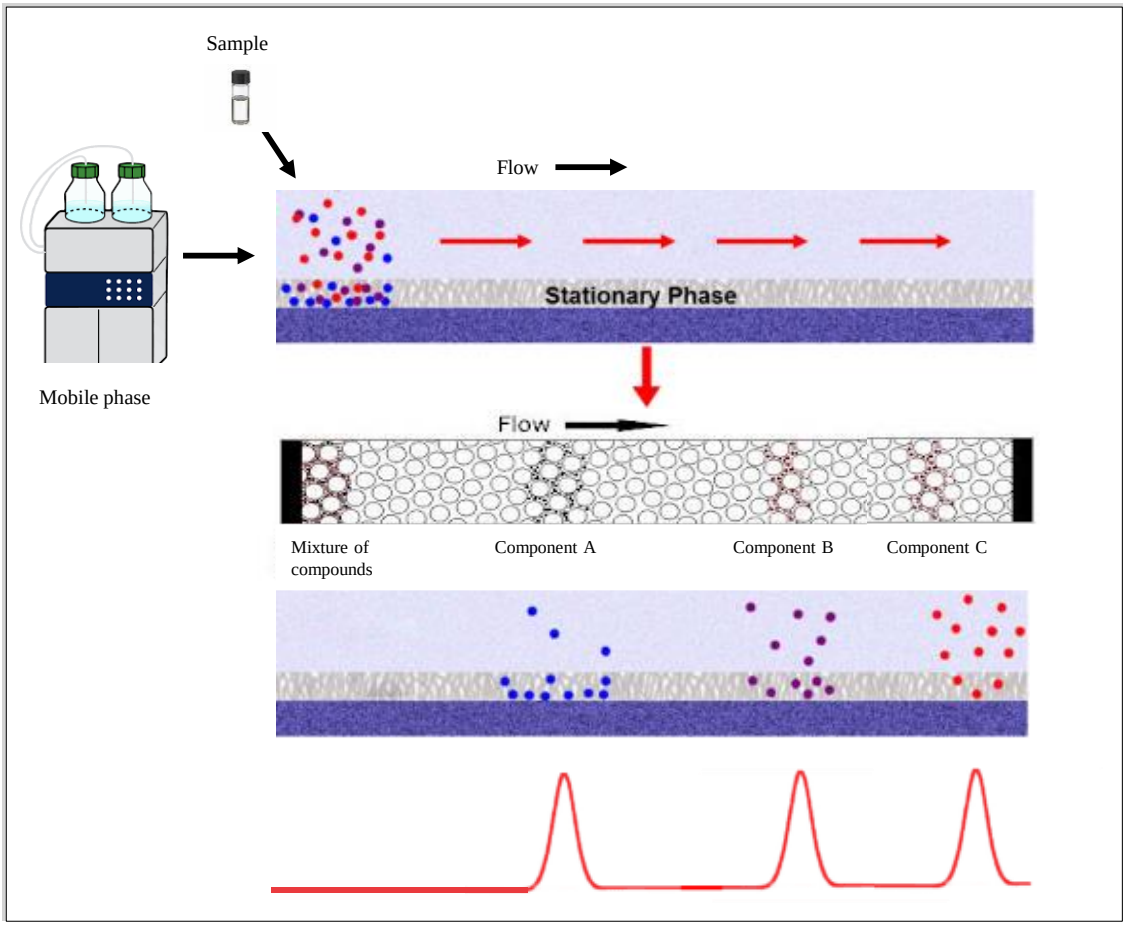

Figure 3. Mechanism of Separation of Components by HPLC.

There are two variations of HPLC separations depending on the relative polarity of the solvents and the stationary phases. Normal phase separation is based on a column filled with silica particles, and the solvent used is non-polar. Polar compounds in the mixture pass through the column and stay for longer in the polar phase if compared with non-polar compounds that pass more quickly through the column. While the reverse phase separation uses the same 3 μm column size, but the silica is non-polar thanks to the presence of the long hydrocarbon chains to its surface, usually with either 8 or 18 carbon atoms in them. A polar solvent is usually used. In this case, there will be a strong attraction between the polar solvent and polar molecules in the mixture that will cross the column. Non-polar compounds will spend less time in solution in the solvent and this will slow them down on their way through the column.
Mass spectrometry is the most suitable technique to characterise different compounds after chromatographic separation.

3.8.2. Mass Spectrometry (MS)

Mass spectrometry is based on the ionisation of molecules that are subsequently moved and influenced by external electric and magnetic fields. Due to the high reactivity of the ions their formation and manipulation must be conducted under vacuum environment. In a mass spectrometer, an ion source ionizes the sample after column separation. The ionisation can be conducted in positive or in negative ion mode and that depends on the way how the molecules will be ionised. The most used ion sources are the electrospray ionisation (ESI) and the atmospheric pressure chemical ionisation (APCI). The first is recommended for the analysis of polar molecules, while the APCI for the molecules with low polarity. In a typical MS procedure (schematized in **Figure 4**), a sample, which may be solid, liquid, or gaseous, is ionized, for example by bombarding it with a beam of electrons.

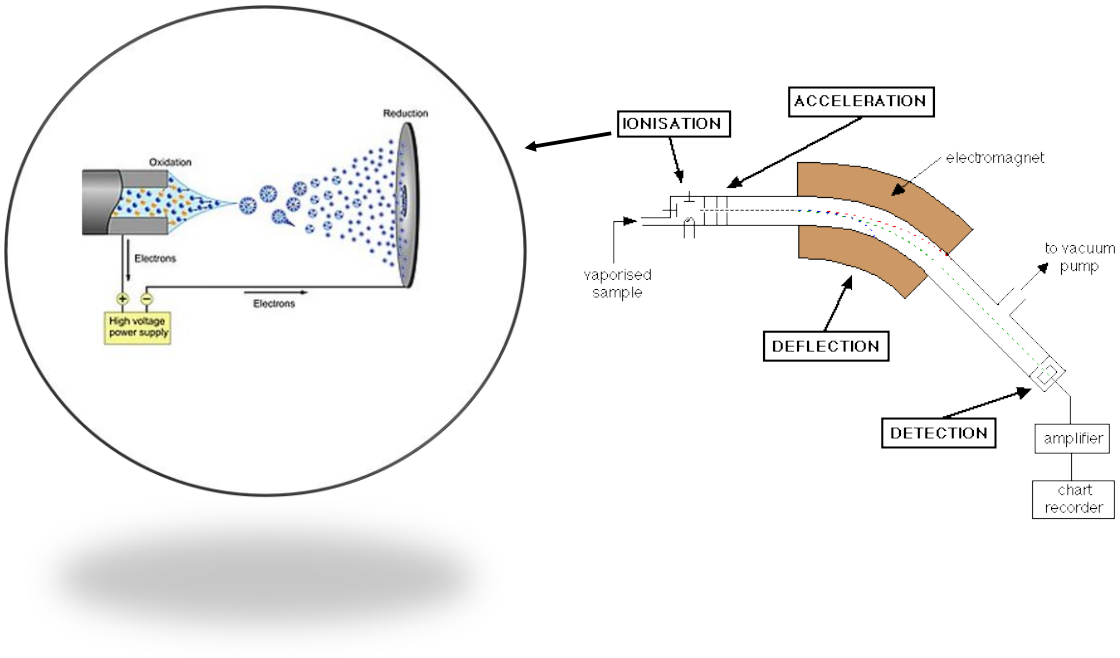

Figure 4. Scheme of a typical Mass Spectrometry procedure.

This may cause some of the sample's molecules to break up into positively or negatively charged fragments or simply become positively or negatively charged without fragmenting. These ions (fragments) are then separated according to their mass-to-charge ratio, for example by accelerating them and subjecting them to an electric or magnetic field: ions of the same mass-to-charge ratio will undergo the same amount of deflection. The ions are detected by a mechanism capable of detecting charged particles, such as an electron multiplier (detector), and then converted in analytical data [21]. In this way, the complex mixture of the sample can be separated, into its different components, in time and space.

3.8.3. Quadrupole Time-of-flight (Q-TOF)

Q-TOF is a mass spectrometry detector in which the correct mass of ions is determined by a time measurement as reported in **Figure 5**.

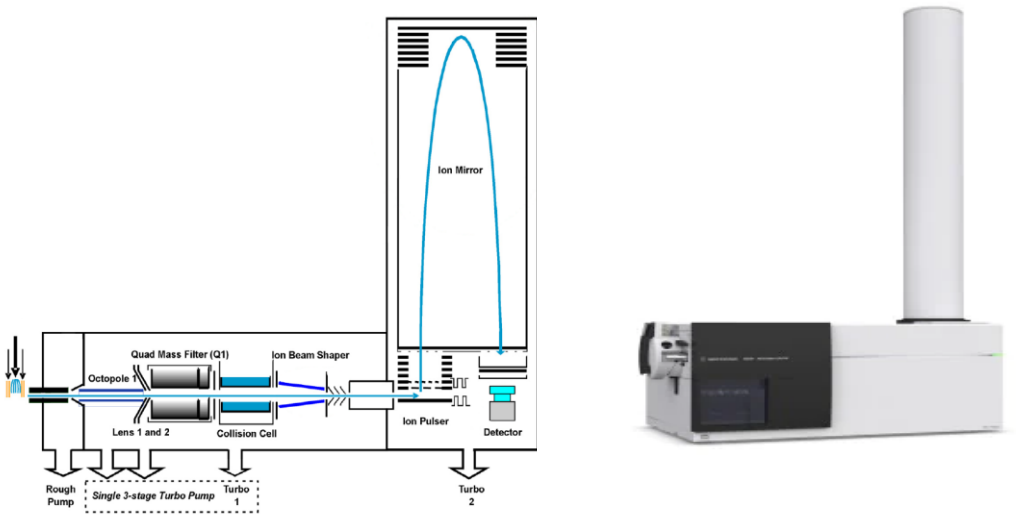

Figure 5. Scheme of a typical Q-TOF detector.

Ions, after ionisation, are accelerated by an electric field that confers a different kinetic energy to the ions according to their charge and mass. The time that each ion subsequently takes to reach the detector through a defined distance is measured. This time will depend on the velocity of the ion, and therefore is a measure of its mass-to-charge ratio (*m/z*). From this ratio and known experimental parameters, it is possible to identify the ion with a very accurate mass [22]. Unfortunately, several compounds have the same mass making their identification difficult. To solve this problem, it is possible to use the tandem mass spectrometry analysis (MS/MS).

3.8.4. MS/MS analysis

MS/MS is an analytical technique used for structure determination and analysis of molecules. Traditionally, MS/MS uses two mass spectrometers in tandem (**Figure 6**).

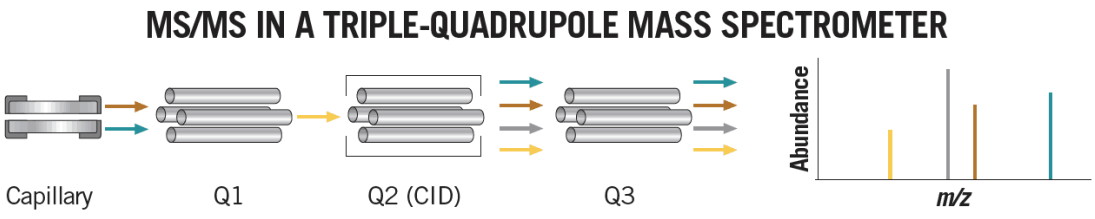

Figure 6. Scheme of a typical MS/MS experiment.

Between the two analysers is sited a collision gas cell (CID). Precursor ions selected by the first spectrometer or quadrupole collide with a high-pressure gas (helium, argon, nitrogen) in the cell and are fragmented. The resulting ions, called fragments, are analysed by the second spectrometer. In the Q-TOF, the collision cell is located between the quadrupole and TOF analyser. Many large molecules such as peptides or lipids have spectra with only a few fragment ions. Usually, each precursor ion has specific fragment ions that can be used for its identification. But in some cases, ions with the same mass have the same fragments and this makes their identification difficult [23]. Ion mobility is one of the latest modern techniques that can be used to achieve this goal.

3.8.5. Ion mobility

Ion mobility is an analytical technique used to separate ions in gas phase based on their dimension and shape, as well as their *m/z* ratio and their chemical characteristics. Coupled with mass spectrometry, this technique is used to obtain complementary information about analytes. In the instrumental setup used here and reported in **Figure 7,** a tunnel (drift tube) is placed after the ion source.

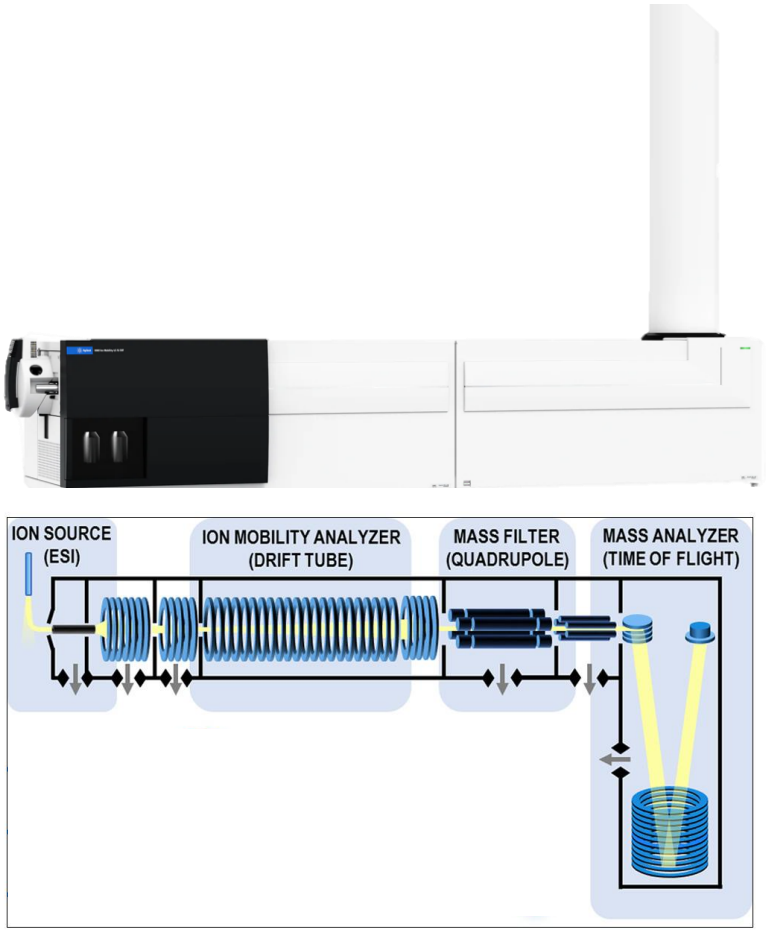

Figure 7. Scheme of a typical Ion Mobility experiment.

The ionised molecules in the drift tube move towards the MS thanks to the presence of an electric field, and their velocity is influenced by collision with molecules of a buffer gas (nitrogen or helium) in the tube, as well as their shape and charge. Ions with multiple charges cross the tunnel with more efficiency than those charged singularly because they exert more strength than the others due to their electrical field. On the other hand, ions with a large impact section are held more easily in the tunnel. This happens because the resistance force, resulted from the ions collision with the buffer gas, acts against their acceleration imposed by the electric field. By measuring the time required for an ion to cross the drift tube and reach the mass spectrometer detector (drift time, DT) it is possible to calculate the collisional cross section (CCS) using the Mason-Schamp equation [24],

$$K = \frac{3}{16}\sqrt{\frac{2\pi}{\mu kT}}\frac{Q}{n\sigma}$$

where, Q is the ion charge, n is the drift gas number density, μ is the reduced mass of the ion and the drift gas molecules, k is Boltzmann constant, T is the drift gas temperature, and σ is the collision cross section between the ion and the drift gas molecules. Hence, the advantages of using ion mobility include obtaining a further layer of separation compared to LC alone, as well as having an extra physicochemical property (CCS) which in combination to the retention time and *m/z* can aid in the identification process [24].

3.8.6. Capillary Electrophoresis.

Capillary electrophoresis-mass spectrometry (CE-MS) has emerged as a powerful new tool for comprehensive analysis of electrically charged compounds suitable in metabolome analysis. Capillary electrophoresis (CE) is a new separation technique that can provide high resolution efficiency which means high resolution and require small volume sample, and minor sample treatment [25] (**Figure 8**).

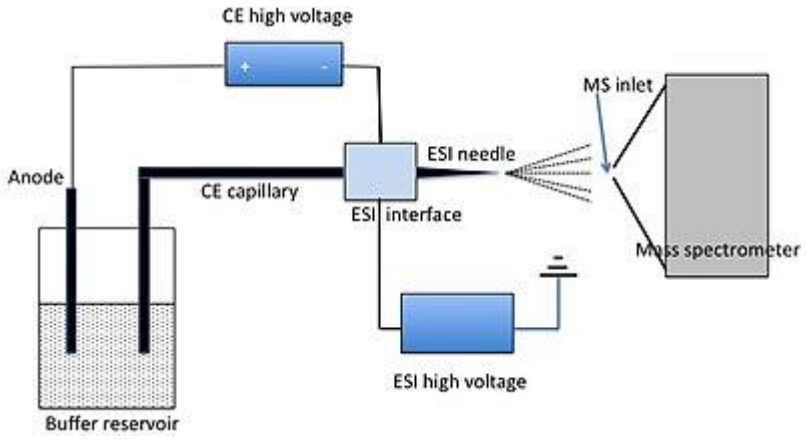

Figure 8. Scheme of CE-MS instrumental setup.

Capillary electrophoresis in the simplest mode, capillary zone electrophoresis (CZE) is a separation technique based on the differential transportation of charged species in an electric field through a conductive medium. In CE methods, analytes migrate through electrolyte solutions under the influence of an electric field. Analytes can be separated according to ionic mobility and/or partitioning into an alternate phase via non-covalent interactions. Additionally, analytes may be concentrated or "focused" by means of gradients in conductivity and pH. Since CE is based on a different separation mechanism to HPLC it also shows a different selectivity and is considered a technique complementary to chromatography. Within the CE system, selectivity can be changed by changing the polarity, coating capillaries or by changing the electrolyte. Regarding the electrical interfacing, there are two types of instruments: (i) with the CE outlet capillary connected at ground and the electrospray voltage applied from the MS, which makes CE separation conditions independent from MS operation conditions, (ii) the end of the capillary is at a high voltage, and it is reduced or increased by the electrospray voltage. In most systems, the capillary outlet is introduced into an ion source that utilizes

electrospray ionization (ESI). The resulting ions are then analysed by the mass spectrometer. This setup requires volatile buffer solutions, which will affect the range of separation modes that can be employed and the degree of resolution that can be used [26].

3.9. Chemometric analysis

From the chromatogram pre-processing, using the software named Profinder, a data matrix was created and subsequently was elaborated using SIMCA Software (14.0, Umetrics, Umeå, Sweden). Among the several mathematical and statistical analysis of data exploration, in this thesis principal component analysis (PCA) and partial least square-discriminant analysis (PLS-DA) with its orthogonal extension (OPLS-DA) were achieved.

3.9.1. Chemometrics

Chemometrics is the science of relating the measurements of a data system or process to their state or treatment through mathematical and statistical methods [27]. A multivariate system, showed in **figure 9**, is represented by a matrix X of N rows (samples) and K columns (variables). Generally, the observed samples can be analytical samples, clinical samples or chemical reactions, while variables can have different origins such as, spectral intensities (from NIR, NMR, IR, UV analysis), chromatographic response or physical measurements. In this thesis several extracts of plasma and erythrocytes samples were used as observations, while spectral peak intensities were used as variables.

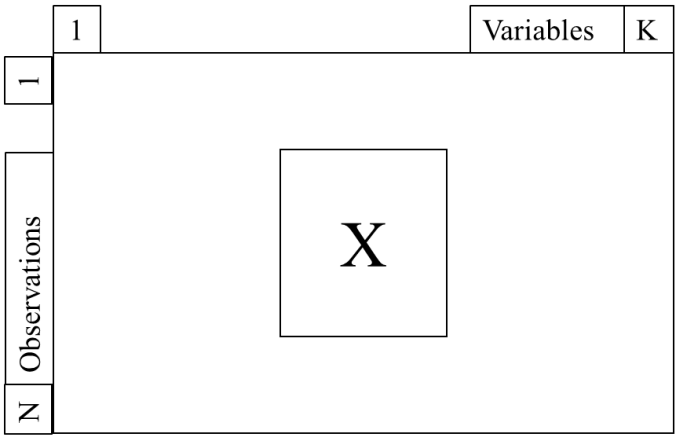

Figure 9. Matrix annotation of a typical dataset.

3.9.2. Scaling

In a multivariate analysis the variables must be comparable each other. For this reason, data set must be pre-treated with the aim to be converted in a more eligible form for the

analysis. In the case of variables that characterized by different scales, we need to give the same importance to each one. This means that the length of each coordinate in the variable space must be regulated following a predetermined criterion. To accomplish this task, a mathematical transformation of the data, termed scaling, needs to be used. In this work, pareto scaling was chosen as preferred method. Pareto scaling uses the square root of the standard deviation as the scaling factor. This action reduces the large differences in intensity between different features, which would otherwise bias the results by conferring a higher importance to most abundant variables [28].

3.9.3. Principal component analysis

Principal component analysis (PCA) is a multivariate unsupervised projection technique used to highlight the most prominent structure present in the data.

PCA is used to show the complexity of a phenomenon constituted by many variables using a small number of summary indicators called latent variables.

PCA is an explorative method that identifies the distribution of a data set, highlights similarities and differences no suspected among the data and compresses the data reducing their dimensions into a smaller number of new variables called principal components (pc). Principal components describe the data variability, reveal groups of normal and abnormal objects (outliers) and find the relations between the objects and the variables and even between the variables. After the data pre-processing and scaling, the cloud of samples (point in the multidimensional space of the metabolites) will be centered around the origin and PCA will look for the directions of maximal dispersion (assuming that dispersion means “information”) (**Figure 10**).

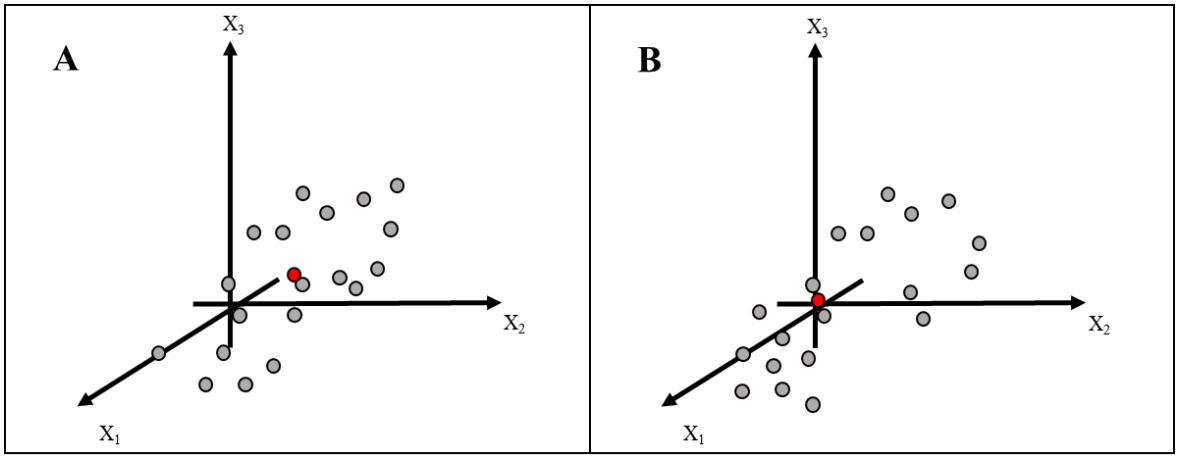

Figure 10. The mean-centering correspond to the movement of the origin system for coincide with the median point represented with a red circle. A: distribution before mean centering, B: distribution after mean-centering.

The position of the points in this new coordinate system are called “scores”. Usually, only one pc it is not sufficient to show all the system variations and for this reason a second pc is also calculated. This component is shown as an orthogonal line to the first pc that passes across the average point (**Figure 11**).

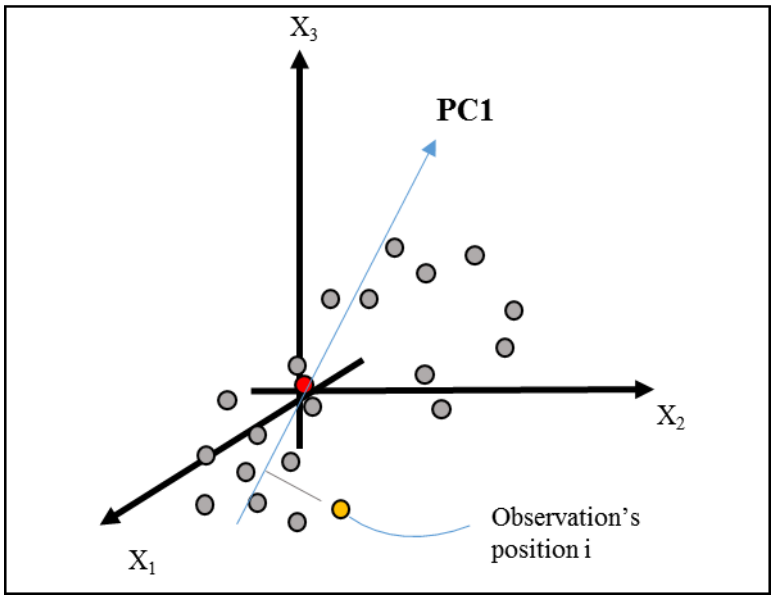

Figure 11. First principal component is the line that describes the shape of set point. It represents the direction of maximum data variance. PC1= first principal component.

The principal components can be considered as new variables (therefore as new cartesian axes) which can be expressed mathematically as linear combinations of the original variables, orthogonal to each other, and each explaining a fraction of the information contained in the original data (explained variance). Each object can be projected onto these new axes: the new coordinates thus obtained, on the main components, are called scores. The cosines of the angles that each principal component forms with the axes of the original variables (directing cosines) are defined as loads: the values of these coefficients, ranging from ± 1, are an index of the contribution of each original variable in defining a given principal component. The first pc direction compared to original variables is formed due to the angles of cosine α1, α2 and α3. These values indicated as the original variables x1, x2 and x3 influenced the first pc. These are called loadings. Similarly, a second set of loadings creates the direction of a second pc compared to the original variables (**Figure 12**).

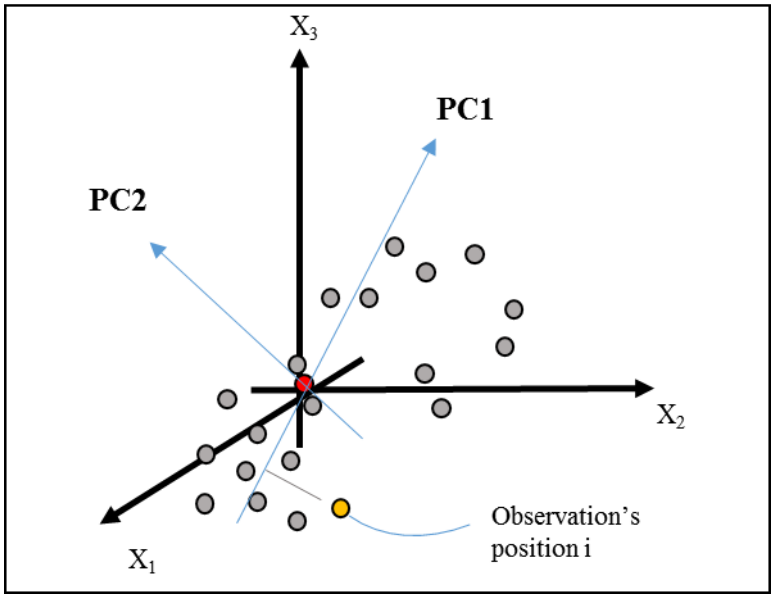

Figure 12. Scores Plot. The two principal components build a plan. This plan represents a window inside the multidimensional space that can be showed graphically. PC1,2: first and second principal components respectively.

The number of pc is related to the variance of the model and by that it is possible to understand how much information is explained by the model.

PCA results are reported into different plots. PCA is a technique that allows highly informative graphical representations of both objects only (score plot) and variables only (loading plot) and objects and variables simultaneously (biplot). The scores plot

reported the samples projection into the model space, calculated using principal components, while the loadings plot reports the projection of variables, using the same rules.

Since the relevant information is generally contained in a limited number of main components, can be easily and effectively displayed. Assuming that the first principal components (i.e. those that explain most of the variance) define the useful information and the subsequent ones are due to spurious information, it is possible to apply PCA as a technique for the synthetic visualization of a data set, achieving both a reduction in the number of variables is an elimination of noise.

The quality of the model can be evaluated by the R^2 and Q^2 statistical parameters. The R^2 is the fraction of the variation of the variables explained by the model. Q^2 is an estimate of the predictive ability of the model. It is calculated by cross-validation. The sample data set is divided into n parts (n = 7 in SIMCA by default), then the model is built on n-1 parts (training set) and tested on the remaining part (test set). By performing these steps for as many iterations as allowed by the initial division of the dataset into sub-sets, it is possible to calculate the sum of square error for the whole dataset. This is then called the Predicted Residual Sum of Squares. The closer the R^2 is close to 1 the more the model is close to the referred experimental models. If the system is homogenous R^2 and Q^2 will be similar, whereas if the system is heterogeneous Q^2 will be lower than R^2. Furthermore, it is possible to highlight the outliers, namely samples that differ excessively if compared with the others and are not very well described by the model. These observations have a high leverage to the model. The leverage is proportional to the distance between an observation and the dataset centre. The variance explained, usually measured as the total variance percentage, is a variance proportional measurement of data taken in consideration by the pc. The variance that is not explained is called residual. To greater appreciate the presence of outliers it is possible to use two analyses: Hotelling's T^2 and DmodX analysis [29].

3.9.4. Partial least square-discriminant analysis and its orthogonal variation (O/PLS-DA)

Partial least square-discriminant analysis (PLS-DA is) a discriminant analysis that classifies one object (sample) based on its belonging class. PLS-DA a supervised

analysis that uses as a prerogative the necessity of a sample classification that is collected in a second matrix called Y matrix. The generated two matrices, the X matrix (constituted by the observation and the variables) and the Y matrix (constituted by the samples classes) are placed in relation and the quality of the model is valuated with different parameters (**Figure 13**).

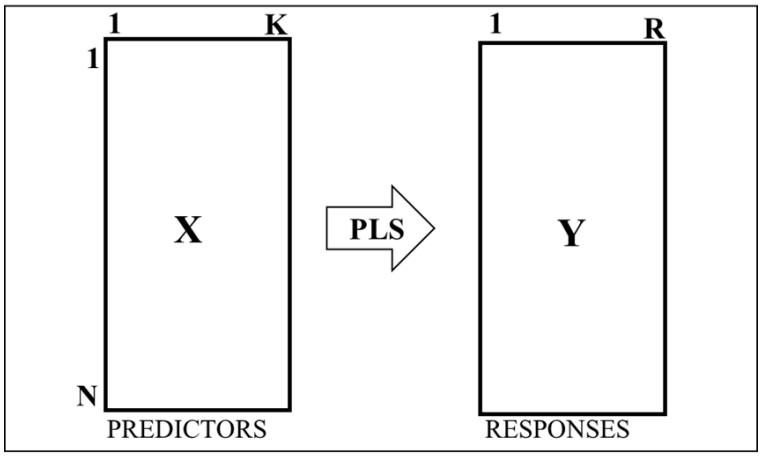

Figure 13. PLS-DA model. The generated two matrices, the X matrix (constituted by the observation and the variables) called predictors and the Y matrix (constituted by the samples classes) called response, are put in relation.

The generated R^2 and Q^2 values described the reliability and the predictive ability of the fitting, respectively. Q^2 is made based on a cross-validation analysis. R^2Y describes the classificatory power of the model. The non-parametric test, Permutation test, is also achieved to highlights the significance of the classificatory power of the model. This test use random shuffles of the data to get the correct distribution of a test statistic under a null hypothesis. Three parameters are used for this analysis: the null hypothesis which determines what we permute, the test statistic which affects the power and the number of permutations, which affects precision of the estimated p-value. This test collects the correct false positive amount from the distributional characteristics of the data. In the case of a non-directly correlation between Y matrix and variables an Orthogonal Projections to Latent Structures (OPLS) can be useful to interpret the problem by incorporating an orthogonal signal correction (OSC) filter into a PLS model. This model separates the Y -predictive variation from the Y -uncorrelated variation in X. It is important to highlight that OPLS-DA does not provide predictive advantage over PLS-DA.

In any case, attention must be paid to Occam's Razor, or the principle of parsimony, which requires the use of models and procedures that contain everything necessary for modeling but nothing more. For example, if a regression model with 2 predictors is sufficient to explain y, then no more than these two predictors should be used. Overfitting is the use of models or procedures that violate parsimony, that is, that include more terms than necessary or use more complicated approaches than necessary [30].

With the aim to study the possible discriminant variables for the project, different analyses can be performed. In more detail, a variable importance in the project test (VIP) gives a measure of a variable's importance in the PLS-DA model. VIP summarizes the influence of a variable in the model. The VIP score of a variable is calculated as a percentage variation sum of the squared correlations between the PLS-DA components and the original variable. All the variables that have a value of VIP lower than 1 are not influencing the classification.

3.10 Univariate statistical analysis.

To understand if discriminants metabolites were correlated to microgravity or to the sampling time, we performed a two-way analysis of variance (ANOVA). With this in mind, the data matrix was analysed using univariate data analysis using MATLAB R2021 software (Mathworks, Inc., Natick, USA), applying an ANOVA test to obtain statistically significant signals. ANOVA (Analysis of Variance) is a statistical test used to analyse the difference between the means of more than two groups. A two-way ANOVA is used to estimate how the mean of a quantitative variable changes according to the levels of two categorical variables. Two-way ANOVA is used when two independent variables, in combination, affect a dependent variable.

References

[1] G. H. Rose and M. Orlander, “Improved procedure for the extraction of lipids from human erythrocytes,” *J. Lipid Res.*, vol. 6, 1965.

[2] C. A. Nickerson, C. M. Ott, J. W. Wilson, R. Ramamurthy, and D. L. Pierson, “Microbial Responses to Microgravity and Other Low-Shear Environments,” *Microbiol. Mol. Biol. Rev.*, vol. 68, no. 2, pp. 345–361, 2004.

[3] R. Herranz *et al.*, “Ground-based facilities for simulation of microgravity: Organism-specific recommendations for their use, and recommended terminology,” *Astrobiology*, vol. 13, no. 1, pp. 1–17, 2013.

[4] K. Mukundakrishnan, H. Hu, and P. S. Ayyaswamy, *J. Fluid Mech.* 2008.

[5] J. Smedsgaard and J. Nielsen, “Metabolite profiling of fungi and yeast: From phenotype to metabolome by MS and informatics,” *J. Exp. Bot.*, vol. 56, no. 410, pp. 273–286, 2005.

[6] O. Fiehn, “Metabolomics - The link between genotypes and phenotypes,” *Plant Mol. Biol.*, vol. 48, no. 1–2, pp. 155–171, 2002.

[7] S. G. Villas-Bôas, S. Mas, M. Åkesson, J. Smedsgaard, and J. Nielsen, “Mass spectrometry in metabolome analysis,” *Mass Spectrom. Rev.*, vol. 24, no. 5, pp. 613–646, 2005.

[8] B. Daviss, “Growing pains for metabolomics: the newest ’omic science is producing results--and more data than researchers know what to do with.,” *Sci.*, vol. 19, no. 8, p. 25, 2005.

[9] W. B. Dunn, N. J. C. Bailey, and H. E. Johnson, “Measuring the metabolome: Current analytical technologies,” *Analyst*, vol. 130, no. 5, pp. 606–625, 2005.

[10] A. H. Murtagh, *Multivariate Data Analysis*, Vol (131). Springer Science & Business Media, 2012.

[11] A. Hirayama, M. Wakayama, and T. Soga, “Metabolome analysis based on capillary electrophoresis-mass spectrometry,” *TrAC - Trends Anal. Chem.*, vol. 61, pp. 215–222, 2014.

[12] H. M. Lin, N. A. Helsby, D. D. Rowan, and L. R. Ferguson, “Using metabolomic analysis to understand inflammatory bowel diseases,” *Inflamm. Bowel Dis.*, vol. 17, no. 4, pp. 1021–1029, 2011.

[13] B. Burla *et al.*, “MS-based lipidomics of human blood plasma: A community-initiated position paper to develop accepted guidelines,” *J. Lipid Res.*, vol. 59, no. 10, pp. 2001–2017, 2018.

[14] T. Hyötyläinen, L. Ahonen, P. Pöhö, and M. Orešič, “Lipidomics in biomedical research-practical considerations,” *Biochim. Biophys. Acta - Mol. Cell Biol. Lipids*, vol. 1862, no. 8, pp. 800–803, 2017.

[15] B. Alberts, *Molecular Biology of the Cell*. Garland Science, 2007.

[16] S. Hein, P. van der Sluijs, and G. van Meer, “How proteins move lipids and lipids move proteins,” *Mol. CELL Biol.*, vol. 2, no. 1, pp. 88–100, 2001.

[17] J. Goldstein *et al., Scanning Electron Microscopy and X-Ray Microanalysis: A Text for Biologists, Materials Scientists, and Geologists 2nd Edition*, 3th ed. Extra materials, 1986.

[18] P. Hortolà, “SEM examination of human erythrocytes in uncoated bloodstains on stone: Use of conventional as environmental-like SEM in a soft biological tissue (and hard inorganic material),” *J. Microsc.*, vol. 218, no. 2, pp. 94–103, 2005.

[19] S. M. Chesnut and J. J. Salisbury, “The role of UHPLC in pharmaceutical development,” *J. Sep. Sci.*, vol. 30, no. 8, pp. 1183–1190, 2007.

[20] H. Ogiso, T. Suzuki, and R. Taguchi, “Development of a reverse-phase liquid chromatography electrospray ionization mass spectrometry method for lipidomics, improving detection of phosphatidic acid and phosphatidylserine,” *Anal. Biochem.*, vol. 375, no. 1, pp. 124–131, 2008.

[21] J. H. Gross, *Mass Spectrometry: A Textbook*. Springer Science & Business Media., 2006.

[22] R. Weimar, R. Romberg, S. P. Frigo, B. Kassühlke, and P. Feulner, “Time-of-flight techniques for the investigation of kinetic energy distributions of ions and neutrals desorbed by core excitations,” *Surf. Sci.*, vol. 451, no. 1, pp. 124–129, 2000.

[23] F. W. McLafferty, “Tandem Mass Spectrometry,” *Science (80-.).*, vol. 214, pp. 1–4, 1981.

[24] F. Lanucara, S. W. Holman, C. J. Gray, and C. E. Eyers, “The power of ion mobility-mass spectrometry for structural characterization and the study of conformational dynamics,” *Nat. Chem.*, vol. 6, no. 4, pp. 281–294, 2014.

[25] C. Barbas, E. P. Moraes, and A. Villaseñor, “Capillary electrophoresis as a metabolomics tool for non-targeted fingerprinting of biological samples,” *J. Pharm. Biomed. Anal.*, vol. 55, no. 4, pp. 823–831, 2011.

[26] S. Banerjee and S. Mazumdar, “Electrospray Ionization Mass Spectrometry: A Technique to Access the Information beyond the Molecular Weight of the Analyte,” *Int. J. Anal. Chem.*, vol. 2012, pp. 1–40, 2012.

[27] S. Wold, “Chemometrics; what do we mean with it, and what do we want from it?,” *Chemom. Intell. Lab. Syst.*, vol. 30, no. 1, pp. 109–115, 1995.

[28] R. A. van den Berg, H. C. J. Hoefsloot, J. A. Westerhuis, A. K. Smilde, and M. J. van der Werf, “Centering, scaling, and transformations: Improving the biological information content of metabolomics data,” *BMC Genomics*, vol. 7, pp. 1–15, 2006.

[29] L. Eriksson, T. Byrne, E. Johansson, J. Trygg, and C. Vikström, *Multi- and Megavariate Data Analysis Basic Principles and Applications*, VOLUME 1. Umetrics Academy, 2013.

[30] D. M. Hawkins, “The Problem of Overfitting,” J. Chem. Inf. Comput. Sci., vol. 44, no. 1, pp. 1–12, 2004.

International Journal of *Molecular Sciences*

MDPI

Article

Untargeted Lipidomics of Erythrocytes under Simulated Microgravity Conditions

Cristina Manis [1,2], Antonio Murgia [1], Alessia Manca [3], Antonella Pantaleo [3], Giacomo Cao [2] and Pierluigi Caboni [1,*]

[1] Department of Life and Environmental Sciences, Cittadella Universitaria di Monserrato, Blocco A, Room 13, 09042 Monserrato, Italy; cristina.manis@unica.it (C.M.); amurgia@unica.it (A.M.)
[2] Department of Mechanical, Chemical and Materials Engineering, University of Cagliari, Via Marengo 2, 09123 Cagliari, Italy; giacomo.cao@unica.it
[3] Department of Biomedical Science, University of Sassari, Viale San Pietro, 07100 Sassari, Italy; alessia_manca@hotmail.it (A.M.); apantaleo@uniss.it (A.P.)
* Correspondence: caboni@unica.it; Tel.:+39-070-6758617; Fax: +39-070-6758612

Citation: Manis, C.; Murgia, A.; Manca, A.; Pantaleo, A.; Cao, G.; Caboni, P. Untargeted Lipidomics of Erythrocytes under Simulated Microgravity Conditions. *Int. J. Mol. Sci.* 2023, *volume number*, x. https://doi.org/10.3390/xxxxx

Academic Editor: Francesco Misiti

Received: 18 January 2023
Revised: 13 February 2023
Accepted: 20 February 2023
Published: 22 February 2023

Abstract: Lipidomics and metabolomics are nowadays widely used to provide promising insights into the pathophysiology of cellular stress disorders. Our study expands, with the use of a hyphenated ion mobility mass spectrometric platform, the understanding of the cellular processes and stress due to microgravity. By lipid profiling of human erythrocytes, we annotated complex lipids such as oxidized phosphocholines, phosphocholines bearing arachidonic in their moiety, as well as sphingomyelins and hexosyl ceramides associated with microgravity conditions. Overall, our findings give an insight into the molecular alterations and identify erythrocyte lipidomics signatures associated with microgravity conditions. If the present results are confirmed in future studies, they may help to develop suitable treatments for astronauts after return to Earth.

Keywords: lipidomics; mass spectrometry; microgravity condition; erythrocytes

List of abbreviations:

fatty acid (FA); phosphatidylethanolamine (PE); ether-linked phosphatidylcholine (Ether-PC); phosphatidylcholine (PC); lysophosphocholine (LPC); sphingomyelin (SM);

1. Introduction

The term microgravity in general refers to the existing residual accelerations. When gravitation is the only force acting on an object then the object is in free fall, and hence, it will experience microgravity [1]. Weightlessness is the state in which a body having a certain weight is balanced by another force or remains in free-fall without feeling the effects of the atmosphere, equivalent to the situation faced by an astronaut aboard a spaceship. The effects of microgravity on human physiology have been studied extensively since the time of Yuri Gagarin (in 1961) who experienced the first man-on-board orbital flight, revealing profound implications for human health [2]. Despite the great interest and commitment of the scientific community, the mechanisms by which microgravity exerts its effects on the human body are not entirely clear.

Acute changes in normal physiology are typically seen in astronauts as a response and adaptation to abnormal environments. Such peculiar alterations require the attention of doctors and scientists [3]. In addition to alterations at the genetic level [4], microgravity experienced by space travelers also induces profound alterations also at the cellular level. These alterations occurring at the cellular level are reflected in a series of pathological conditions such as reduction of bone density muscle atrophy, endocrine disorders, cognitive disorders and cardiovascular disfunctions, body fluid and electrolyte reduction, motion sickness, immune inhibition and anemia [5]. For these reasons, ground-based experiments simulating factors of a spaceflight are needed.

Microgravity is studied in several scientific and technological fields with the aim to highlight processes that on Earth are masked by the effects of the high gravitational field. Furthermore, the study of physiological processes in microgravity conditions allows the identification of the molecular mechanisms involved in different pathologies [6].

Roughly 350 people have experienced spaceflight in the past four decades, making it difficult to develop higher levels of clinical evidence to evaluate the effectiveness of space medicine interventions [7]. This great limitation and the great importance of studying the alterations at the cellular level that affect astronauts, have led various research groups to study and build instruments capable of simulating space gravitational conditions on Earth.

The most employed methods to simulate microgravity are random positioning machines (RPM) and clinostats [8]. By controlled simultaneous rotating of the two axes, the clinostat cancels the cumulative gravity vector at the centre of the device, producing an environment with an average of 10^{-3} g. This is accomplished by the rotation of a chamber at the centre of the device to disperse the gravity vector uniformly within a spherical volume at a constant angular speed [9].

Bioactive lipid molecules known as signaling molecules, such as fatty acid, eicosanoids, diacylglycerol, phosphatidic acid, lysophosphatidic acid, ceramide, sphingosine, sphingosine-1-phosphate, phosphatidylinositol-3 phosphate, and cholesterol, are involved in the activation or regulation of different signaling pathways leading to apoptosis. Furthermore, alterations in the lipid composition determine membrane rigidity and fluidity, and play a crucial role in membrane organization, dynamics, and function [10]. Because of their biological role, lipids have been the subject of an intense area of research since the 1960s, which unfortunately was held back due to limited instrument platforms. Nowadays, lipidomics is considered an emerging science of fundamental importance for clarifying the biochemical pathways involved in several pathologies or cellular stress adaptations [11]. Advances in mass spectrometry (MS) and data processing, as well as the incorporation of soft ionization techniques, as ESI-MS^2 method, has revolutionized the use of mass spectrometry, ushering this analytical tool in the field of lipidomics [12]. The lipidomics study can be applied as untargeted and targeted approaches, each with its own advantages and limitations [13]. Untargeted lipidomics focuses on the analysis of all detectable metabolites in a sample, including unknown chemicals, while targeted lipidomics is the measurement of defined groups of metabolites. While the strength of the targeted approach is validating one or more hypotheses, untargeted lipidomics allows for the discovery of new compounds that have led to a number of breakthroughs in understanding human disease risks [14]. Untargeted analyses can be performed with or without the addition of internal rules. When internal

standards are added to samples, the method can provide pseudoconcentration results for particular metabolites or for metabolites with similar physicochemical properties (e.g., lipids). While these results are not truly quantitative, they may be accurate enough for case/control comparisons [15].

Despite the great relevance of the topic, currently few studies have been carried out to investigate the behavior of lipids in erythrocyte samples cultured under simulated gravity conditions. In 2009, Ivanova et al. investigated blood samples from Russian cosmonauts by observing significant changes in the phospholipids class [16]. An increase in the percentage of phosphatidylcholine may be clearly associated with the increase in membrane rigidity. On the other hand, changes in the physicochemical properties of the plasma membrane of erythrocytes (microviscosity and permeability) can influence the efficiency of oxygen transfer, the state of the haemoglobin, and changes in the conformation of hematoporphyrin. Furthermore, changes in the erythrocyte structure through an ultrastructural morphological analysis can be assessed by atomic force microscopy [17]. However, the study conducted by Ivanova's team reported data deriving mainly from studies carried out after the end of a space flight, while only few data are related to changes that occur during a space flight. Moreover, lipid and phospholipid compositions of erythrocyte membranes were assayed by thin layer chromatography followed by densitometric measurement of stained dots. This technique provides information on the entire lipid class, but hardly allows the recognition of the specific lipid compounds. Since no data are reported on this subject, we decided to exploit the potential offered by chromatographic and mass spectrometry innovations to better understand the lipid modifications suffered by erythrocytes during simulated microgravity conditions. For this reason, with the aim to better understand which metabolic and/or structural changes occur in the erythrocytes subjected to low gravity, an experimental analysis of the erythrocytes' lipid profile and their morphology under normal- and micro-g conditions was carried out following a recent investigation on the subject [18]. In detail, human erythrocytes were cultured in simulated gravity conditions, and they were collected at different times of clinorotation. For each sample, the organic phase was collected and analysed through ion mobility Q-TOF mass spectrometer (UHPLC-IM-QTOF-MS).

2. Results and Discussion

To investigate the erythrocytes' lipid profile after clinorotation and to describe possible variations among the different lipid categories, samples were analysed by IM-QTOF-LC/MS and representative total ion chromatograms are shown in **Figure 1**.

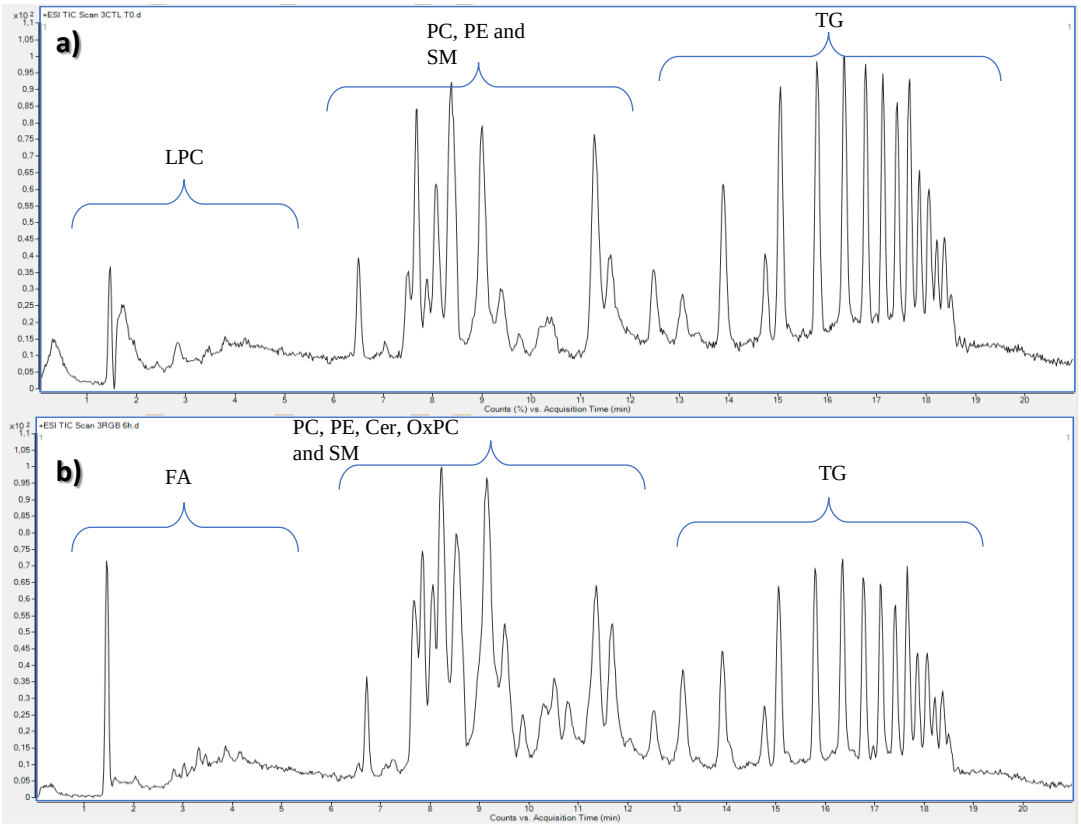

Figure 1. Representative total ion chromatograms of erythrocytes cultured in terrestrial gravity conditions and used as control (a) and compared with erythrocytes cultured in simulated gravity conditions (b) both collected after six hours of experiment.

Data processing yielded 215 and 160 features for the positive (PIA) and negative ionization analysis (NIA), respectively, which were subjected to multivariate statistical analysis (MVA). Chemical composition analysis indicated that the lipid fraction was composed of lipids from the following classes: free fatty acid (FA), lysophosphatidylcholines (LysoPC), phosphatidylcholines (PC), phosphatidylethanolamines (PE), sphingomyelins (SM), ceramides (Cer), and ether-

linked oxidized phosphatidylcholine (EtherOxPC). Initially, to study sample distribution, to detect outliers, and to highlight differences or common features, a PCA was performed. The unsupervised analysis of both PIA and NIA features did not indicate any sample clustering correlated to clinorotation as shown in **Figure 2**.

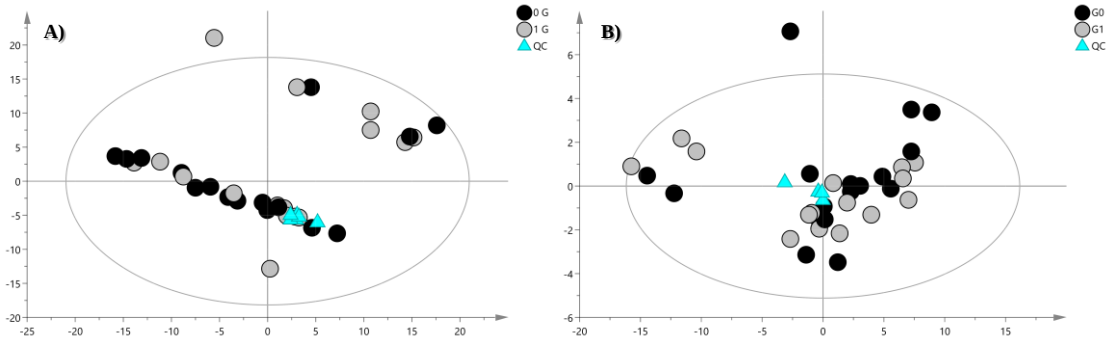

Figure 2. PCA score plot of (A) positive ion mode data and (B) negative ion mode data. The black circles represent the clinorotated samples, while grey circles represent control samples. The PCA analysis for PIA shows the following validation parameters: R2X = 0.808 and Q2 = 0.629; for the NIA model: R2X = 0.721, Q2 = 0.572.

However, the arrangement of the samples in the multivariate space appeared to be influenced by the time factor. Thus, to further limit the time factor influence, for each time point, we performed a PLS-DA. The validation parameters of the PIA and NIA models built for the samples collected at 6, 9, and 24 h are reported in the caption of the resulting plots (**Figure 3**).

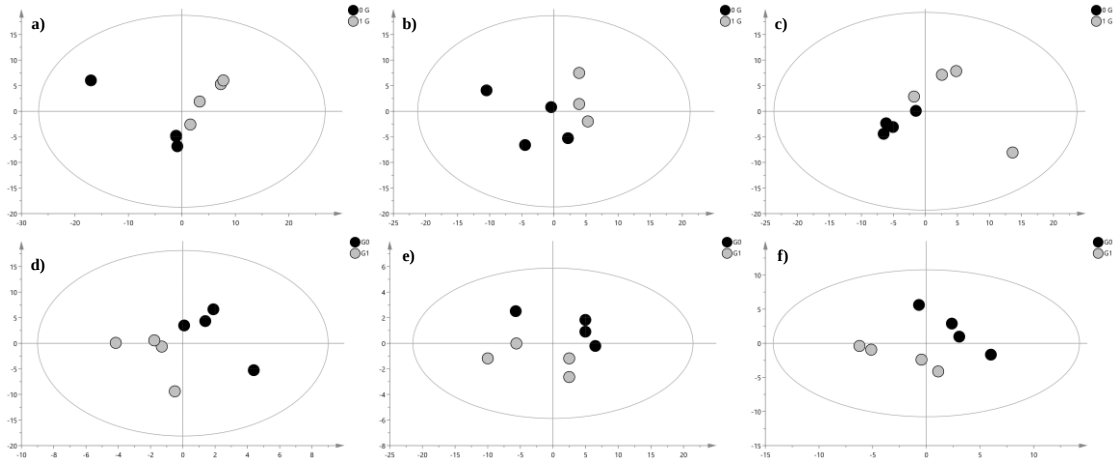

Figure 3. PLS-DA score plot. The grey circles represent the control samples, while black circles represent clinorotated erythrocytes samples. (a) 6 h clinorotated samples vs. 6 h control samples (PIA): R2X = 0.686, R2Y = 0.747, and Q2 = 0.434; (b) 9 h clinorotated samples vs. 9 h control samples (PIA): R2X = 0.849, R2Y = 0.945, and Q2 = 0.66; (c) 24 h clinorotated samples vs. 24 h control samples (PIA): R2X = 0.741, R2Y = 0.984, and Q2 = 0.421; (d) 6 h clinorotated samples vs. 6 h control samples (NIA): R2X = 0.776, R2Y = 0.994, and Q2 = 0.599; (e) 9 h clinorotated samples vs. 9 h control samples (NIA): R2X = 0.85, R2Y = 0.971, and Q2 = 0.147; (f) 24 h clinorotated samples vs. 24 h control samples (NIA): R2X = 0.692, R2Y = 0.995, and Q2 = 0.837.

To identify metabolites that can discriminate for the two classes of samples (clinorotated vs. control samples), an OPLS-DA model of the IM-QTOF-LC/MS data was performed for each time point and for both polarities of acquisition. The OPLS-DA score plots are reported in **Figure 4**. In **Table 1**, we reported the discriminant metabolites between two classes and selected based on VIP value.

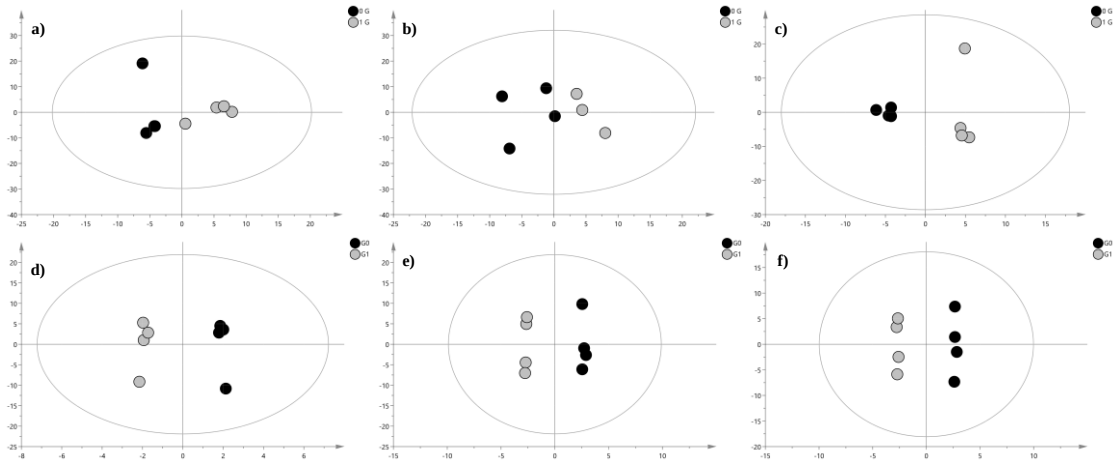

Figure 4. OPLS-DA score plot. The grey circles represent the control samples, while black circles represent clinorotated erythrocytes samples. (a) 6 h clinorotated samples vs. 6 h control samples (PIA): R2X = 0.868, R2Y= 0.862, and Q2 = 0.503; (b) 9 h clinorotated samples vs. 9 h control samples (PIA): R2X = 0.646, R2Y= 0.708, and Q2 = 0.199; (c) 24 h clinorotated samples vs. 24 h control samples (PIA): R2X = 0.741, R2Y= 0.984, and Q2 = 0.284; (d) 6 h clinorotated samples vs. 6 h control samples (NIA): R2X = 0.776, R2Y= 0.994, and Q2 = 0.482; (e) 9 h clinorotated samples vs. 9 h control samples (NIA): R2X = 0.883, R2Y= 0.998, and Q2 = 0.033; (f) 24 h clinorotated samples vs. 24 h control samples (NIA): R2X = 0.788, R2Y= 0.998, and Q2 = 0.721.

Table 1. Discriminant metabolites of human erythrocyte samples annotated by LC/DTIM-QTOF-MS.

Lipid	Adduct	*m/z Experimental*	*m/z Theoretical*	Δ (ppm)	RT (min)	Fatty Acid Composition	$^{DT}CCS_{N2}$ (Å^2)	VIP	Significance Level	Regulation in G0 Cells
6 h										
LysoPC16:1	$+H^+$	494.3216	494.3241	5.1	6.55	16:1	231.58	1.73	ns	up
PC 32:2	$+H^+$	730.5394	730.5381	1.3	7.77	32:2	286.75	1.71	**	up
PC 38:5	$+H^+$	808.5871	808.5851	2.0	8.05	18:1, 20:4	292.87	1.50	**	up
PC 33:5	$+H^+$	738.5070	738.5068	0.3	7.74		287.33	1.26	ns	down
SM d34:0	$+H^+$	705.5930	705.5905	3.5	8.01	16:0, 18:0	285.87	1.10	*	down
PC 38:4	$+H^+$	810.6021	810.6007	1.7	9.23	18:0, 20:4	295.11	1.05	**	up
PC 36:2	$+H^+$	786.6031	786.6007	3.0	9.43	18:1, 18:1	291.56	1.00	*	up
SM d 38:1	$+H^+$	759.6328	759.6375	6.0	11.31		297.55	1.00	**	down
PC 36:1	$+H^+$	788.6192	788.6164	3.2	10.43		293.88	0.99	*	up
FA 16:2	$-H^-$	251.2021	251.2017	1.6	3.59	16:2	114.95	1.38	**	down
HexCer_AP t37:1	$+(C_2H_3O_2)^-$	832.6152	832.6164	1.5	10.43	22:1, 15:0	296.27	1.46	**	up

Etn-1-P-Cer 32:1	$-H^-$	687.5469	687.5446	3.4	7.51	14:1, 18:0	265.47	1.13	***	up
EtherOxPC 36:4e + 1O	$+(CHO_2)^-$	828.5761	828.5781	2.4	8.3	16:0, 20:4	293.50	1.07	*	up
SM d40:1	$+(CHO_2)^-$	831.6632	831.6597	4	11.66		301.49	1.06	ns	up
PE 36:3	$-H^-$	740.5249	740.5236	2	7.50	18:2, 18:1	270.58	1.02	ns	up
9 h										
PC 38:6	$+H^+$	806.5700	806.5694	0.74	8.48	18:2, 20:4	293.14	1.79	*	up
SM d 38:1	$+H^+$	759.6328	759.6375	6.0	11.31		297.55	1.75	**	down
PC 35:5	$+H^+$	766.5399	766.5381	2.3	8.33	15:1, 20:4	280.17	1.73	***	up
PE 36:1	$+H^+$	746.5712	746.5694	2.1	10.71	18:0, 18:1	281.87	1.71	**	up
PC 36:5	$+H^+$	780.5541	780.5538	0.3	8.11	16:1, 20:4	228.33	1.70	**	up
PC 32:0	$+H^+$	734.572	734.5694	3.5	8.92	16:0, 16:0	284.83	1.64	**	up
PC 36:2	$+H^+$	786.6031	786.6007	3.0	9.25	18:1, 18:1	291.56	1.63	**	up
SM d34:0	$+H^+$	705.5930	705.5905	3.5	8.01	16:0, 18:0	285.87	1.61	**	up
PC 35:5	$+H^+$	766.5407	766.5381	3.4	8.51		288.55	1.60	**	down
PE 38:6	$+H^+$	764.524	764.5225	2.0	7.89	16:0, 22:6	279.42	1.59	**	up
PC 36:3	$+H^+$	784.5872	784.5851	2.7	8.25	18:1, 18:2	289.42	1.57	**	up
PC 35:4	$+H^+$	768.5593	768.5538	7.0	8.73	15:0, 20:4	289.52	1.56	**	up
SM d44:5	$+H^+$	835.6691	835.6688	1.0	11.61	14:3, 30:2	305.48	1.52	**	up
SM 42:3	$+H^+$	811.6713	811.6688	3.1	10.49		302.65	1.48	**	up
PC 38:7	$+H^+$	804.554	804.5 538	0.3	7.93	18:3, 20:4	292.2	1.45	ns	up
PC 34:0	$+H^+$	762.6032	762.6007	3.3	10.27		290.86	1.38	ns	up
PC 36:5	$+H^+$	780.5541	780.5538	0.3	8.11		289.42	1.37	*	up
PC 36:4	$+H^+$	782.5701	782.5694	1.0	9.08	16:0, 20:4	229.67	1.36	**	up
PC 34:3	$+H^+$	756.554	759.5538	0.3	8.92	18:1, 16:2	286.35	1.33	*	up
PE 34:2	$+H^+$	716.5251	716.5225	3.5	8.37	16:0, 18:2	273.06	1.23	ns	up
PC 36:1	$+H^+$	788.6192	788.6164	3.2	10.43		293.88	1.21	*	up
SM d42:2	$+H^+$	813.6870	813.6844	3.2	11.61		305.35	1.21	**	up
PC 38:5	$+H^+$	808.5870	808.5851	2.3	8.04	16:0, 22:5	292.87	1.20	ns	up
PC 33:5	$+H^+$	738.5070	738.5068	0.3	7.74		287.33	1.07	*	down
PE 36:3	$+H^+$	742.5399	742.5381	2.5	8.51	16:0, 20:3	276.61	1.04	ns	up
PE 36:4	$+H^+$	740.5239	740.5225	2.0	8.19	16:0, 20:4	276.93	1.03	**	up
SM d42:2	$+H^+$	813.6870	813.6844	3.2	11.61		305.03	1.00	**	up
EtherOxPC 36:4e + 1O	$+(CHO_2)^-$	828.5761	828.5781	2.4	8.3	16:0, 20:4	293.50	1.56	*	down
PE 36:2	$-H^-$	742.5403	742.5392	1.5	9.55	18:1, 18:1	271.52	1.16	**	up
PC 38:6	$+(CHO_2)^-$	850.5613	850.5604	1.1	7.62	18:2, 20:4	296.34	1.01	ns	up

24 h										
PC 35:4	$+H^+$	768.5593	768.5538	7.0	8.73	15:0, 20:4	289.52	1.84	**	up
PE 36:4	$+H^+$	740.5239	740.5225	2.0	8.19	16:0, 20:4	276.93	1.84	**	up
PC 36:2	$+H^+$	786.6031	786.6007	3.0	9.25	18:1, 18:1	291.56	1.64	**	up
PC 32:0	$+H^+$	734.572	734.5694	3.5	8.92	16:0, 16:0	284.83	1.61	ns	up
SM d42:2	$+H^+$	813.6870	813.6844	3.2	11.98		305.03	1.46	*	up
SM 42:3	$+H^+$	811.6713	811.6688	3.1	10.49		302.65	1.40	**	up
PC 36:3	$+H^+$	784.5872	784.5851	2.7	8.25	18:1, 18:2	289.42	1.35	*	up
PE 36:1	$+H^+$	746.5712	746.5694	2.1	10.71	18:0, 18:1	281.87	1.34	ns	up
PE 38:6	$+H^+$	764.524	764.5225	2.0	7.89	18:2, 20:4	279.42	1.21	**	up
PC 36:4	$+H^+$	782.5701	782.5694	1.0	9.08	16:0, 20:4	229.67	1.20	***	up
PC 36:5	$+H^+$	780.5541	780.5538	0.3	8.11		289.42	1.20	*	up
PC 38:4	$+H^+$	810.6021	810.6007	1.7	9.23	18:0, 20:4	295.11	1.19	**	up
PC 34:0	$+H^+$	762.6032	762.6007	3.3	10.27		290.86	1.13	*	up
PC 35:5	$+H^+$	766.5399	766.5381	2.3	8.33	15:1, 20:4	280.17	1.11	*	down
PE 36:3	$+H^+$	742.5399	742.5381	2.5	8.52	16:0, 20:3	276.61	1.11	ns	up
SM d44:5	$+H^+$	835.6691	835.6688	1.0	11.61	14:3, 30:2	305.48	1.09	**	up
SM d42:2	$+H^+$	813.6870	813.6844	3.2	11.62		305.35	1.05	ns	up
PC 35:5	$+H^+$	766.5407	766.5381	3.4	8.51		288.55	1.03	*	down
LysoPC16:1	$+H^+$	494.3216	494.3241	5.1	6.55	16:1	231.58	1.01	*	up
FA 16:2	$-H^-$	251.2021	251.2017	1.6	3.59	16:2	114.95	1.99	ns	up
Cer 42:1	$+(CHO_2)^-$	694.6369	694.6355	2.1	15.27	18:1, 24:0	278.31	1.02	*	down
HexCer_AP t37:2	$+(C_2H_3O_2)^-$	830.5979	830.5999	2.5	9.42	22:1, 15:1	295.07	1.01	ns	down
HexCer_AP t37:1	$+(C_2H_3O_2)^-$	832.6152	832.6164	1.5	10.43	22:1, 15:0	296.27	1.01	ns	down

ns: not significant; *** p value < 0.001; ** p value < 0.01; * p value < 0.05.

Using MS/MS fragmentation data and consulting the Metlin and Lipidomics libraries, we were able to tentatively identify the most discriminant metabolites as reported in **Table 1**.

Astronauts, after their return from space missions, manifest significant haematological alterations. Since the earliest space missions, symptoms such as structural alterations of red blood cells [18], anaemia [19], thrombocytopenia, [20,21], 10–17% reduction in plasma volume, and haemolysis [22] were reported. For these reasons, concern about the effects of space flight on haematological processes has been increasing. Several scientific studies allowed different theories to be proposed that may explain the

alterations in the size and number of erythrocytes [23,24,25]. Recently, Trudel et al. showed in astronauts a degradation and 54% reduction in red blood cells [26]. Different factors can lead a human cell to programmed death, such as changes to lipid signal activity [27].

Human cells determine the characteristics of the plasma membrane bilayer by tightly controlling lipid composition and recruiting cytosolic proteins involved in structural functions or signal transduction [28]. The cell membrane is a lipid bilayer essentially formed by phospholipids, cholesterol, and glycolipids [29]. Small variations in percentage composition and molar ratio of the different classes of phospholipids and glycolipids might induce changes in the cell membrane's fluidity and permeability. In particular, phospholipids are the main components of cell membranes and perform important biological functions.

From our results, it appears that after 6 h of clinorotation, levels of phosphocholines were increased in human erythrocytes. In particular, PC 18:1_20:4, PC 18:0_20:4, PC18:1_18:1, and PC 18:2_18:1 were found to be upregulated. Notably, PC with the arachidonic acid in their moiety were found discriminants. In particular, the proportion of sn-2-arachidonoyl-phosphatidylcholine (20:4-PC) has been shown to be inversely correlated with the activity of protein kinase B (Akt), an important kinase which promotes cell proliferation and survival. 20:4-PC reduces cell proliferation by interfering with the S-phase cell transition and by suppressing Akt downstream signalling and the expression of cyclin, such as LY294002, which is a specific inhibitor of the phosphatidylinositol-3-kinase/Akt [30]. At 9 and 24 h, erythrocytes showed other 20:4-PC upregulated: PC 18:2_20:4, PC 18:3_20:4 and PC 16:0_20:4, and PC 15:0_20:4, 15:1_20:4 and 16:0_20:4, respectively.

With the classical techniques of liquid chromatography coupled to mass spectrometry, the annotation of lipids and thus phosphocholine fatty acid composition with a good confidence interval is difficult due to the large variety of lipid species with different regiochemistry. In our study, the use of an analytical platform such as ion mobility coupled to mass spectrometry providing the collision cross section (CCS) value allows a better and more confident annotation of each metabolite. Each CCS was compared with an internal database and against the unified collision cross section compendium available on LipidMaps [31].

Additionally, a different fatty acid composition of membrane components can result in a greater sensitivity to peroxidative stress, with a consequent increase in membrane

fragility. Phosphatidylcholine species containing polyunsaturated fatty acids in their moiety, particularly arachidonate, at the sn-2 position are susceptible to free radical oxidation [32]. An example is represented by 1-palmitoyl-2-arachidonoyl-sn-glycero-3-phosphatidylcholine (PC16.0_20:4), which is a common cell membrane constituent, and circulates within cholesterol particles. At 6 h of clinorotation, erythrocytes showed an upregulation of EtherOxPC 16:0_20:4, while the respective phosphocholine, PC 16:0_20:4, was found to be not discriminant. Simulated microgravity conditions increase reactive oxygen species (ROS) production in various cell types [33]. Generally, in microgravity conditions a different management of cellular resources was observed. In fact, in G0 conditions, there is a more rapid consumption of intracellular ATP, and an increase in ATP expulsion compared to cells cultured under terrestrial gravity conditions, coupled with a reducing power [8] resulting in a more oxidant environment. Furthermore, inflammation and oxidative stress are associated with lipid peroxidation and the formation of bioactive lipids such as oxidized phosphocholines [34]. C-reactive protein (CRP), an acute-phase protein of hepatic origin that binds to specific structures expressed on the surface of dead or dying cells, promotes phagocytosis as macrophages may bind to these PC-oxidized species. Furthermore, recent studies demonstrate an enrichment of oxidized phosphatidylcholine in apoptotic cells [35]. Indeed, CRP can selectively bind on oxidized phosphatidylcholine but not on native phosphatidylcholine. In addition, oxidized phospholipids are recognized by macrophage scavenger, implying that these innate immune responses participate in cell clearance due to their proinflammatory properties [36]. Moreover, oxidized phosphatidylcholine, specifically oxidized-1-palmitoyl-2-arachidonoyl-sn-glycero-3-phosphatidylcholine (EtherOxPC 16:0_20:4), seems to be involved in ROS production. According to the study of Rouhanizadeh et al., EtherOxPC 16:0_20:4 was able to induce vascular endothelial superoxide production [37].

On the contrary, after 9 h of clinorotation, EtherOxPC(16:0_20:4) was downregulated, while PC 16:0_20:4 was upregulated, resulting non-discriminant after 24 h. These findings can lead us to hypothesize the complex adaptive response of cells.

Interestingly, several sphingomyelins were found to be downregulated for each experimental time point. This should not be surprising considering the mechanism of sphingomyelin synthesis. Indeed, sphingomyelinases (SMases) catalyse the hydrolysis of sphingomyelin to form ceramide and phosphocholine [38].

Taken together, these findings indicate that there are probably several mechanisms underlying spatial anaemia: inhibition of 20:4 PC-mediated cell proliferation and a simultaneous increase in pro-apoptotic signals.

3. Materials and methods

3.1 Chemicals.

Analytical LC-grade methanol, chloroform, acetonitrile, 2-propanol, and ammonium acetate and formiate were purchased from Sigma Aldrich (Milan, Italy). Bi-distilled water was obtained with a MilliQ purification system (Millipore, Milan, Italy). A SPLASH® LIPIDOMIX® standard component mixture was purchased from Sigma Aldrich (Milan, Italy): PC (15:0–18:1) (d7), PE (15:0–18:1) (d7), PS (15:0–18:1) (d7), PG (15:0–18:1) (d7), PI (15:0–18:1) (d7), PA (15:0–18:1) (d7), LPC (18:1) (d7), LPC 25, LPE (18:1) (d7), Chol Ester (18:1) (d7), MG (18:1) (d7), DG (15:0–18:1) (d7), TG ((15:0–18:1) (d7)-15:0)), SM (18:1) (d9), cholesterol (d7).

3.2 Cell culture.

Freshly drawn blood (Rh+) from 9 healthy adults of both sexes (men and women) was used, heparin was added and preserved in citrate-phosphate-dextrose with adenine (CPDA-1). Data are the average ± SD of three independent experiments. RBCs were separated from plasma and leukocytes by washing three times with phosphate-buffered saline (127 mM NaCl, 2.7 mM KCl, 8.1 mM Na_2HPO_4, 1.5 mM KH_2PO_4, 20 mM HEPES, 1 mM $MgCl_2$, and pH 7.4) supplemented with 5 mM glucose (PBS glucose) to obtain packed cells. This study was conducted in accordance with Good Clinical Practice guidelines and the Declaration of Helsinki. No ethical approval has been requested as human blood samples were used only to sustain in vitro cultures and patients provided written, informed consent in ASL. 1-Sassari (Azienda Sanitaria Locale. 1-Sassari) centre before entering the study.

3.3 Microgravity simulation.

In order to study the effects caused by microgravity on human erythrocytes, the gravity simulator 3D Random Positioning Machine (RPM, Fokker Space, Netherlands) was used at the laboratory of the Department of Biomedical Sciences, University of Sassari, Sardinia, Italy. The 3D Random Positioning Machine (RPM) is a micro-weight ('microgravity') simulator based on the principle of 'gravity-vector-averaging', built by Dutch Space. The 3D RPM is constructed from two perpendicular frames that rotate independently. This setup was used to constantly change the mean value of the gravity vector to zero. In this way, the 3D RPM provides a simulated microgravity less than 10^{-3} g. The dimensions of the 3D RPM are limited to 1000 × 800 × 1000 mm (length × width × height). The 3D RPM is connected to a computer, and through a specific software the mode and speed of rotation were selected. Random Walk mode with an 80 degree/s (rpm) was chosen.

The red blood cell samples were carefully deposited in 2 mL tubes together with PBS-glucose (30% haematocrit, approximately 3.4 × 109 cells) in a dedicated room at 37 °C. The control group samples were placed in the static bar at 1 g to undergo the same vibrations as the samples placed in µg conditions. Both control (1 g) and case (0 g) samples were collected after different time points (0, 6, 9, 24 h). Subsequently, the red blood cells were centrifuged and resuspended in 1 mL of lysis buffer [5 mM Na_2HPO_4, 1 mM EDTA (pH 8.0)] and stored at −20 °C until use for lipidomic analysis.

3.4 Sample Preparation for UHPLC-IM-QTOF-MS Analysis.

In order to investigate changes in the lipidome, analysis by UHPLC- IM-QTOF-MS requires the extraction of lipid content from cells [39]. An amount of 50 µL of human erythrocyte solution was extracted following the Folch procedure using 0.700 mL of a

methanol and chloroform mixture (2/1, *v/v*). Samples were vortexed every 15 min up to 1 h, when 0.350 mL of chloroform and 0.150 mL of water were subsequently added. The solution thus obtained was centrifuged at 17,700 rcf for 10 min, and 0.600 mL of the organic layer was transferred into a glass vial and dried under a nitrogen stream. The dried chloroform phase was reconstituted with 50 µL of a methanol and chloroform mixture (1/1, v/v) and 75 µL isopropanol:acetonitrile:water mixture (2:1:1 v/v/v). Quality control (QC) samples were prepared taking an aliquot of 10 µL of each sample. All samples thus prepared were injected in UHPLC-IM-QTOF-MS/MS and acquired in negative ionization mode, while for positive ionization mode they were diluted in ratio 1:10.

3.5 UHPLC-IM-QTOF-MS/MS analysis.

The chloroform phase was analysed with a 6560-drift tube ion mobility LC-QTOF-MS coupled with an Agilent 1290 Infinity II LC system. An aliquot of 4.0 µL from each sample was injected in a Luna Omega C18, 1.6 µm, 100 mm x 2.1 mm chromatographic column (Phenomenex, Castel Maggiore (BO), Italy). The column was maintained at 50 °C at a flow rate of 0.4 mL/min. The mobile phase for positive ionization mode consisted of (A) 10 mM ammonium formate solution in 60% of milliQ water and 40% of acetonitrile and (B) 10 mM ammonium formate solution containing 90% of isopropanol, 10% of acetonitrile. In positive ionization mode, the chromatographic separation was obtained with the following gradient: initially 80% of A, then a linear decrease from 80% to 50% of A in 2.1 min then at 30% in 10 minutes. Subsequently the mobile phase A was again decrease from 30% at 1%% and staying at this percentage for 1.9 minutes and then brought back to the initial conditions in 1 min. The mobile phase for the

chromatographic separation in the negative ionization mode differed only for the use of 10 mM ammonium acetate instead of ammonium formate.

An Agilent jet stream technology source which was operated in both positive and negative ion modes with the following parameters: gas temperature, 200 °C; gas flow (nitrogen) 10 L/min; nebulizer gas (nitrogen), 50 psig; sheath gas temperature, 300 °C; sheath gas flow, 12 L/min; capillary voltage 3500 V for positive and 3000 V for negative; nozzle voltage 0 V; fragmentor 150 V; skimmer 65 V, octapole RF 7550 V; mass range, 50−1700 *m/z*; capillary voltage, 3.5 kV; collision energy 20 eV in positive and 25 eV in negative mode, mass precursor per cycle = 3. High purity nitrogen (99.999%) was used as a drift gas with a trap fill time and a trap release time of 2000 and 500 µs, respectively. Before the analysis, the instrument was calibrated using an Agilent tuning solution at the mass range of *m/z* 50-1700. Samples were evaporated with nitrogen at the pressure of 48 mTorr and at the temperature of 375 °C, while an Agilent reference mass mix for mass re-calibration was continuously injected during the run schedule.

The Agilent MassHunter LC/MS Acquisition console (revision B.09.00) from The MassHunter suite was used for data acquisition.

3.6 Data analysis.

Data acquired with the Agilent 6560 DTIM Q-TOF LC-MS were pre-processed with the software MassHunter Workstation suite (Agilent Technologies, Santa Clara, CA, USA). This software (Mass Profiler 10.0) allowed us to perform mass re-calibration, DTCCSN2 re-calibration, time alignment, and deconvolution of signals, yielding a matrix containing all features present across all samples. The removal of background noise and unrelated ions was performed by a recursive feature extraction tool, yielding

a matrix containing all the features present across all samples. Furthermore, to eliminate non-specific information, data matrix quality assurance was performed. This filtered matrix was then subjected to multivariate statistical analysis using SIMCA software 15.0 (Umetrics, Umeå, Sweden).

First, a principal component analysis (PCA) was carried out. This unsupervised analysis allows an observation of samples and variables distribution in the multivariate space on the basis of their similarity and dissimilarity. This was followed by partial least square-discriminant analysis (PLS-DA) with its orthogonal extension (OPLS-DA), which was used as a classificatory model to visualize and evaluate the differences between sample classes.

3. Conclusions

Spatial anaemia in astronauts has been noted since the earliest space missions, while the contributing mechanisms during space flight remained unclear. To investigate the molecular mechanisms that induce a reduction in the number of erythrocytes during spaceflight, we decided to analyse the lipid profile of human erythrocytes under microgravity conditions. Thanks to the advancement of hyphenated techniques and mass analysers, we were able to identify biologically active complex lipids susceptible to microgravity, allowing new possible hypotheses that explain the anaemia experienced by astronauts.

In more detail, lipidomic analysis of erythrocytes revealed a double mechanism that generates the reduction in the number of red blood cells. On one hand, there is an increase in the levels of 20:4 PC, reducing cellular proliferation. On the other hand, the increase in the levels of EtherOxPC 16:0_20:4 stimulates the immune response by attracting the C-reactive protein and macrophages and induces an increase in ROS production [33,34]. This accumulation acts as a pro-apoptotic signal condemning the erythrocytes to death.

In this study, we reported a set of lipid discriminants or potential biomarkers linked to microgravity exposure with the aim to explore in the future specific lipid pathways and form the foundation in the development of novel therapeutics in hopes of reducing the effects of space flights. However, further studies are needed to accurately measure lipids in erythrocytes samples to better understand the clinical effects of microgravity.

Acknowledgments

We acknowledge the CeSAR (Centro Servizi d'Ateneo per la Ricerca) of the University of Cagliari, Italy for the IMQTOFMSMS experiments performed with an Agilent 6560.

References

1. Riwaldt, S.; Corydon, T.J.; Pantalone, D.; Sahana, J.; Wise, P.; Wehland, M.; Krüger, M.; Melnik, D.; Kopp, S.; Infanger, M.; et al. Role of Apoptosis in Wound Healing and Apoptosis Alterations in Microgravity. *Front. Bioeng. Biotechnol.* **2021**, *9*, 1–22. https://doi.org/10.3389/fbioe.2021.679650.
2. Bizzarri, M.; Fedeli, V.; Piombarolo, A.; Angeloni, A. Space Biomedicine: A Unique Opportunity to Rethink the Relationships between Physics and Biology. *Biomedicines* **2022**, *10*, 2633. https://doi.org/10.3390/biomedicines10102633.
3. Thirsk, R.; Kuipers, A.; Mukai, C.; Williams, D. The space-flight environment: The International Space Station and beyond. *CMAJ* **2009**, *180*, 1216–1220. https://doi.org/10.1503/cmaj.081125.
4. Sheyn, D.; Pelled, G.; Netanely, D.; Domany, E.; Gazit, D. The Effect of Simulated Microgravity on Human Mesenchymal Stem Cells Cultured in an Osteogenic Differentiation System: A Bioinformatics Study. *Tissue Eng.-Part A* **2010**, *16*, 3403–3412. https://doi.org/10.1089/ten.tea.2009.0834.
5. Hughes-Fulford, M.; Tjandrawinata, R.; Fitzgerald, J.; Gasuad, K.; Gilbertson, V. Effects of microgravity on osteoblast growth. *Gravit. Space Biol. Bull.* **1998**, *11*, 51–60.
6. Han, X.; Qiu, L.; Zhang, Y.; Kong, Q.; Wang, H.; Wang, H.; Li, H.; Duan, C.; Wang, Y.; Song, Y.; et al. Transplantation of Sertoli-Islet Cell Aggregates Formed by Microgravity: Prolonged Survival in Diabetic Rats. *Exp. Biol. Med.* **2009**, *234*, 595–603. https://doi.org/10.3181/0812-rm-359.
7. NSBRI. National Space Biomedical Research Institute Strategic Plan 2010. *Biomed Res*. 2010.

http://nsbri.org/wp-content/uploads/2015/08/NSBRI_strategic_plan1.

8. Dinarelli, S.; Longo, G.; Dietler, G.; Francioso, A.; Mosca, L.; Pannitteri, G.; Boumis, G.; Bellelli, A.; Girasole, M. Erythrocyte's aging in microgravity highlights how environmental stimuli shape metabolism and morphology. *Sci. Rep.* **2018**, *8*, 5277. https://doi.org/10.1038/s41598-018-22870-0.
9. Poon, C. Factors implicating the validity and interpretation of mechanobiology studies in simulated microgravity environments. *Eng. Rep.* **2020**, *2*, 1–18. https://doi.org/10.1002/eng2.12242.
10. Maxfield, F.R.; Tabas, I. Role of cholesterol and lipid organization in disease. *Nature* **2005**, *438*, 612–621. https://doi.org/10.1038/nature04399.
11. Wenk, M.R. The emerging field of lipidomics. *Nat. Rev. Drug Discov.* **2005**, *4*, 594–610. https://doi.org/10.1038/nrd1776.
12. Carrasco-Pancorbo, A.; Navas-Iglesias, N.; Cuadros-Rodríguez, L. From lipid analysis towards lipidomics, a new challenge for the analytical chemistry of the

21st century. Part I: Modern lipid analysis. *TrAC-Trends Anal. Chem.* **2009**, *28*, 263–278. https://doi.org/10.1016/j.trac.2008.12.005.

13. Roberts, L.D.; Souza, A.L.; Gerszten, R.E.; Clish, C.B. Targeted Metabolomics. *Curr. Protoc. Mol. Biol.* **2012**, *98*, 30.2.1–30.2.24. https://doi.org/10.1002/0471142727.mb3002s98.

14. Wang, Z.; Klipfell, E.; Bennett, B.J.; Koeth, R.; Levison, B.S.; DuGar, B.; Feldstein, A.E.; Britt, E.B.; Fu, X.; Chung, Y.-M.; et al. Gut Flora Metabolism of Phosphatidylcholine Promotes Cardiovascular Disease. *Nature* **2011**, *472*, 57–63. https://doi.org/10.1038/nature09922.

15. Cajka, T.; Fiehn, O. Toward Merging Untargeted and Targeted Methods in Mass Spectrometry-Based Metabolomics and Lipidomics. *Anal. Chem.* **2016**, *88*, 524–545. https://doi.org/10.1021/acs.analchem.5b04491.

16. Ivanova, S.M.; Morukov, B.V.; Labetskaia, O.I.; IuV, I.; Levina, A.A.; Kozinets, G.I. Morphobiochemical assay of the red blood system in members of the prime crews of the International Space Station. *Hum. Physiol*. **2009**, *43*, 43-47.

17. Girasole, M.; Pompeo, G.; Cricenti, A.; Congiu-Castellano, A.; Andreola, F.; Serafino, A.; Frazer, B.; Boumis, G.; Amiconi, G. Roughness of the plasma membrane as an independent morphological parameter to study RBCs: A quantitative atomic force microscopy investigation. *Biochim. Biophys. Acta (BBA)-Biomembr.* **2007**, *1768*, 1268–1276. https://doi.org/10.1016/j.bbamem.2007.01.014.

18. Manis, C.; Manca, A.; Murgia, A.; Uras, G.; Caboni, P.; Congiu, T.; Faa, G.; Pantaleo, A.; Cao, G. Understanding the Behaviour of Human Cell Types under Simulated Microgravity Conditions: The Case of Erythrocytes. *Int. J. Mol. Sci.* **2022**, *23*, 6876. https://doi.org/10.3390/ijms23126876.

19. Alfrey, C.P.; Udden, M.M.; Leach-Huntoon, C.; Driscoll, T.; Pickett, M.H. Control of red blood cell mass in spaceflight. *J. Appl. Physiol.* **1996**, *81*, 98–104. https://doi.org/10.1152/jappl.1996.81.1.98.

20. Taylor, G.R. Advances in experimental medicine. In *Advances in Experimental Medicine and Biology*; Plenum Press: New York, NY, USA; London, UK, 1997; Volume 225, pp. 269–271. Available online: http://linkinghub.elsevier.com/retrieve/pii/0020711X84902064 (accessed on 18 January 2022).

21. Meehan, R.T.; Neale, L.S.; Kraus, E.T.; Stuart, C.A.; Smith, M.L.; Cintron, N.M.; Sams, C.F. Alteration in human mononuclear leucocytes following space flight. *Immunology* **1992**, *76*, 491–497.

22. Diedrich, A.; Paranjape, S.Y.; Robertson, D. Plasma and Blood Volume in Space. *Am. J. Med. Sci.* **2007**, *334*, 80–86. https://doi.org/10.1097/maj.0b013e318065b89b.

23. Erslev, A.J. Erythropoietin. *N. Engl. J. Med.* **1991**, *324*, 1339–1344. https://doi.org/10.1056/nejm199105093241907.

24. Koury, M.J.; Bondurant, M.C. Erythropoietin Retards DNA Breakdown and Prevents Programmed Death in Erythroid Progenitor Cells. *Science* **1990**, *248*, 378–381. https://doi.org/10.1126/science.2326648.

25. Leach, C.S.; Johnson, P.C. Influence of Spaceflight on Erythrokinetics in Man. *Science* **1984**, *225*, 216–218. https://doi.org/10.1126/science.6729477.

26. Trudel, G.; Shahin, N.; Ramsay, T.; Laneuville, O.; Louati, H. Hemolysis contributes to anemia during long-duration space flight. *Nat. Med.* **2022**, *28*, 59–62. https://doi.org/10.1038/s41591-021-01637-7.

27. Crimi, M.; Degli Esposti, M. Apoptosis-induced changes in mitochondrial lipids. *Biochim. Biophys. Acta (BBA)-Mol. Cell Res.* **2011**, *1813*, 551–557. https://doi.org/10.1016/j.bbamcr.2010.09.014.

28. Sprong, H.; Van Der Sluijs, P.; van Meer, G. How proteins move lipids and lipids move proteins. *Nat. Rev. Mol. Cell Biol.* **2001**, *2*, 504–513. https://doi.org/10.1038/35080071.

29. Robertson, J.L. The lipid bilayer membrane and its protein constituents. *J. Gen. Physiol.* **2018**, *150*, 1472–1483. https://doi.org/10.1085/jgp.201812153.

30. Koeberle, A.; Shindou, H.; Koeberle, S.C.; Laufer, S.A.; Shimizu, T.; Werz, O. Arachidonoyl-phosphatidylcholine oscillates during the cell cycle and counteracts proliferation by suppressing Akt membrane binding. *Proc. Natl. Acad. Sci. USA* **2013**, *110*, 2546–2551. https://doi.org/10.1073/pnas.1216182110.

31. Picache, J.A.; Rose, B.S.; Balinski, A.; Leaptrot, K.L.; Sherrod, S.D.; May, J.C.; McLean, J.A. Collision cross section compendium to annotate and predict multi-omic compound identities. *Chem. Sci.* **2019**, *10*, 983–993. https://doi.org/10.1039/c8sc04396e.

32. Subbanagounder, G.; Leitinger, N.; Schwenke, D.C.; Wong, J.W.; Lee, H.; Rizza, C.; Watson, A.D.; Faull, K.F.; Fogelman, A.M.; Berliner, J.A. Determinants of bioactivity of oxidized phospholipids: Specific oxidized fatty acyl groups at the sn-2 position. *Arterioscler. Thromb. Vasc. Biol.* **2000**, *20*, 2248–2254. https://doi.org/10.1161/01.atv.20.10.2248.

33. Ran, F.; An, L.; Fan, Y.; Hang, H.; Wang, S. Simulated microgravity potentiates generation of reactive oxygen species in cells. *Biophys. Rep.* **2016**, *2*, 100–105. https://doi.org/10.1007/s41048-016-0029-0.

34. Ashraf, M.Z.; Kar, N.S.; Podrez, E.A. Oxidized phospholipids: Biomarker for cardiovascular diseases. *Int. J. Biochem. Cell Biol.* **2009**, *41*, 1241–1244. https://doi.org/10.1016/j.biocel.2008.11.002.

35. Huber, J.; Vales, A.; Mitulović, G.; Blumer, M.; Schmid, R.; Witztum, J.L.; Binder, B.R.; Leitinger, N. Oxidized Membrane Vesicles and Blebs from Apoptotic Cells Contain Biologically Active Oxidized Phospholipids That Induce Monocyte-Endothelial Interactions. *Arterioscler. Thromb. Vasc. Biol.* **2002**, *22*, 101–107. https://doi.org/10.1161/hq0102.101525.

36. Chang, M.-K.; Binder, C.J.; Torzewski, M.; Witztum, J.L. C-reactive protein binds to both oxidized LDL and apoptotic cells through recognition of a common ligand: Phosphorylcholine of oxidized phospholipids. *Proc. Natl. Acad. Sci. USA* **2002**, *99*, 13043–13048. https://doi.org/10.1073/pnas.192399699.

37. Rouhanizadeh, M.; Hwang, J.; Clempus, R.E.; Marcu, L.; Lassègue, B.; Sevanian, A.; Hsiai, T.K. Oxidized-1-palmitoyl-2-arachidonoyl-sn-glycero-3-phosphorylcholine induces vascular endothelial superoxide production: Implication of NADPH oxidase. *Free Radic. Biol. Med.* **2005**, *39*, 1512–1522. https://doi.org/10.1016/j.freeradbiomed.2005.07.013.

38. Patwardhan, G.A.; Beverly, L.J.; Siskind, L.J. Sphingolipids and mitochondrial apoptosis. *J. Bioenerg. Biomembr.* **2016**, *48*, 153–168. https://doi.org/10.1007/s10863-015-9602-3.

39. Ulmer, C.Z.; Jones, C.M.; Yost, R.A.; Garrett, T.J.; Bowden, J.A. Optimization of Folch, Bligh-Dyer, and Matyash sample-to-extraction solvent ratios for human plasma-based lipidomics studies. *Anal. Chim. Acta* **2018**, *1037*, 351–357. https://doi.org/10.1016/j.aca.2018.08.004.

International Journal of *Molecular Sciences*

MDPI

Article

Understanding the Behaviour of Human Cell Types under Microgravity Conditions: The Case of Erythrocytes

Cristina Manis [1,2], Alessia Manca [3], Antonio Murgia [1], Giuseppe Uras [4], Pierluigi Caboni [1], Terenzio Congiu [5], Gavino Faa [5], Antonella Pantaleo [3,*,‡] and Giacomo Cao [2,6,7,*]

[1] Department of Life and Environmental Sciences, Cittadella Universitaria di Monserrato, Blocco A, Room 13, 09042 Monserrato, Italy; cristina.manis@outlook.it (C.M.); a-murgia@hotmail.it (A.M.); caboni@unica.it (P.C.)
[2] Department of Mechanical, Chemical and Materials Engineering, University of Cagliari, Piazza d'Armi, 09123 Cagliari, Italy
[3] Department of Biomedical Science, University of Sassari, Viale San Pietro, 07100 Sassari, Italy; alessia_manca@hotmail.it
[4] Department of Clinical and Movement Neurosciences, Institute of Neurology, University of College London, London NW3 2PF, UK; g.uras@ucl.ac.uk
[5] Department of Medical Sciences and Public Health, Monserrato's Campus, SS554, 09042 Monserrato, Italy; terenzio.congiu@unica.it (T.C.); gavinofaa@gmail.com (G.F.)
[6] Center of Advanced Studies, Research and Development in Sardinia (CRS4), Loc. Piscina Manna, Building 1, 09050 Pula (CA), Italy
[7] Sardinia AeroSpace District (DASS), c/o Sardegna Ricerche, Via G. Carbonazzi 14, 09123 Cagliari, Italy
* Correspondence: apantaleo@uniss.it (A.P.); giacomo.cao@unica.it (G.C.)
‡ Senior co-author.

Abstract: Erythrocytes are highly specialized cells in human body, and their main function is to ensure the gas exchanges, O_2 and CO_2, within the body. The exposure to microgravity environment leads to several health risks such as those affecting red blood cells. In this work, we investigated the changes that occur in the structure and function of red blood cells under simulated microgravity, compared to terrestrial conditions, at different time points using biochemical and biophysical techniques. Erythrocytes exposed to simulated microgravity showed morphological changes, a constant increase in reactive oxygen species (ROS), a significant reduction in total antioxidant capacity (TAC), a remarkable and constant decrease in total glutathione (GSH) concentration, and an augmentation in malondialdehyde (MDA) at increasing times. Moreover, experiments were performed to evaluate the lipid profile of erythrocyte membranes which showed an upregulation in the following membrane phosphocholines: PC16:0_16:0, PC 33:5, PC18:2_18:2, PC 15:1_20:4 and SM d42:1. Thus, remarkable changes in erythrocyte cytoskeletal architecture and membrane stiffness due to oxidative damage have been found under microgravity conditions, in addition to factors that contribute to the plasticity of the red blood cells (RBCs)

including shape, size, cell viscosity and membrane rigidity. This study represents our first investigation into the effects of microgravity on erythrocytes and will be followed by other experiments towards understanding the behaviour of different human cell types in microgravity.

Keywords: erythrocytes; microgravity; confocal and scanning electron microscopy; oxidative stress; mass spectrometry; lipidomics

1. Introduction

Red blood cells (RBCs) are peculiar within the human body, given their unique physiological role as transporters of O_2 and CO_2, with a specialized molecular apparatus for gas exchange [1]. In addition to this, RBCs present a differentiated membrane which allows them to be physically dynamic in terms of shape and structure in order to sustain the stresses within the blood flow [2].

RBCs have peculiar characteristics, such as absence of DNA, simplified structure and a metabolism that suggests that these cells have a special relationship with the external environment. They are very sensitive to their surroundings and also well equipped with antioxidant systems which essentially contribute to their function and integrity [1].

It is well known that the presence of gravity on Earth deeply influenced the evolution of living organisms [3]. During the past century, human space activities have opened new scientific challenges related to understand the effects caused by the low gravity environment (microgravity) on organisms at the cellular as well as systemic level [4]. Microgravity (μg) can regulate the behaviour and structural properties of cells and regarding RBCs effectively acts as modulator of their shape and function through various mechanisms [5]. Microgravity environment has resulted in modified transcriptome and cytoskeletal changes, resulting in both short and long-term morphological changes in the cells [6]. Propelled by the constant increase in the human presence within space environment such as the International Space Station (ISS), there has been increased attention on the effects of modelled microgravity on cells physiological functions.

The exposure to microgravity conditions during space flight is associated with various health risks, which potentially affect the body, making it vulnerable to secondary conditions such as the effects of radiation, physiological changes lysis, neocytolysis, muscle atrophy, hydrostatic pressure changes, and metabolic changes [7–9]. During spaceflight, astronauts are also subjected to a variety of stress factors, such as microgravity conditions and radiation, which lead to negative health consequences [10,11]. The main cause of cellular damage to astronauts is oxidative stress [12], which is caused by an imbalance between oxidant and antioxidant species [13,14]. Previous studies [15–17] have been conceived to report the most recent knowledge about band 3 protein, with specific regard to its functions in oxidative stress conditions, including oxidative stress-related diseases. The produced reactive oxygen species (ROS) are

mainly superoxide anion (O2-), hydrogen peroxide (H2O2) and free radicals. An increase in oxidants causes an imbalance in favour of oxidizing species, which are the cause of several pathologies in humans, as well as being one of the causes of aging. In more detail, the astronauts are affected, on their return to Earth, by several health problems such as reduction in bone density up to 20%, muscle atrophy, endocrine, immune system and cognitive disorders in addition to cardiovascular dysfunctions [18]. In particular, blood samples from Russian cosmonauts have been investigated observing significant changes in phospholipids [19]. An increase in the percentage of phosphatidylcholine may be clearly associated with the increase in membrane rigidity. On the other hand, changes in physicochemical properties of the plasma membrane of erythrocytes (microviscosity and permeability) can influence the efficiency of oxygen transfer, the state of the haemoglobin and changes in the conformation of haematoporphyrin. Moreover, lipid and phospholipid compositions of erythrocyte membranes were assayed by thin layer chromatography followed by densitometric measurement of stained dots. This technique provides information on the entire lipid class, but hardly allows the recognition of the specific molecules that belong to that class, making it difficult to understand the biochemical mechanisms involved in achieving the final result [19]. However, most previous studies have investigated data derived after the end of a space flight, while only a few data related to changes occurring during a space flight are described in the literature. Concerning RBCs, it is known that spaceflight induces oxidative stress [20], although the direct role of microgravity is still unclear, while there are several pieces of evidence of blood homeostasis alterations such as the so-called space anaemia or Pseudopolycythemia [21]. During the early days of low gravity conditions, astronauts show a reduction in plasma volume and therefore an increase in erythrocytes relative volume [22,23]. The body's adaptive response to this new condition consists of an increase in erythrocytes clearance and a decrease in erythropoietin synthesis [24]. Therefore, haemoconcentration occurs with an increase in the haematocrit that is favoured by the rapid decrease in erythrocytes selective counting and haemolysis [25].

On the basis of the considerations above, due to the high cost of space experiments, there is an increasing demand of the development of technologies to guarantee nearly zero-gravity environmental conditions on Earth [26].

To model microgravity conditions observed on the ISS, a g force between 10−3 and 10−6 has to be achieved, resulting in a weightless environment [1]. In order to do to so,

international space agencies validated machines, namely random positioning machines (RPM) and 3D-clinostats, have been employed [1,27] (Figure 1). Such instruments simply produce a fast rotation within three axes, resulting in a null gravity [28,29].

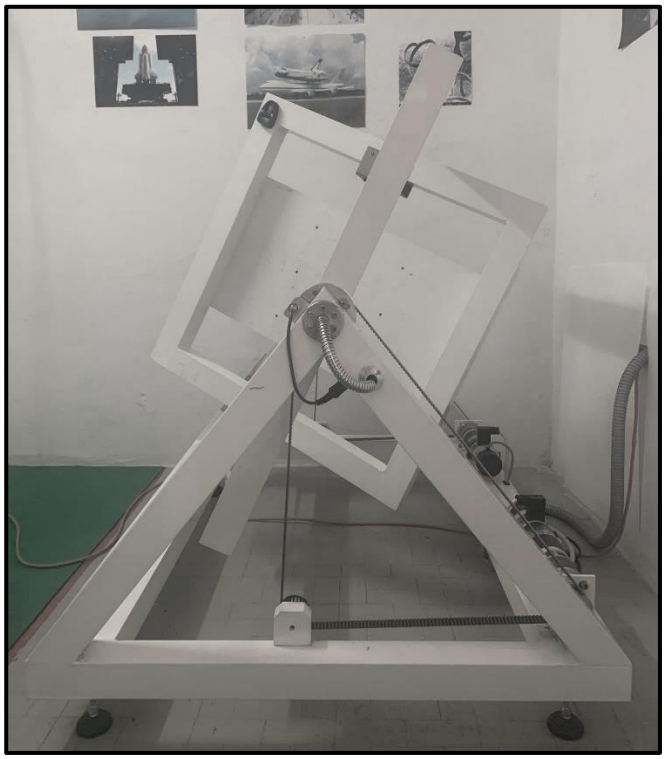

Figure 1. Random Positioning Machine (RPM, Fokker Space, Netherlands).

Despite the great relevance of the topic, currently few studies have been carried out to investigate the behaviour of RBCs under simulated gravity conditions which demonstrated that these cells undergo a rapid sensing of the environment initially translated into a metabolic adaptive response and subsequently fixed in structural and morphological alterations, thus in modulations or alterations of functionality [1,30].

Since no other data on this subject are available in the literature, here we present a novel approach to understand the changes to RBCs under microgravity conditions, specifically related to their membrane components, using different biochemical and biophysical techniques, such as scanning electron microscopy (SEM) and confocal microscopy together with the exploitation of the great potential offered by chromatographic and mass spectrometry to comprehensively evaluate the structure and function of RBCs in normal and in 3D-clinostat-delivered microgravity conditions. These analyses collectively provide additionally insights into red cell morphology and membrane property changes in direct relation to biological mechanisms.

2. Results and Discussion

To understand how RBCs sense microgravity and transduce this stimulus into morphological modification, confocal and scanning electron microscopy were used. RBCs were clinorotaded at given time-points. Specifically, 0, 6, and 9 h were set up, while control RBCs were placed in the static bar at 1 g to undergo the same vibration of the samples under microgravity conditions. Figures 2 and 3 allow us to visualize, by confocal and scanning electron microscopy respectively, the progressive changes in RBCs morphology related to microgravity condition. Clinorotated RBCs already at 6 h differ significantly in shape and size when compared to RBCs at 1 g. No significant alterations were in fact present at 1 g (Panels A, B, C of Figures 2 and 3), since RBCs showed a biconcave shape, at 6 and 9 h being their conditions identical at T_0. On the contrary, the microgravity-exposed RBCs showed, at increasing times (Panels E, F of Figures 2 and 3) more severe morphological defects, probably due to a faster occurrence of structural weakening and alterations.

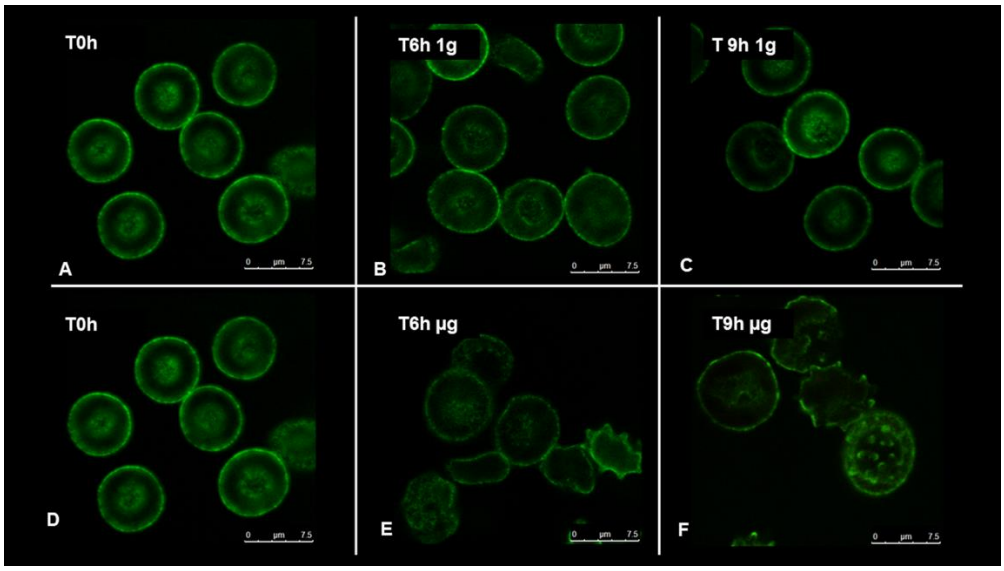

Figure 2. Confocal images of RBCs incubated for 6 and 9 h under terrestrial (1 g) (**A,B**,**C**) and microgravity conditions (µg) (**D**,**E**,**F**). Images were acquired using the same magnification with a Leica TCS SP5 X (Leica Microsystems, Germany) confocal microscope equipped with a 60 × 1.4 numerical aperture oil immersion lens. The scale bar in the figure is 7.5 µm.

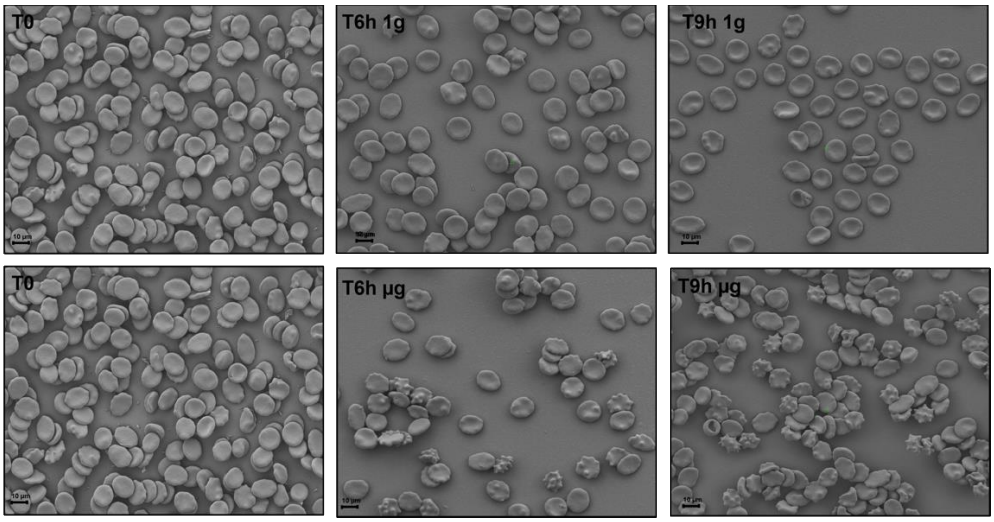

Figure 3. Scanning electron microscopy images of RBCs incubated for 6 and 9 h under terrestrial (1 g) (A–C) and microgravity conditions (µg) (D–F). Images were acquired using a SEM (ZEISS SIGMA 300). The scale bar in the figure is 10 µm.

In fact, cells were in the form of echinocytes characterized by convex rounded protrusions or spicules evenly spaced around the cell circumference, with a sharp increase in the spicules morphology at 9 h of clinorotation, usually considered as a more severe marker of cell senescence and corresponding oxidative stress.

These observations can be certainly correlated with the redox power (e.g., the GSH/GSSH ratio) and the intracellular and extracellular ATP which determine cell's resources and the corresponding metabolic status [1]. Concerning RBCs, we are aware of space-flight-induced oxidative stress [20] in which the direct role of microgravity is still controversial. The relationship between metabolic adaptations induced by microgravity and their structural or morphological characteristics is still unclear.

It is worth mentioning that the observed landscape obtained by microscopy analysis was indicative of a progressive loss of the cellular function and defence, coupled with a degradation of RBCs' structures. On the basis of these premises, we quantified oxidant and antioxidant species to better understand some of the RBCs' metabolic strategies exerted under stress and compared their time-dependent evolution under static or microgravity conditions. To analyse the oxidative stress experienced and the imbalances between antioxidant species by red blood cells during the performed experiments, we decided to evaluate ROS and malondialdehyde (MDA-TBARS) levels as markers of oxidative stress. In addition, total antioxidant capacity (TAC) and glutathione (GSH) were measured, as antioxidant defence species, which can prevent cellular damage

caused by oxidant species such as ROS and MDA. The measurement of TAC allows one to estimate the ability of cells to counteract oxidative stress-induced damage in cells. The evaluation of antioxidant and ROS species was carried out on plasma samples exposed to simulated microgravity (µg) and Earth gravity condition (1 g). Figure 4 Panel A shows the extracellular ROS level at different time point (T_0, 30–60-90 min and 2–3-6–9 hours). Samples exposed to simulated microgravity showed a constantly increase in ROS levels compared to the control samples at 1 g. After 30 mins, level of ROS increased by 50% in microgravity samples and up to 100% at 9 h. In Figure 4, Panel B the TAC expressed in µmol/L is reported. It is seen that clinorotated samples displayed a significative reduction, approximately by 60% of TAC concentration at 2 h as compared to control samples which remains fairly constant. Figure 4, Panel C shows the total GSH concentration expressed in µmol/L. Samples exposed to clinorotation display a significant and constant decrease approximately by 85% in concentration up to 9 h while a non-significant decrease was observed under 1 g condition. Figure 4, Panel D shows the MDA concentration expressed in µmol/L. MDA concentration was higher in samples exposed to microgravity condition.

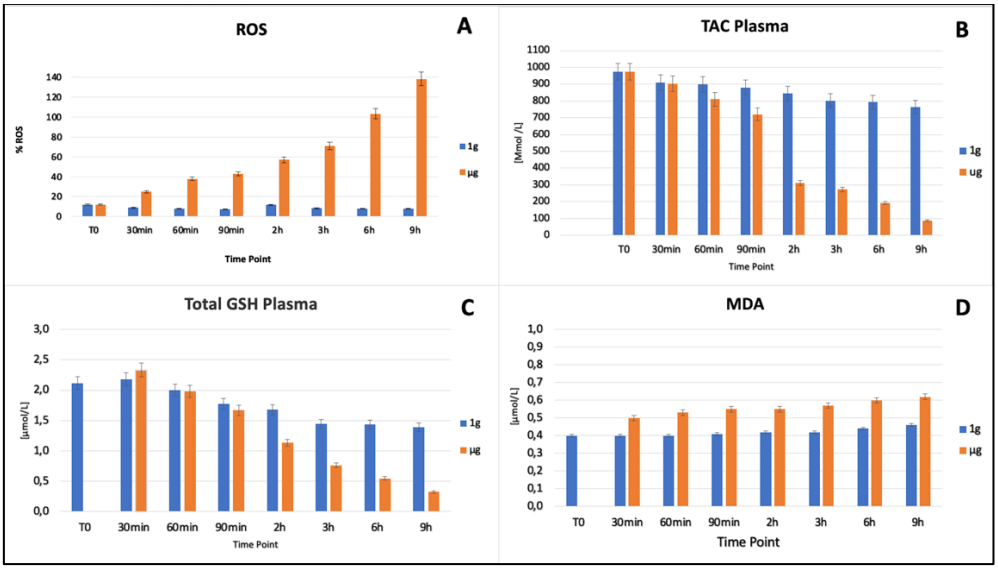

Figure 4. Evaluation of extracellular ROS level (A), TAC (B), GSH (C), and MDA (D) on plasma samples exposed to simulated microgravity (µg) and earth gravity conditions (1 g) at different time point (T0, 30-60-90 min and 2-3-6-9 hours). Data are the average ± SD of three independent ex-periments.

These results provide a confirmation of remarkable changes in red cell cytoskeletal architecture and membrane stiffness due to oxidative damage, validated in our study by

the marked increase in ROS and by a significant decrease in TAC. RBC's antioxidant defence system become no longer able to reduce the levels of reactive oxygen species (ROSs). Progressive incubation under microgravity condition is also thought to be a consequence of oxidative damage due to the increase in MDA concentration and the decrease in GSH. All these factors contribute to the deformability of the RBCs including shape, size, cell viscosity, and membrane rigidity.

To evaluate the overall impact of simulated microgravity on membrane modifications, we decided to investigate the lipid profile of erythrocytes under normal and microgravity conditions by LC-QTOF-MS. The unsupervised principal component analysis (PCA) is able to extract meaning information from data without training a model on labelled data. The PCA model for the data acquired in positive (PCA R2X = 0.67, Q2 = 0.54) and negative ionization mode (PCA R2X = 0.432 and Q2 = 0.195), respectively, did not indicate any clusters related to clinorotation. However, the arrangement of the samples in the multivariate space appeared to be influenced by the time factor. To further limit the time factor influence, for each time point, we performed a Partial Least Square-Discriminant Analysis (PLS-DA). The validation parameters of the positive ionization acquisition (PIA) model built for the samples collected at 6 h showed a good classifying power and a good predictive ability ($R^2X = 0.729$; $R^2Y = 0.856$; $Q^2 = 0.514$), while the latter one decreased in PLS-DA of samples collected at 9 and 24 h ($R^2X = 0.699$; $R^2Y = 0.432$; $Q^2 = 0.165$ and $R^2X = 0.602$; $R^2Y = 0.678$; $Q^2 = 0.107$), respectively. Due to the greater predictive ability of the PLS-DA model relating to samples collected after 6 h of experiment, we focused on metabolites that discriminate the class of clinorotated erythrocytes from those ones at 1g conditions. Finally, an OPLS-DA was performed to find the discriminant metabolites. For the positive and negative ionization mode the OPLS-DA score plot reported in Figure 5a and 5b, respectively, the following parameters were obtained: $R^2X = 0.755$; $R^2Y = 0.998$ and $Q^2 = 0.409$ $R^2X = 0.432$ and $Q^2 = 0.195$, respectively. Among the most discriminant compounds, resulting by PIA OPLS-DA model, the membrane phosphocholines PC16:0_16:0 and PC 33:5 were found to be upregulated in erythrocytes clinorotated for six hours when compared with control samples. The significance of the discriminating character of these metabolites was assessed on the basis of the VIP value, which was 1.1089 and 1.8294, respectively. On the other hand, from the negative ionization acquisition (NIA) OPLS-DA model, the phosphocholine PC18:2_18:2, PC 15:1_20:4

and sphingomyelin SM d42:1 (VIP values: 1.1197, 1.4849, and 1.5191) were upregulated in RBCs clinorotated for six hours when compared with control samples.

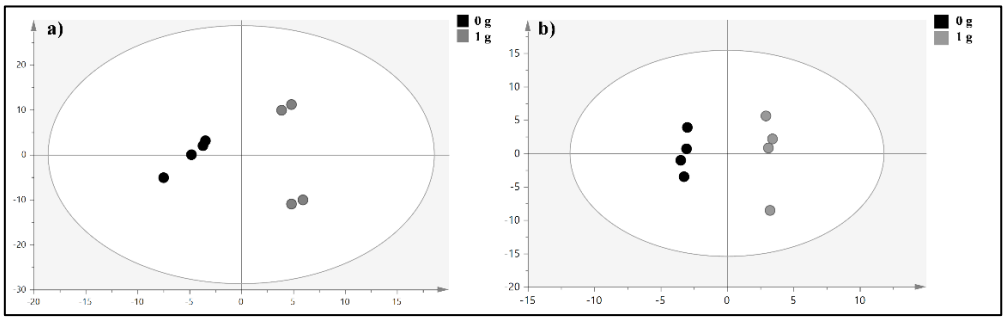

Figure 5. (a) OPLS-DA score plot for the PIA model and **(b)** OPLS-DA score plot for the NIA model. The grey circles represent the control samples, while black circles represent clinorotated erythrocytes samples.

Considering the results of the analysis and the general literature on the topic, it can be concluded that RBCs are very sensitive to their surroundings, changing shape and reacting to their environment. In an ideal situation, the RBC exists as a biconcave disc, of which the structure, shape, and modifications to physical stress are defined by the cytoskeletal architecture supporting the plasma membrane [31,32]. Modifications in the cytoskeletal proteins involved in structural function alter the RBCs spectrin network and membrane integrity when re-shaping in response to an induced stress [33,34]. Dysfunctional responses to physical change can result in a loss of function in RBCs, recapitulating a disease-like scenario [35].

Recently, several studies have shown an upregulation of phosphocholines class in different cell types such as epidermal stem cells [36] or gastric cancer cells subjected to simulated gravity conditions [37]. The same studies were performed on blood samples from Russian cosmonauts by Ivanova et al. [19]. In this case, the research team observed that during the voyage there was an increase in the percentage of phosphatidylcholine lipid class associated with the increase in membrane rigidity. In fact, an increase in phosphatidylcholine is associated with an increase in the rigidity of the cell membrane. The specific composition of the membrane provides the RBCs a certain fluidity, necessary to modulate cell functions, while loss of such fluidity affects normal functions and cellular signalling. From the analysis of our samples, it appears that the 42: 1 sphingomyelin was upregulated in erythrocytes cultured under simulated microgravity conditions. Sphingomyelins are often associated with inflammation processes. In this case, the latter ones could be triggered by the known increase in ROS. Furthermore, the

upregulation of phosphocholines substantially affects the phosphocholines PC 18: 2_18: 2 and PC 15: 1_20: 4. Both of these phosphocholines have different unsaturation, considerably increasing the possible rigidity of the cell membrane, in particular this effect occurs within the first six hours of clinorotation.

3. Materials and Methods

3.1. Cell Culture

Freshly drawn blood (Rh+) from healthy adults of both sexes was used. Patients provided written, informed consent in the ASL. 1-Sassari (Azienda Sanitaria Locale.1-Sassari) centre before entering the study. This study was conducted in accordance with Good Clinical Practice guidelines and the Declaration of Helsinki. No ethical approval was requested as human blood samples were used only to perform in vitro experiments. Blood anti-coagulated with heparin was stored in citrate-phosphate-dextrose with adenine (CPDA-1) prior to use. RBCs were separated from plasma and leukocytes by washing three times with phosphate-buffered saline (127 mM NaCl, 2.7 mM KCl, 8.1 mM Na2HPO4, 1.5 mM KH2PO4, 20 mM HEPES, 1 mM MgCl2, and pH 7.4) supplemented with 5 mM glucose (PBS glucose) to obtain packed cells.

3.2. Microgravity Simulation

To verify whether RBCs could be affected by microgravity conditions, experiments were performed using a 3D random positioning machine (RPM, Fokker Space, Netherlands) at the laboratory of the Department of Biomedical Sciences, University of Sassari, Sardinia, Italy. The 3D RPM is a micro-weight (microgravity) simulator based on the principle of ‘gravity-vector-averaging’, built by Dutch Space. The 3D RPM is constituted by two perpendicular frames that rotate independently. The direction of the gravity vector is constantly changed so that the average of the gravity vector simulates a microgravity environment. The 3D RPM provides a simulated microgravity less than 10-3 g. The dimensions of the 3D RPM are of 1000 × 800 × 1000 mm (length × width × height). The 3D RPM is connected to a computer and through a specific software the mode and speed of rotation were selected. Random Walk mode with an 80 degree/sec (rpm) was chosen.

To simulate the effect of all the operating conditions, the following procedure was adopted.

Two millilitre tubes were carefully filled with packed RBCs and PBS-glucose (30% haematocrit) without air bubbles to avoid shearing of the fluid, in a dedicated room at 37 °C. Controls were placed in the static bar at 1g to undergo the same vibration of the sample under µg conditions. Different time points were set (0-6-9-12-24-36-48 h). Subsequently, RBCs were centrifuged and resuspended in 1mL of lysis buffer [5 mM Na2HPO4, 1 mM EDTA (pH 8.0)] and stored at −20 °C until use for further characterizations.

3.3. Confocal Microscopy Analysis

Once the experiments under micro and normal gravity conditions were performed at 0, 6, and 9 h, RBCs, after being fixed for 5 min in 0.5% acrolein in PBS, samples were rinsed three times, then permeabilized in PBS containing 0.1 M glycine (rinsing buffer) plus 0.1% Triton X-100 for 5 min and rinsed again 3× in rinsing buffer. To ensure complete neutralization of unreacted aldehydes, the cells were then incubated in rinsing buffer at room temperature for 30 min. After incubation, all nonspecific bindings were blocked by incubation for 60 min in blocking buffer (PBS containing 0.05 mM glycine, 0.2% fish skin gelatin and 0.05% sodium azide). Staining was performed using specific antibodies diluted in blocking buffer. After labelling, RBCs were allowed to attach to cover slips coated with poly-l-lysine, which were then mounted onto glass slides using Aqua-Mount (Lerner Laboratories, New Haven, CT, USA). Samples were imaged with a Leica TCS SP5 confocal microscope equipped with a 60 × 1.4 numerical aperture oil immersion lens.

3.4. Scanning electron microscopy (SEM) characterization

For three-dimensional SEM imaging and a fine resolution of erythrocytes structure, samples were fixed with 1% paraformaldehyde in 0.1 M Na-cacodylate buffer (pH 7.4) for 1 h at room temperature. After washing in Na-cacodylate buffer, samples have been decanted on microscope slides overnight. After numerous washes in PBS (Phosphate Buffered Saline), slides were dehydrated in ascending ethanol scales, dried at critical point in CO2 and then mounted on aluminium support (stub) with double-sided tape.

Finally, samples were covered with a gold conductive film and observed at SEM (ZEISS SIGMA 300).

3.5. Oxidative Stress Analysis

Oxidative stress analyses were performed in lysate red blood cells and/or plasma according to the manufacturer's instructions. Total antioxidant capacity (Cayman Antioxidant Assay kit 709001, Cayman Chemical) [38,39], reduced glutathione (GSH) (Cayman glutathione assay kit 703002, Cayman Chemical) [40,41], and thiobarbituric acid reactive substance (TBARS) (Cayman TBARS assay kit 10009055, Cayman Chemical) [38,39] were evaluated. Reactive oxygen species (ROS) level analysis was performed accordingly with method described by Tsamesidis et al. [14].

3.6. UHPLC-QTOF-MS Analysis

Prior to mass spectrometric analysis, 50 µL of human erythrocytes were extracted following the Folch procedure using 0.7 mL of a methanol and chloroform mixture (2/1, v/v). Samples were vortexed every 15 min up to 1 h, when 0.35 mL of chloroform and 0.15 mL of water were subsequently added. The solution was centrifuged at 12,000 rpm for 10 min, and 0.4 mL of the organic layer was transferred into a glass vial and dried under a nitrogen stream. The dried chloroform phase was reconstituted with 50 µL of a methanol and chloroform mixture (1/1, v/v) and 75 µL isopropanol:acetonitrile:water mixture (2:1:1 v/v). Quality control (QC) samples were prepared taking an aliquot of 10 µL of each sample. All samples thus prepared were injected in UHPLC-QTOF-MS/MS and acquired in negative ionization mode, while for positive ionization mode they were diluted in ratio 1:10. The chloroform phase was analysed with a LC-QTOF-MS coupled with an Agilent 1290 Infinity II LC system. An aliquot of 4.0 µL from each sample was injected in a Luna Omega C18, 1.6 µm, 100 mm × 2.1 mm chromatographic column (Phenomenex, Bologna, Italy). The column was maintained at 50 °C at a flow rate of 0.4 mL/min. The mobile phase for positive ionization mode consisted of (A) 10 mM ammonium formate solution in 60% of water and 40% of acetonitrile and (B) 10 mM ammonium formate solution containing 90% of isopropanol, 10% of acetonitrile. In positive ionization mode, the chromatographic separation was obtained with the following gradient: initially 80% of A, then a linear decrease from 80% to 50% of A in

2.1 min then at 30% in 10 min. Subsequently the mobile phase A was again decreased from 30% to 1% and was maintained at this percentage for 1.9 min and then brought back to the initial conditions in 1 min. The mobile phase for the chromatographic separation in the negative ionization mode differed only for the use of 10 mM ammonium acetate instead of ammonium formate. An Agilent jet stream source which was operated in both positive and negative ion modes with the following parameters: gas temperature, 200 °C; gas flow (nitrogen) 10 L/min; nebulizer gas (nitrogen), 50 psig; sheath gas temperature, 300 °C; sheath gas flow, 12 L/min; capillary voltage 3500 V for positive and 3000 V for negative; nozzle voltage 0 V; fragmentor 150 V; skimmer 65 V, octapole RF 7550 V; mass range, 50−1700 m/z; capillary voltage, 3.5 kV; collision energy 20 eV in positive and 25 eV in negative mode, mass precursor per cycle = 3. High purity nitrogen (99.999%) was used as a drift gas with a trap fill time and a trap release time of 2000 and 500 µs, respectively.

3.7. Multivariate Data Analysis

Mass spectrometric data acquired were pre-processed with the software MassHunter Workstation suite (Agilent Technologies, Santa Clara, CA, USA). This software (Mass Profiler 10.0) allowed us to perform mass deconvolution, yielding a matrix containing all features present across all samples. This matrix was further processed with a pipeline based on the KNIME analytic platform [42], KniMet for the post-processing of metabolomics MS-based data [43]. Features were filtered based on their presence in QC samples (threshold = 40%) and the remaining features were collected in a data matrix subsequently processed using SIMCA software 14.0 (Umetrics, Umeå, Sweden). First, a Principal Component Analysis (PCA) was carried out. This unsupervised statistical analysis allowed us to observe samples and variables distribution in the multivariate space based on their similarity and dissimilarity. This was followed by partial least square-discriminant analysis (PLS-DA) with its orthogonal extension (OPLS-DA).

4. Conclusions

In this work we investigated, using different approaches, the behaviour of human RBCs under simulated microgravity conditions. No significant changes were present at 1 g in different time points, while the performed investigations using SEM and confocal microscopy, ROS, TAC, GSH, and MDA analysis, and lipid profile evaluation demonstrated that samples exposed to simulated microgravity conditions exhibited remarkable changes in red cell cytoskeletal architecture and membrane stiffness.

This work represents the first step of our research group towards the understanding the behaviour of human cells under microgravity conditions. Work is underway not only to analyse additional cell types with particular emphasis towards those ones that might be more important for future human missions but also to involve institutions and researchers at the national and international levels to strengthen the cooperation in this crucial field of enquiry.

It is apparent that the implications of this research work and the corresponding future developments are related to the basic investigation of the intrinsic mechanisms underlying the behaviour of several human cell types under microgravity conditions which will be able to provide a useful contribution towards both the understanding and the potential prevention of classical health risks associated to the astronauts involved in deep space exploration scenarios.

Acknowledgments: We acknowledge the CeSAR (Centro Servizi d'Ateneo per la Ricerca) of the University of Cagliari, Italy for the IMQTOFMSMS experiments performed with an Agilent 6560. The authors would also like to thank Dr. Claudio Fozza for his scientific contribution. C.M and A.M, also acknowledge the PhD program in Innovation Science and Technologies available at University of Cagliari and Life Science and Biotechnologies available at University of Sassari, respectively.

References

1. Dinarelli, S.; Longo, G.; Dietler, G.; Francioso, A.; Mosca, L.; Pannitteri, G.; Boumis, G.; Bellelli, A.; Girasole, M. Erythrocyte's Aging in Microgravity Highlights How Environmental Stimuli Shape Metabolism and Morphology. *Sci. Rep.* **2018**, *8*, 5277. https://doi.org/10.1038/S41598-018-22870-0.

2. Qiang, Y.; Liu, J.; Dao, M.; Suresh, S.; Du, E. Mechanical Fatigue of Human Red Blood Cells. *Proc. Natl. Acad. Sci. USA* **2019**, *116*, 19828–19834. https://doi.org/10.1073/PNAS.1910336116/-/DCSUPPLEMENTAL.

3. Adamopoulos, K.; Koutsouris, D.; Zaravinos, A.; Lambrou, G.I. Gravitational Influence on Human Living Systems and the Evolution of Species on Earth. *Molecules* **2021**, *26*, 2784. https://doi.org/10.3390/MOLECULES26092784.

4. Guarnieri, S.; Morabito, C.; Bevere, M.; Lanuti, P.; Mariggiò, M.A. A Protective Strategy to Counteract the Oxidative Stress Induced by Simulated Microgravity on H9C2 Cardiomyocytes. *Oxidative Med. Cell. Longev.* **2021**, *2021*, 9951113. https://doi.org/10.1155/2021/9951113.

5. Girasole, M.; Cricenti, A.; Generosi, R.; Congiu-Castellano, A.; Boumis, G.; Amiconi, G. Artificially Induced Unusual Shape of Erythrocytes: An Atomic Force Microscopy Study. *J. Microsc.* **2001**, *204*, 46–52. https://doi.org/10.1046/J.1365-2818.2001.00937.X.

6. Boonstra, J. Growth Factor-Induced Signal Transduction in Adherent Mammalian Cells Is Sensitive to Gravity. *FASEB J. Off. Publ. Fed. Am. Soc. Exp. Biol.* **1999**, *13*, S35–S42. https://doi.org/10.1096/FASEBJ.13.9001.S35.

7. Schcolnik-Cabrera, A.; Labastida-Mercado, N.; Nancy, D.; Mercado, L. How Is Hematology Involved in the Era of Aerospace Medicine?: Systemic and Hematological Changes in the Astronaut. *Rev. Hematol. Mex.* **2014**, *15*, 122–128.

8. Schimmerling, W. Space and Radiation Protection: Scientific Requirements for Space Research. *Radiat. Environ. Biophys.* **1995**, *34*, 133–137. https://doi.org/10.1007/BF01211538.

9. Buonanno, M.; De Toledo, S.M.; Howell, R.W.; Azzam, E.I. Low-Dose Energetic Protons Induce Adaptive and Bystander Effects That Protect Human Cells against DNA Damage Caused by a Subsequent Exposure to Energetic Iron Ions. *J. Radiat. Res.* **2015**, *56*, 502–508. https://doi.org/10.1093/jrr/rrv005.

10. Garrett-Bakelman, F.E.; Darshi, M.; Green, S.J.; Gur, R.C.; Lin, L.; Macias, B.R.; McKenna, M.J.; Meydan, C.; Mishra, T.; Nasrini, J.; et al. The NASA Twins Study: A Multidimensional Analysis of a Year-Long Human Spaceflight. *Science* **2019**, *364*, eaau8650. https://doi.org/10.1126/SCIENCE.AAU8650/SUPPL_FILE/AAU8650_TABLE_S9.XLSX.

11. Afshinnekoo, E.; Scott, R.T.; MacKay, M.J.; Pariset, E.; Cekanaviciute, E.; Barker, R.; Gilroy, S.; Hassane, D.; Smith, S.M.; Zwart, S.R.; et al. Fundamental Biological Features of Spaceflight: Advancing the Field to Enable Deep-Space Exploration. *Cell* **2020**, *183*, 1162–1184. https://doi.org/10.1016/j.cell.2020.10.050.

12. Stein, T.P.; Leskiw, M.J. Oxidant Damage during and after Spaceflight. *Am. J. Physiol.—Endocrinol. Metab.* **2000**, *278*, 375–382. https://doi.org/10.1152/ajpendo.2000.278.3.e375.

13. Pizzino, G.; Irrera, N.; Cucinotta, M.; Pallio, G.; Mannino, F.; Arcoraci, V.; Squadrito, F.; Altavilla, D.; Bitto, A. Oxidative Stress: Harms and Benefits for Human Health. *Oxid. Med. Cell. Longev.* **2017**, *2017*, 8416763. https://doi.org/10.1155/2017/8416763.

14. Tsamesidis, I.; Egwu, C.O.; Pério, P.; Augereau, J.M.; Benoit-Vical, F.; Reybier, K. An LC–MS Assay to Measure Superoxide Radicals and Hydrogen Peroxide in the Blood System. *Metabolites* **2020**, *10*, 175. https://doi.org/10.3390/METABO10050175.

15. Remigante, A.; Morabito, R.; Marino, A. Band 3 protein function and oxidative stress in erythrocytes. *J. Cell. Physiol.* **2021**, *236*, 6225–6234. https://doi.org/10.1002/jcp.30322.

16. Pantaleo, A.; Ferru, E.; Pau, M.C.; Khadjavi, A.; Mandili, G.; Mattè, A.; Spano, A.; De Franceschi, L.; Pippia, P.; Turrini, F. Band 3 Erythrocyte Membrane Protein

Acts as Redox Stress Sensor Leading to Its Phosphorylation by p (72) Syk. *Oxid. Med. Cell. Longev*. **2016**, *2016*, 6051093. https://doi.org/10.1155/2016/6051093.

17. Morabito, R.; Remigante, A.; Marino, A. Protective Role of Magnesium against Oxidative Stress on SO4 = Uptake through Band 3 Protein in Human Erythrocytes. *Cell. Physiol. Biochem.* **2019**, *52*, 1292–1308. https://doi.org/10.33594/000000091.

18. Hughes-Fulford, M.; Tjandrawinata, R.; Fitzgerald, J.; Gasuad, K.; Gilbertson, V. Effects of Microgravity on Osteoblast Growth. *Gravit. Space Biol. Bull. Publ. Am. Soc. Gravit. Space Biol.* **1998**, *11*, 51–60.

19. Ivanova, S.M.; Morukova, B.V.; Maksimovb, G.V.; Bryzgalovab, N.Y.; Labetskayaa, O.I.; Yarlykovaa, Y.V.; Levina, A.A. Morphobiochemical Assay of the Red Blood System in Members of the Prime Crews of the International Space Station. *Hum. Physiol.* **2009**, *43*, 43–47.

20. Rizzo, A.M.; Corsetto, P.A.; Montorfano, G.; Milani, S.; Zava, S.; Tavella, S.; Cancedda, R.; Berra, B. Effects of Long-Term Space Flight on Erythrocytes and Oxidative Stress Of Rodents. *PLoS ONE* **2012**, *7*, e32361. https://doi.org/10.1371/journal.pone.0032361.

21. Alfrey, C.P.; Udden, M.M.; Leach-Huntoon, C.; Driscoll, T.; Pickett, M.H. Control of Red Blood Cell Mass in Spaceflight. *J. Appl. Physiol.* **1996**, *81*, 98–104. https://doi.org/10.1152/jappl.1996.81.1.98.

22. Kunz, H.; Quiriarte, H.; Simpson, R.J.; Ploutz-Snyder, R.; McMonigal, K.; Sams, C.; Crucian, B. Alterations in Hematologic Indices during Long-Duration Spaceflight. *BMC Hematol.* **2017**, *17*, 12. https://doi.org/10.1186/s12878-017-0083-y.

23. Trudel, G.; Shahin, N.; Ramsay, T.; Laneuville, O.; Louati, H. Hemolysis Contributes to Anemia during Long-Duration Space Flight. *Nat. Med.* **2022**, *28*, 59–62. https://doi.org/10.1038/s41591-021-01637-7.

24. Charles, J.; Bungo, M.; Fortner, G. Cardiopulmonary Function. In *Space Physiology and Medicine*, 3rd ed.; Lea & Febiger: Philadelphia, PA, USA, 1994.

25. Risso, A.; Ciana, A.; Achilli, C.; Antonutto, G.; Minetti, G. Neocytolysis: None, One or Many? A Reappraisal and Future Perspectives. *Front. Physiol.* **2014**, *5*, 54. https://doi.org/10.3389/fphys.2014.00054.

26. Unsworth, B.R.; Lelkes, P.I. Growing Tissues in Microgravity. *Nat. Med.* **1998**, *4*, 901–907. https://doi.org/10.1038/NM0898-901.

27. Van Loon, J.J.W.A. Some History and Use of the Random Positioning Machine, RPM, in Gravity Related Research. *Adv. Space Res.* **2007**, *39*, 1161–1165. https://doi.org/10.1016/j.asr.2007.02.016.

28. Herranz, R.; Anken, R.; Boonstra, J.; Braun, M.; Christianen, P.C.M.; De Geest, M.; Hauslage, J.; Hilbig, R.; Hill, R.J.A.; Lebert, M.; et al. Ground-Based Facilities for Simulation of Microgravity: Organism-Specific Recommendations for Their Use, and Recommended Terminology. *Astrobiology* **2013**, *13*, 1–17. https://doi.org/10.1089/AST.2012.0876.

29. Wuest, S.L.; Richard, S.; Kopp, S.; Grimm, D.; Egli, M. Simulated Microgravity: Critical Review on the Use of Random Positioning Machines for Mammalian Cell Culture. *BioMed Res. Int.* **2015**, *2015*, 971474. https://doi.org/10.1155/2015/971474.

30. Serova, L.V.; Leon, G.A.; Chel'naia, N.A.; Sidorenko, L.A. The Effect of Weightlessness on Erythrocyte Resistance In Vivo and In Vitro—PubMed. Available online: https://pubmed.ncbi.nlm.nih.gov/8012303/ (accessed on).

31. Buys, A.V.; Van Rooy, M.J.; Soma, P.; Van Papendorp, D.; Lipinski, B.; Pretorius, E. Changes in Red Blood Cell Membrane Structure in Type 2 Diabetes: A Scanning Electron and Atomic Force Microscopy Study. *Cardiovasc. Diabetol.* **2013**, *12*, 25. https://doi.org/10.1186/1475-2840-12-25.

32. Girasole, M.; Pompeo, G.; Cricenti, A.; Congiu-Castellano, A.; Andreola, F.; Serafino, A.; Frazer, B.H.; Boumis, G.; Amiconi, G. Roughness of the Plasma Membrane as an Independent Morphological Parameter to Study RBCs: A Quantitative Atomic Force Microscopy Investigation. *Biochim. Biophys. Acta* **2007**, *1768*, 1268–1276. https://doi.org/10.1016/J.BBAMEM.2007.01.014.

33. Bennett-Guerrero, E.; Veldman, T.H.; Doctor, A.; Telen, M.J.; Ortel, T.L.; Reid, T.S.; Mulherin, M.A.; Zhu, H.; Buck, R.D.; Califf, R.M.; et al. Evolution of Adverse Changes in Stored RBCs. *Proc. Natl. Acad. Sci. USA* **2007**, *104*, 17063–17068. https://doi.org/10.1073/PNAS.0708160104.

34. Ferru, E.; Giger, K.; Pantaleo, A.; Campanella, E.; Grey, J.; Ritchie, K.; Vono, R.; Turrini, F.; Low, P.S. Regulation of Membrane-Cytoskeletal Interactions by Tyrosine Phosphorylation of Erythrocyte Band 3. *Blood* **2011**, *117*, 5998–6006. https://doi.org/10.1182/BLOOD-2010-11-317024.

35. Pantaleo, A.; De Franceschi, L.; Ferru, E.; Vono, R.; Turrini, F. Current Knowledge about the Functional Roles of Phosphorylative Changes of Membrane Proteins in Normal and Diseased Red Cells. *J. Proteom.* **2010**, *73*, 445–455. https://doi.org/10.1016/J.JPROT.2009.08.011.

36. Li, B.B.; Chen, Z.Y.; Jiang, N.; Guo, S.; Yang, J.Q.; Chai, S.B.; Yan, H.F.; Sun, P.M.; Hu, G.; Zhang, T.; et al. Simulated Microgravity Significantly Altered Metabolism in Epidermal Stem Cells. *In Vitr. Cell. Dev. Biol.—Anim.* **2020**, *56*, 200–212. https://doi.org/10.1007/s11626-020-00435-8.

37. Chen, Z.Y.; Jiang, N.; Guo, S.; Li, B.B.; Yang, J.Q.; Chai, S.B.; Yan, H.F.; Sun, P.M.; Zhang, T.; Sun, H.W.; et al. Effect of Simulated Microgravity on Metabolism of HGC-27 Gastric Cancer Cells. *Oncol. Lett.* **2020**, *19*, 3439–3450. https://doi.org/10.3892/ol.2020.11451.

38. Armstrong, D.; Browne, R. The Analysis of Free Radicals, Lipid Peroxides, Antioxidant Enzymes and Compounds Related to Oxidative Stress as Applied to the Clinical Chemistry Laboratory. *Adv. Exp. Med. Biol.* **1994**, *366*, 43–58. https://doi.org/10.1007/978-1-4615-1833-4_4.

39. Yagi, K. Simple Assay for the Level of Total Lipid Peroxides in Serum or Plasma. *Methods Mol. Biol.* **1998**, *108*, 101–106. https://doi.org/10.1385/0-89603-472-0:101.

40. Eyer, P.; Podhradský, D. Evaluation of the Micromethod for Determination of Glutathione Using Enzymatic Cycling and Ellman's Reagent. *Anal. Biochem.* **1986**, *153*, 57–66. https://doi.org/10.1016/0003-2697(86)90061-8.

41. Baker, M.A.; Cerniglia, G.J.; Zaman, A. Microtiter Plate Assay for the Measurement of Glutathione and Glutathione Disulfide in Large Numbers of Biological Samples. *Anal. Biochem.* **1990**, *190*, 360–365. https://doi.org/10.1016/0003-2697(90)90208-Q.

42. Berthold, M.R.; Hand, D.J. *Intelligent Data Analysis*; Springer: Berlin/Heidelberg, Germany, 2003. https://doi.org/10.1007/978-3-540-48625-1.

43. Liggi, S. *Sonial/KniMet: First Release of KniMet (Version v1.2.0): Zenodo*; https://doi.org/10.5281/Zenodo.11964 07.2018.

Chapter 6

CE-MS metabolomics of human plasma under simulated microgravity conditions

Cristina Manis[1,3], Carolina Gonzalez-Riano[2], Angeles Lopez-Gonzalvez[2], Coral Barbas[2], Antonella Pantaleo[2], Giacomo Cao[3], Pierluigi Caboni[*1]

[1]Department of Life and Environmental sciences, Cittadella Universitaria di Monserrato, Blocco A, Room 13, 09042, Monserrato, Italy

[2] Centre for Metabolomics and Bioanalysis (CEMBIO), Facultad de Farmacia, Universidad CEU San Pablo, Madrid, Spain.

[3] Department of Mechanical, Chemical and Materials Engineering, University of Cagliari, Piazza d'Armi, 09123 Cagliari, Italy.

[4] Department of Biomedical Science, University of Sassari, Viale San Pietro, 07100 Sassari, Italy.

[ǂ]Corresponding author:

Prof. Pierluigi Caboni,

Department of Life and Environmental sciences, Cittadella Universitaria di Monserrato,

Blocco A, Room 13, 09042, Monserrato, Italy

Tel. 0039 070 6758617, Fax 0039 070 6758612,

email: caboni@unica.it

Running head: Metabolomics of human plasma under microgravity conditions.

Abstract

The absence of gravity is considered as an extreme biological stressor and the human body's adaptive response to microgravity conditions triggers a series of metabolic rewiring that are often associated with bone density loss, skeletal muscle atrophy, nervous system dysfunction, and anemia. To investigate the biological mechanisms underlying aerospace anemia we used an analytical metabolomics approach to study the biological changes of human plasma subjected to simulated microgravity conditions. Metabolomics analysis revealed that microgravity induced an increase of glycolysis, Krebs cycle and fatty acids β-oxidation perturbations, and lactic acid production. Overall, these findings indicate an evident damage of circulating mitochondria causing a defective respiratory chain, oxidative environment, and incomplete β-oxidation of fatty acids with consequent accumulation of carnitines.

Key Words: capillary electrophoresis, mass spectrometry, multivariate analysis, clinostat.

1. Introduction

Bioastronautics is a discipline, developed by NASA, dealing with the study of the biological and medical effects of space flight on human beings. In this context, astronauts are considered a critical space flight system as well as propulsion, thermal and power systems. In order to develop space flight guidelines able to optimize the performance and health of astronauts[1], it would be necessary to clearly know the mechanisms underlying the physiological changes that occur in astronauts during the space missions. All space travelers are exposed to several risks or stressors, i.e. gravity, radiation, hostile enclosed environment and distance from Earth, that depend on the design of their space mission [2].

Life and, consequently, the structure and physiology of the human body, have developed and adapted, during of evolution, in constant presence of gravity conditions. For this reason, when the gravitational force no longer acts on the body, drastic changes occur. Some of these changes occur immediately, others progress only slowly [3], and, more worryingly some remain for shorter or longer time after their return to Earth [4].

Astronauts returning from missions show an overall health condition similar to aging [5] with main clinical disorders including bone and muscle mass loss [6], immune dysfunction [7], central nervous system [2] and cardiovascular disorders [8]. Additionally, astronauts develop several haematological abnormalities, anaemia [9], thrombocytopenia, and modifications of red blood cell structure [10][11][12], reduction of plasma volume by 10-17% and hemolysis [13]. Furthermore, it is not known whether hemolysis occurs at an intravascular or extravascular level, in the spleen, liver or bone marrow [4] while pseudopolycythemia in astronauts occur due to the rapid redistribution of blood and the increase in renal function. According to Leach and Johnson [14] Trudel et al. showed, a reduction of 54% in red blood cells during spaceflight when compared to gravity experienced on Earth [15]. A major advance for the future in long-term space exploration requires a thorough understanding of the impact of space flight on human physiology [16] and in particular their mechanisms at cellular levels.

In our previous work we reported how after six hours of simulated gravity, the erythrocytes morphologically changed at the level of the plasma membrane. These alterations progress over time leading the erythrocyte death [12]. In order to investigate the biological mechanisms underlying aerospace anemia we used an analytical

metabolomics approach to study the biological changes of human plasma subjected to simulated microgravity conditions. To achieve this, plasma samples were submitted to a metabolomics workflow using capillary electrophoresis coupled to mass spectrometry and multivariate data analysis.

2. Materials and methods

2.1. Chemicals. Analytical LC grade methanol, chloroform, acetonitrile and formic acid were purchased from Sigma Aldrich (Milan, Italy). Methionine sulfone as IS (99% purity), MES and paracetamol were acquired from Sigma (Steinheim, Germany); and sodium hydroxide was acquired from Panreac, (Barcelona, Spain). Ultrapure water was used to prepare the aqueous solution, this was obtained from a Milli-Q® system (Millipore, Billerica, MA, USA).

2.2. Plasma samples. Freshly drawn blood (Rh+) from healthy adult volunteers (men and women), heparin was added and preserved in citrate-phosphate-dextrose with adenine (CPDA-1). Plasma samples and RBCs were separated by washing three times with phosphate-buffered saline as reported in Manis et al. This study was conducted in accordance with Good Clinical Practice guidelines and the Declaration of Helsinki. No ethical approval has been requested and patients provided written, informed consent to the Azienda Sanitaria Locale (Sassari) before entering the study.

2.3. Microgravity simulation. Microgravity experiments were performed using a 3D random positioning machine (RPM, Fokker Space, Netherlands). The 3D Random Positioning Machine (RPM) is a micro-weight simulator based on the "gravity vector mean" principle providing simulated microgravity of less than 10-3g selecting the Random Walk mode with 80 degrees/sec (Leiden, The Netherlands). The 3D RPM consists of two perpendicular frames that rotate independently. The direction of the gravity vector is constantly changed so that the gravity vector average simulates a microgravity environment.

Practically, 2 mL tubes were carefully filled with bubble-free human plasma in a dedicated room at 37° C. Control samples were placed in the static bar at 1 g to undergo the same vibration of the samples subjected to the µg conditions. Different sampling time points were chosen (0, 6, 9, 24 h). After the experiments samples were centrifuged and stored at -20 ° C until use for metabolomics analysis.

2.4. CE-MS Analysis

2.4.1. Sheath liquid preparation and BGE. Sheath liquid consisted of a water/methanol (1:1 *v/v*) mixture, containing purine, phosphazene, hexakis(1H,1H,3H-

tetrafluoropropoxy) as reference compounds (Agilent Technologies, Santa Clara, CA, USA). Sheath liquid was freshly prepared and degassed by sonication for 5 min before use. Background electrolyte (BGE) solution was prepared using formic acid (1.0 M) in ultrapure water with MeOH 10% (*v/v*). The apparent pH of the BGE was 2.04.

2.4.2. Sample preparation for CE-MS analysis. Prior to the CE-MS analysis, 50 µL of human plasma solution were extracted following the Folch procedure using 0.700 mL of a methanol and chloroform mixture (1:1, *v/v*). Samples were vortexed every 15 min up to 1 h, when 0.350 mL of chloroform and 0.150 mL of fresh ultrapure water were subsequently added. The solution was centrifuged at 12,000 rpm for 10 min, and 0.200 mL of the aqueous phase was transferred into a glass vial and dried under a gentle nitrogen stream. The dried aqueous phase was reconstituted with 75 µL of a standard mix solution consisting of formic acid (0.025M), methionine sulfone (0.2mM), 2-(N-morpholino) ethanesulfonic acid (MES) (0.2mM) and paracetamol (1mM) and vortexed for 30 min. At this point, 0.175 mL of a methanol and water mixture (3:1, v/v) was added to each sample and vortexed again for 20 min. Then, 0.240 mL of the supernatant was taken from each sample, deposited in new eppendorf and placed in a desiccator (Hyper Vac) for 4 h at 40° C. Samples were reconstituted with 0.075 mL of an aqueous solution of 0.025 M formic acid and vortexed for 20 min. Subsequently, the samples were centrifuged for 10 min at 16000 rpm and at 4° C. Finally, the supernatant of each sample was collected and transferred to the respective vial of CE. Quality control (QC) samples were prepared taking an aliquot of 5 µL of each sample. All samples thus prepared were injected in CE-MS and acquired in positive and negative ionization mode.

2.4.3. CE-MS analysis of cationic metabolites. The samples were analyzed by CE (7100 Agilent) coupled to a MS with time-of-flight analyzer, TOF-MS (6230 Agilent). The coupling was performed with an electrospray source, using a sheath liquid to compensate the volume and increase the necessary volatility for MS. This auxiliary liquid was supplied by an isocratic pump (1260 Infinity II Agilent).

Metabolite separation was performed in a fused silica capillary (100 cm x 50 µm i.d. x 360 µm o.d., Agilent Technologies), previously conditioned with NaOH, water and background

electrolyte (BGE). Before each analysis, the BGE was automatically replaced. The capillary was then rinsed for 5 min (950 mbar) with BGE, and a voltage of 30 kV was

applied for 10 s in order to displace the BGE ions. Then the sample was introduced applying 50 mbar for 50 s and then BGE was introduced for 20 s at 100 mbar. The separation was achieved in the capillary by means of a pressure of 25 mbar and a voltage of 30 kV, the current observed under these conditions was 23 µA.

Once the separated compounds from the sample leave the capillary, a positively charged spray is formed by a flow of 0.6 mL min^{-1} (1:100 split) of the auxiliary liquid a nebulization pressure of 10 psig with nitrogen and voltages: capillary voltage 3500 V. This spray was dried with a hot nitrogen flow of 10 mL min^{-1} at 200°C. The ions formed in the gaseous state were directed to the TOF by the following fragmentor voltages: (125 V and 200 V), skimmer (65 V) and octopole (750 V). The data was collected in the ESI (+) positive ion mode and mass range from 50 and 1050 *m/z* was acquired at a scanning rate of 1.02 scans/s. CE-MS system was controlled and monitored by MassHunter Workstation (Agilent Technologies). Two voltages were used in the fragmentor: i) 125 V for adducts, dimmers and transformation data (MS1); and ii) 200 V for the acquisition of in-source fragment ions (pseudo-MS/MS).

2.4.4. CE-MS analysis of anionic metabolites. A fused-silica capillary (Agilent Technologies) (100 cm; i.d., 50 µm) was used for the separation in normal polarity with a background electrolyte containing 50 mM ammonium acetate solution (pH=8.5). Samples were hydrodynamically injected at 50 mBar for 35 s. The stacking was carried out by applying the background electrolyte (BGE) at 100 mBar for 20 s. The separation voltage was 30 kV. The internal pressure was 50 mbar, and the analyses were carried out in 50 min. The current observed during the experiment under these conditions was 30 µA. The sheath liquid was continuously infused at 10 µL min^{-1} and consisted of methanol/water (1:1 *v/v*) containing 2.5 mM ammonium acetate solution (pH=8.5) and purine and HP-0921 as reference masses. MS acquisition was conducted in the negative ion mode, and the parameters were: drying gas temperature, 250 °C; nebulizer pressure, 10 psi; flow rate, 10 L min^{-1}; capillary voltage, 4000 V; fragmentor, 120 V; skimmer, 65 V; and octupole, 750 V. Data were acquired with a full scan from *m/z* 60 to 1000 at a rate of 1.41 scan s^{-1}.

2.5. Data analysis.

CE-MS data acquired in positive and negative ionization modes, were pre-processed with the software Mass Profinder 10.0 (Agilent Technologies, Santa Clara, USA) for time alignment and deconvolution of signals. The removal of background noise and unrelated ions was performed by recursive feature extraction tool, yielding a matrix containing all the features present across all samples. With the aim to minimize the observed instrumental variation data were normalized using the Quality Control Samples and Vector Regression Support (QC-SVRC) algorithm (Kuligowski et al., 2015). The SVR algorithm uses a radial-based function kernel to fix the instrumental drift within a sample using data acquired from quality control samples. Furthermore, in order to eliminate non-specific information, data matrix quality assurance was performed. This filtered matrix was then subjected to multivariate statistical analysis using SIMCA software 16.0 (Umetrics, Umeå, Sweden). First, a Principal Component Analysis (PCA) was carried out. This unsupervised analysis allowed us to observe samples and variables distribution in the multivariate space based on their similarity and dissimilarity. This was followed by partial least square-discriminant analysis (PLS-DA) with its orthogonal extension (OPLS-DA), which was used as classificatory model to visualize and evaluate the differences between sample classes. The quality of the models was evaluated based on the cumulative parameters R^2Y and Q^2Y and the variable importance in projection (VIP) scores in the predictive component of pairwise OPLS-DA were analyzed and only the metabolites having VIP values > 1 were considered as discriminant.

Furthermore, in the specific case of our study, we were interested in evaluating the combined effect of two experimental factors, for example, the condition of microgravity to which the samples were subjected and the time that the samples remained in this condition, to highlight possible interactions. A two-way ANOVA was performed to discern the effect microgravity and time variables using MATLAB (Mathworks, Inc., Natick, USA).

Finally, metabolite percentage change was calculated by comparing case vs. control sample. The metabolites that turned out to be statistically significant (p-value < 0.05) and showed % change >20% were tentatively annotated through databases available online (CEU mass mediator) [18].

3. Results

3.1. Untargeted CE-MS analysis

Untargeted metabolomics analysis of 32 human plasma samples, performed by capillary electrophoresis coupled to high-resolution mass spectrometry (QTOF-MS) provided an overview of the plasma metabolites changes in a simulated microgravity environment. Data processing yielded 233 and 78 features for positive (PIA) and negative ionization analysis (NIA), respectively, which were then subjected to multivariate statistical analysis (MVA). We initially performed a principal component analysis (PCA) on the molecular features across all the sampling times (0, 6, 9, 24 h) to evaluate differences between the samples. After data normalization, the unsupervised PCA analysis of both PIA and NIA was performed. Interestingly, the PCA plots presented a tight clustering of the QC samples, revealing that the instrumental variation detected was effectively corrected (**Figure 1**).

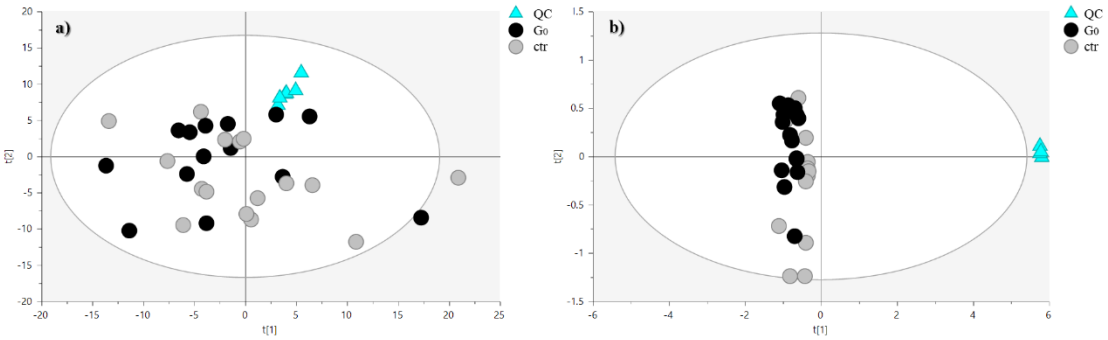

Figure 1. PCA-X score plot. ***a)*** *represent the PCA-X model for CE–MS ESI (+), (R2X =0.671, Q2= 0.35);* ***b)*** *represent the PCA-X model for CE–MS ESI (−), (R2X= 0.927 and Q2= 831). Both models showed very good QC clustering, thereby indicating good system stability and reliability of the results (black circles, human plasma samples subjected at gravity G_0; grey circles, human plasma samples subjected at gravity G_1 (control samples); blue triangles, QCs).*

However, due to the large difference between QCs (external QCs in NIA model) and real samples was very difficult to assess the separation for the two classes of samples. For this reason, another PCA analysis was performed after removing the QCs (**Figure 1.1**). Furthermore, the arrangement of the samples in the multivariate space (**Figure 1.1**) did not show any samples clustering.

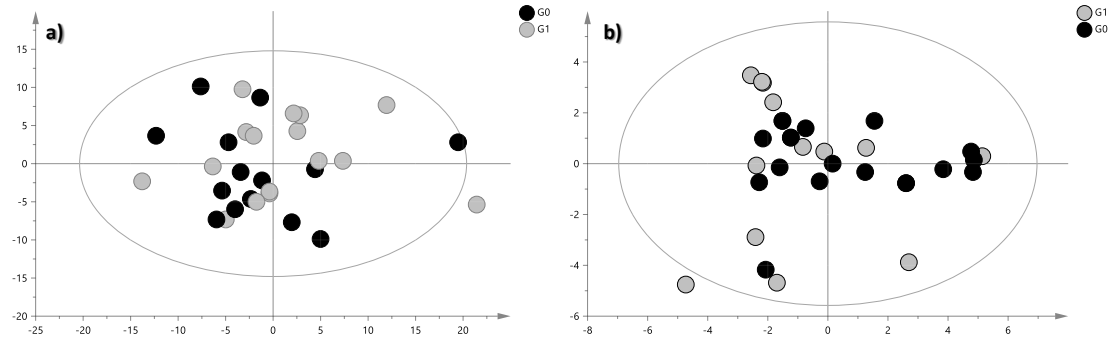

Figure 1.1 PCA-X score plot after removing QC samples. ***a)*** *represent the PCA-X model for CE–MS ESI (+), (R2X =0.665, Q2= 0.258);* ***b)*** *represent the PCA-X model for CE–MS ESI (−), (R2X= 0.546 and Q2= 0.16). The black circles, human plasma samples subjected at gravity G_0; while grey circles human plasma samples subjected at gravity G_1 (control samples).*

We then hypothesized the influence of the sampling time as the main driving factor affecting the metabolic changes, and thus we performed a Partial Least Square-Discriminant Analysis (PLS-DA). The validation parameters of PIA and NIA models built for the samples collected at 6 h showed a good classifying power and a good predictive ability (R^2X= 0.648; R^2Y= 0,987; Q^2= 0.597; R^2X= 0.857; R^2Y= 0,995; Q^2= 0.898, respectively). Also, the statistical model at 9 h showed good quality parameters values (R^2X= 0.484; R^2Y= 0,995; Q^2= 0.167 and R^2X = 0.915; R^2Y = 0,998; Q^2 = 0.982, for PIA and NIA respectively). Likewise, the supervised model at 24 h, showed good quality parameters values of explained variance (PIA: R^2X = 0.459; R^2Y = 0,992; and NIA: R^2X = 0.846; R^2Y = 0,989) and predicted variance (PIA: Q^2 = 0.754; and NIA: 0.766). Furthermore, an OPLS-DA was performed to find discriminant metabolites. The score plots of these statistical models for the positive and negative ionization are reported in **Figure 2.1** and **2.2**, respectively.

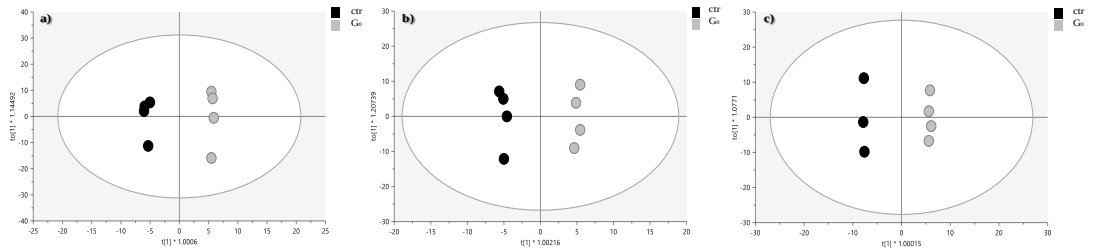

Figure 2.1. Supervised OPLS-DA plot of CE–MS (+) data analysis. *The models presented good quality of variance explained and predicted variance:* ***a)*** *samples subjected at six hours of clinorotation vs relative control samples (R2X = 0.771, R2Y = 0.997, Q2 = 0.573);* ***b)*** *samples subjected at nine hours of clinorotation vs relative control samples (R2X = 0.484, R2Y = 0.995, Q2 = 0.268) and* ***c)*** *samples subjected at twenty-four hours of clinorotation vs relative control samples (R2X = 0.797, R2Y = 0.998, Q2 = 0.945); black circles, human plasma samples subjected at gravity G_0; grey circles, human plasma samples subjected at gravity G_1 (control samples).*

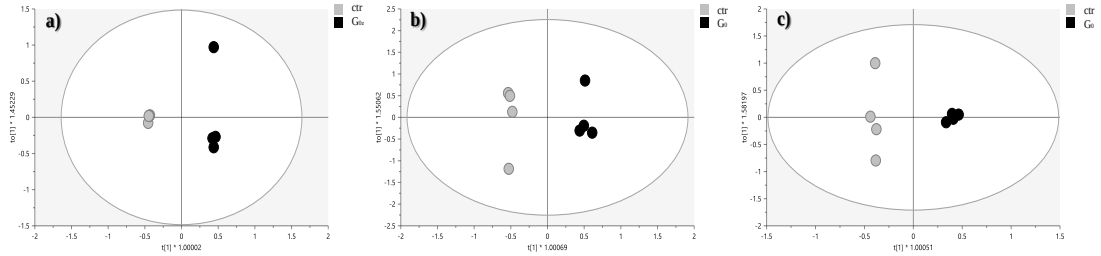

Figure 2.2. Supervised OPLS-DA plot of CE–MS (-) data analysis. *The models presented good quality of variance explained and predicted variance:* ***a)*** *samples subjected at six hours of clinorotation vs relative control samples (R2X = 0.935, R2Y = 0.999, Q2 = 0.985);* ***b)*** *samples subjected at nine hours of clinorotation vs relative control samples (R2X = 0.913, R2Y = 0.992, Q2 = 0.826) and* ***c)*** *samples subjected at twenty-four hours of clinorotation vs relative control samples (R2X = 0.828, R2Y = 0.992, Q2 = 0.447); black circles, human plasma samples subjected at gravity G_0; grey circles, human plasma samples subjected at gravity G_1 (control samples.*

Lastly, based on the prediction coefficients of the OPLS-DA models the most relevant metabolites among the different groups of samples were evidenced. From the OPLS-DA model, metabolites presenting variable importance in projection (VIP)>1, *p* value <0.05 and change variation >20% were selected as statistically significant. For each experiment time point (6, 9, 24 h), annotated discriminants metabolites are reported in **Table 1.**

Table 1: *Metabolites that showed statistical significance when comparing clinorotated samples and controls*.

Metabolite	*m/z*	Formula	RT (min)	RMT	Error (ppm)	VIP	% change	p *value*	polarity
6 h									
Propionylcarnitine	218.1382	$C_{10}H_{19}NO_4$	11.23	0.71	2	2.53	-100.0	0.002	+
Acetylcarnitine	204.1231	$C_9H_{17}NO_4$	12.91	0.82	0	1.66	-51.1	0.058	+
Aspartic acid	134.0433	$C_4H_7NO_4$	18.61	0.78	6	1.04	-18.2	0.033	+
Tyrosine	182.0803	$C_9H_{11}NO_3$	15.26	0.64	5	0.71	-33.4	-	+
Fumaric Acid	115.0037	$C_4H_4O_4$	14.96	0.68	0	2.60	+282.4	0.003	-
Pyruvic acid	87.0088	$C_3H_4O_3$	15.55	0.71	2	2.54	+272.1	0.001	-
Glucose	179.0561	$C_6H_{12}O_6$	17.31	0.79	2	1.17	-41.5	0.034	-
Succinic acid	117.0193	$C_4H_6O_4$	17.15	0.78	7	1.25	+59.3	0.05	-
Malic acid	134.021	$C_4H_6O_5$	16.73	0.76	4	0.88	+51.9	0.004	-
Citric acid	191.0197	$C_6H_8O_7$	16.35	0.74	1	1.04	+67.7	-	-
Lactic acid	89.0245	$C_3H_6O_3$	17.02	0.77	1	0.73	-30.7	0.012	-
9 h									
Propionylcarnitine	218.1382	$C_{10}H_{19}NO_4$	11.23	0.71	2	1.90	-89.6	0.029	+
Tryptophanyl-cysteinyl-glutamine	436.167	$C_{19}H_{25}N_5O_5S$	23.94	1.51	5	1.88	-33.3	0.028	+
Succinic acid	117.0193	$C_4H_6O_4$	17.15	0.78	7	3.22	+108.0	0.002	-
Fumaric Acid	115.0037	$C_4H_4O_4$	14.96	0.68	0	2.57	+198.4	0.0004	-
Glucose	179.0561	$C_6H_{12}O_6$	17.31	0.79	2	1.53	-62.9	0.0003	-
Malic acid	134.021	$C_4H_6O_5$	16.73	0.76	4	0.65	+26.8	0.0023	-
Aminobutyric acid	102.0561	$C_4H_9NO_2$	24.33	1.11	2	0.64	-25.5	0.034	-
Citric acid	191.0197	$C_6H_8O_7$	16.35	0.74	1	0.85	+115.6	-	-
Lactic acid	89.0245	$C_3H_6O_3$	17.02	0.77	1	0.29	-23.8	0.029	-
24 h									
Propionylcarnitine	218.1382	$C_{10}H_{19}NO_4$	11.23	0.71	2	2.18	+113.6	0.000002	+
5,6-dihydrothymine	129.054	$C_5H_8N_2O_2$	23.93	1.51	5	2.01	-25.4	0.0023	+
unknown	274.0411		24.12	1.01		1.64	-33.0	0.025	+
Adenosine	268.1041	$C_{10}H_{13}N_5O_4$	23.98	1.51	0	1.47	-42.1	0.054	+
Alanine	90.0552	$C_3H_7NO_2$	12.93	0.54	3	0.72	+42,4	-	+
Uric acid	167.0211	$C_5H_4N_4O_3$	17.28	0.79	2	2.94	+173.8	0.007	-
Glucose	179.0561	$C_6H_{12}O_6$	17.31	0.79	2	1.81	-55.3	0.008	-
Aminobutyric acid	102.0561	$C_4H_9NO_2$	24.33	1.11	4	1.38	+59.5	0.0257	-
α-ketoglutaric acid	145.0142	$C_5H_6O_5$	16.35	0.75	4	1.34	-45.9	0.026	-
Glutamic acid	146.0455	$C_5H_9NO_4$	24.34	1.11	0	0.75	+88.3	0.078	-
Lactic acid	89.0245	$C_3H_6O_3$	17.02	0.77	1	-	+94.3	0.011	-
Citric acid	191.0197	$C_6H_8O_7$	16.35	0.74	1	0.83	+47.5	-	-

RT retention time expressed in minutes, relative migration time (RMT) based on the migration time of the internal standard added to each sample, % change percentage of change calculated between clinorotated and controls samples, the sign (−) indicates that this metabolite is less abundant in clinorotated samples than in controls and the sign (+) indicates that this metabolite is more abundant in clinorotated than in the controls samples, p-value obtained with the ANOVA test, VIP variable of importance in projection.

Propionyl carnitine was found downregulated on plasma samples after 6 and 9 h, while upregulated at 24 h of clinorotation with percentage change of -100.0, -89.6 and 113.6, respectively.

Furthermore, levels of Krebs metabolites such as pyruvic acid, succinic acid, malic acid and α-ketoglutaric acid were found profoundly affected during the experiment. In particular, after 6 h, pyruvic acid levels were found higher in clinorotated samples with a % change of 272.1 while at 9 h this alteration was not statistically relevant. Fumaric acid, succinic acid and malic acid were upregulated in the clinorotated samples when compared to controls showing percent change of 198.4, 108.0 and 26.8, respectively. Furthermore, uric acid was detected as discriminant metabolite only after 24 h of clinorotation, % change of 173.8, while glucose was *down*-regulated in clinorotated samples at all time-points analyzed.

4. Discussions

The exposure to real or simulated microgravity is sensed as a stress factor by mammalian cells which trigger an adaptative response. After spaceflights, astronauts show different health problems thus over the years researchers have been involved in studying the effects of microgravity at the cellular level using human or animal differentiated cell lines and stem cells. For this reason, different cell lines were studied under simulated gravity conditions, revealing that microgravity is responsible for energy imbalances and cellular damage. In particular, oxidative stress caused by microgravity induced retinal damage and degeneration [19], and alterations of microtubule organization [20], oxidative phosphorylation, glycolysis, and TCA proteins expression [21]. Additionally, oxidative stress altered: the growth and physiology of cells through impacting on intracellular signaling mechanisms [22]; cell secretions, gene expression [23]; and mitochondrial dysfunction [24][25]. Despite a plethora of scientific studies biological processes involved in these alterations remain today unclear.

Currently, no studies have been reported on the metabolic changes of human plasma under microgravity conditions while is known that biochemical composition of plasma can influence the morphology and physiology of differentiated cells [26]. For these reasons, the purpose of this study was to understand the plasma metabolite changes in microgravity conditions and eventually broaden the knowledge of the plasma biochemical alterations. To investigate the microgravity-induced perturbations on human plasma, which is known to contain circulating mitochondria and extracellular exosomes able to perform glycolysis [27][28], a metabolomics comparison was carried out comparing plasma metabolomes from normo- and microgravity.

Multivariate statistical analyses were employed for the CE-MS data sets. After 6 h of clinorotation, we observed how under microgravity conditions, the Kreb's cycle was activated, as indicated by the up-regulation of pyruvic and fumaric acid and a concomitant down-regulation of glucose levels (**Table 1**).

It is known that the microgravity conditions influence the consumption and, consequently, the synthesis of ATP. Dinarelli et al., highlighted how the ATP cellular consumption in microgravity conditions is faster than in the control samples [29]. This evidence may explain how the microgravity condition causes the increase of the Krebs cycle activity to produce more ATP. However, it has become clear that other than energy

generation, mitochondrion produces reactive oxygen species as “side products” of respiration.

After 9 h of microgravity, human plasma samples still showed an upregulation of the Krebs cycle substrates. Indeed, the multivariate statistical analysis carried out at this time point, showed that succinic acid, fumaric acid and malic acid were up regulated, while lactic acid was downregulated. However, considering metabolites percent change value, we can hypothesize that the Krebs cycle activity after 9 h of clinorotation seems to be less marked compared to 6 h. Furthermore, it is important to underline that at 9 h, pyruvic acid is no longer a discriminant, while at 24 h, Krebs cycle metabolites are no longer discriminants. Interestingly at 24 h lactic acid was upregulated by 94%.

In mitochondria-containing cells and in aerobic conditions, pyruvate can enter the citric acid cycle within the mitochondrial matrix and undergo oxidative phosphorylation. However, under oxygen-deficient conditions, the pyruvate produced by glycolysis no longer enters the TCA cycle in the mitochondria but remains within the cytoplasm and is converted to lactate regenerating NAD^+ necessary for the first reactions of glycolysis [30].

Under microgravity conditions, the alteration of the cytoskeleton disrupts the mitochondrial structure, reducing mitochondrial content, oxygen consumption and respiratory capacity [25]. Furthermore, defects of the mitochondrial respiratory chain are often associated with an increased lactic acid/pyruvic acid ratio (L:P) [31]. In our study the L:P ratio was significantly altered in human plasma samples exposed to 24 h of simulated gravity (**Figure 3**), indicating a shift from aerobic to anaerobic energy metabolism (**Figure 4**).

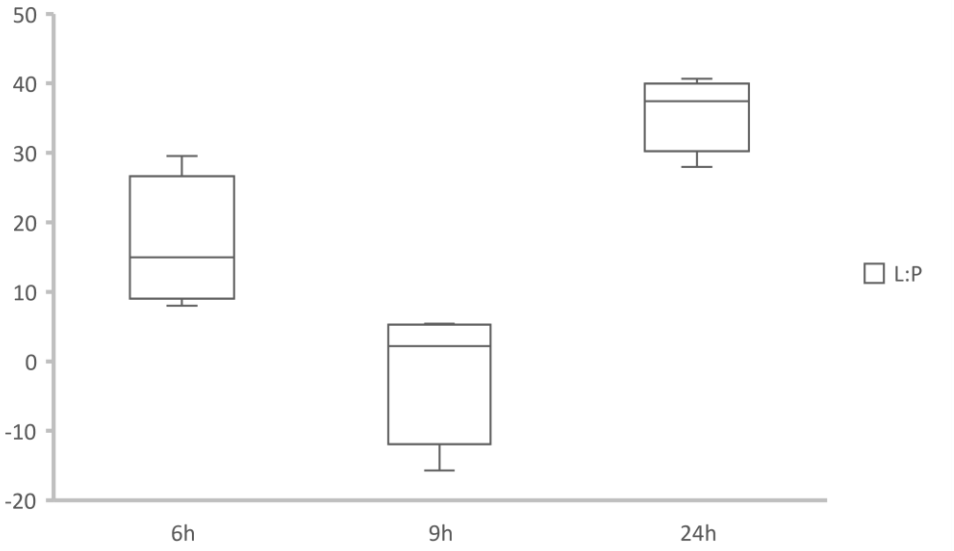

Figure 3. *Boxplot representing the ratio of plasma lactic acid to pyruvic acid at 6, 9 and 24 hours of clinorotation.*

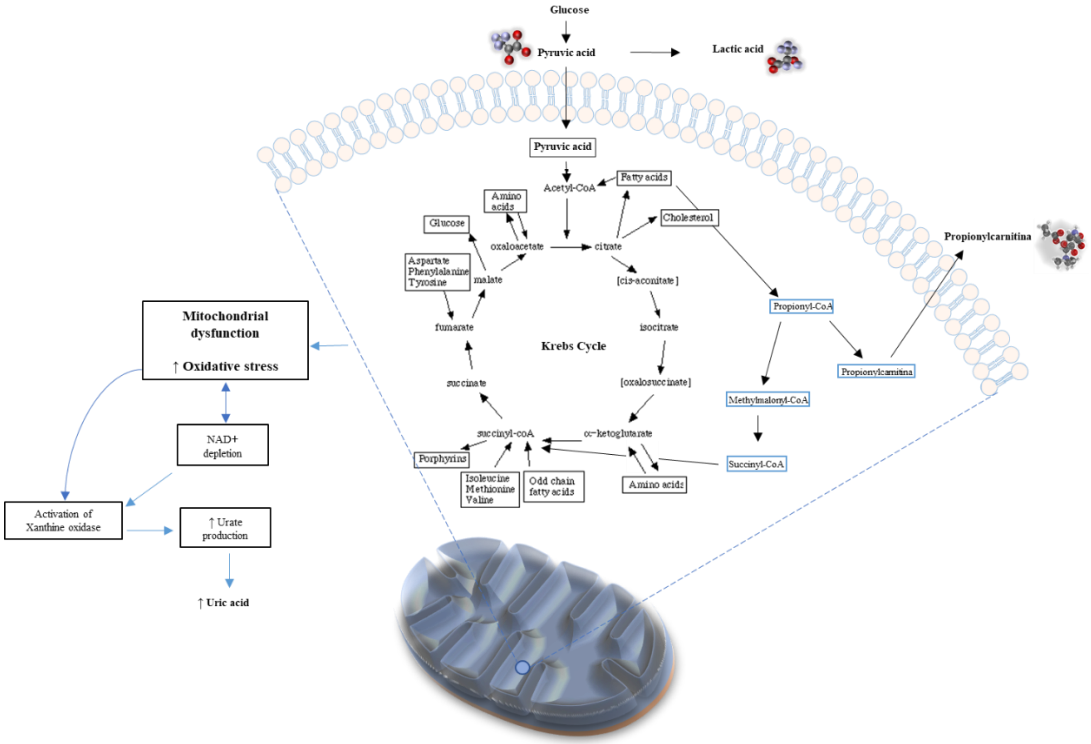

Figure 4. *Crosstalk between Krebs cycle, electron transport chain, β-oxidation of fatty acids, lactic acid, and uric acid production.*

The same evidence was found during the NASA twin study experiments [32]. This metabolic rewiring is often seen in what is called the Warbug effect operated by cancer cells [33]. Most tumor cells downregulate mitochondrial oxidative phosphorylation and increase the rate of glucose consumption and lactate release, independently of oxygen availability [34]. The Warburg effect may simply be a consequence of damage to the mitochondria in cancer [35]. It may also be an adaptation to low-oxygen environments within tumors, or the result of mitochondrial genes shutting down, which are involved in the cell's apoptosis program [36]. In general, microgravity affects mitochondrial dysfunction in all cell types by increasing mitochondrial ROS levels, by causing an imbalance of mitochondrial gene expression, and by damaging DNA [25]. Therefore, it is possible that microgravity, causing genetic alterations at the mitochondrial level, could generate a picture similar to the Warburg effect. Moreover, the production of lactic acid observed following 24 h of clinorotation leads to an acidification of the extracellular environment which can induce cell death via a ROS production [37]. Such an extracellular environment could explain the elevated uric acid levels observed at 24h. In fact, at a physiologic pH, uric acid exists primarily as urate, accounts for a large proportion of the antioxidant capacity of blood, and suppresses oxidative stress [38].

Interestingly, the metabolite with the higher value of statistical significance was propionyl carnitine which was significantly down-regulated at 6 and 9 h, while upregulated at 24 h. This trend may suggest that the increase in activity of the Krebs cycle observed at time points 6 and 9 h was replaced by the β-oxidation of fatty acids at 24 h. With the aim to confirming this hypothesis, we performed a targeted carnitine analysis. The results are summarized in **Figure 5.** Interestingly, propionylcarnitine levels were below the limit of quantitation in plasma samples taken at 6 and 9 h. This fact can be explained considering that propionyl carnitine is produced by carnitine and propionylCoA which can be transformed to methylmalonilCoA and then succinic acid and thus entering the Krebs cycle. Propionyl-L-carnitine, was reported to affect the molecular dynamics of the membrane bilayer region decreasing the molecular packing of phospholipids and modulating erythrocyte membrane stability [39].

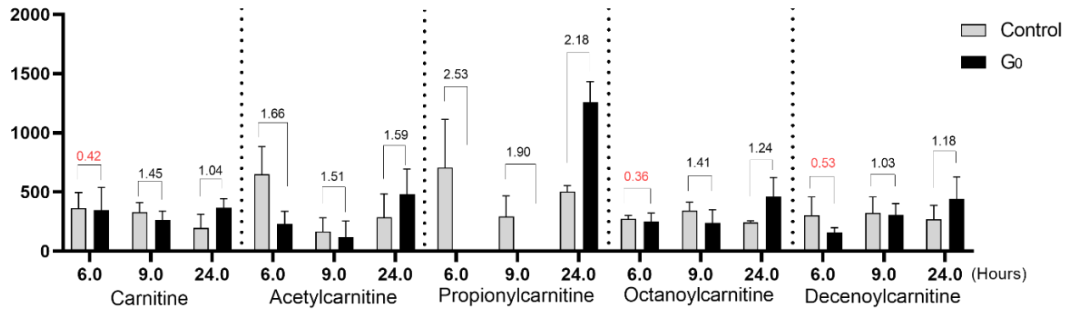

Figure 5. Targeted analysis of carnitines. *This boxplot shown levels of carnitines detected at 6, 9 and 24h reporting the VIP values. In each plot, the black column represents plasma samples under simulated gravity conditions, while white column represents control samples.*

5. Conclusions

In human plasma under microgravity environment, we detected a significant increase of short and medium-chain acylcarnitines that are tightly correlated to a loss of mitochondrial integrity and resulting in incomplete β-oxidation of fatty acids. The strong alterations of both the TCA and the acylcarnitine metabolites observed in microgravity conditions suggest a dysfunctional mitochondrial status in the plasma.

Limitations of our study are related to the low number of metabolites detected by CE-MS compared to the entire plasma metabolome and that microgravity conditions have been reproduced using a laboratory clinostat and not in the international space station. Despite these limitations the plasma metabolomics profile indicates an evident dysregulation of mitochondrial homeostasis with defective respiratory chain, oxidative environment, and incomplete β-oxidation of fatty acids with consequent accumulation of carnitines. Since an ability of propionyl carnitine to affect the plasma membrane of erythrocytes [39] and given the membrane damage observed in our previous study, further in vivo studied are needed. Overall, the mitochondrial production of propionyl carnitine may contribute to the damage seen in the erythrocyte plasma membrane thus worsening the spatial anemia manifested by astronauts.

In summary, the metabolomics investigation of human plasma under simulated microgravity conditions may be useful to understand molecular mechanisms during spaceflight allowing to determine countermeasures effective to overcome low gravity environments effects.

References

[1] G. Fogleman, L. Leveton, and J. B. Charles, “The bioastronautics roadmap: A risk reduction strategy for human exploration,” A Collect. Tech. Pap. - 1st Sp. Explor. Conf. Contin. Voyag. Discov., vol. 1, no. February, pp. 281–291, 2005.

[2] G. R. Clément et al., “Challenges to the central nervous system during human spaceflight missions to Mars,” J. Neurophysiol., vol. 123, no. 5, pp. 2037–2063, 2020.

[3] A. E. Aubert, F. Beckers, and B. Verheyden, “Cardiovascular function and basics of physiology in microgravity,” Acta Cardiol., vol. 60, no. 2, pp. 129–151, 2005.

[4] G. Trudel, J. Shafer, O. Laneuville, and T. Ramsay, “Characterizing the effect of exposure to microgravity on anemia: more space is worse,” American Journal of Hematology, vol. 95, no. 3. pp. 267–273, 2020.

[5] F. Strollo and J. Vernikos, “Aging-like metabolic and adrenal changes in microgravity: State of the art in preparation for Mars,” Neurosci. Biobehav. Rev., vol. 126, no. January, pp. 236–242, 2021.

[6] M. Hughes-Fulford, R. Tjandrawinata, J. Fitzgerald, K. Gasuad, and V. Gilbertson, “Effects of microgravity on osteoblast growth.,” Gravit. Space Biol. Bull., vol. 11, no. 2, pp. 51–60, 1998.

[7] S. H. Jee, J. He, L. J. Appel, P. K. Whelton, I. Suh, and M. J. Klag, “Coffee Consumption and Serum Lipids: A Meta-Analysis of Randomized Controlled Clinical Trials CORE View metadata, citation and similar papers at core.ac.uk,” Am. J. Epidemiol., vol. 153, no. 4, pp. 353–362, 2014.

[8] S. Patel, “The effects of microgravity and space radiation on cardiovascular health: From low-Earth orbit and beyond,” IJC Hear. Vasc., vol. 30, p. 100595, 2020.

[9] C. P. Alfrey, M. M. Udden, C. Leach-Huntoon, T. Driscoll, and M. H. Pickett, “Control of red blood cell mass in spaceflight,” J. Appl. Physiol., vol. 81, no. 1, pp. 98–104, 1996.

[10] R. T. Meehan et al., “Alteration in human mononuclear leucocytes following space flight.,” Immunology, vol. 76, no. 3, pp. 491–497, 1992.

[11] G. R. Taylor, “Advances in experimental medicine,” in ADVANCES IN EXPERIMENTAL MEDICINE AND BIOLOGY, vol. 225, no. 1, 1997, pp. 269–271.

[12] C. Manis et al., “Understanding the Behaviour of Human Cell Types under Simulated Microgravity Conditions: The Case of Erythrocytes,” International Journal of Molecular Sciences, vol. 23, no. 12. 2022.

[13] A. Diedrich, S. Y. Paranjape, and D. Robertson, “Plasma and blood volume in space,” Am. J. Med. Sci., vol. 334, no. 1, pp. 80–86, 2007.

[14] C. S. Leach and P. C. Johnson, “Influence of spaceflight on erythrokinetics in man,” Science (80-.)., vol. 225, no. 4658, pp. 216–218, 1984.

[15] G. Trudel, N. Shahin, T. Ramsay, O. Laneuville, and H. Louati, “Hemolysis contributes to anemia during long-duration space flight,” Nat. Med., vol. 28, no.

1, pp. 59–62, 2022.

[16] W. A. da Silveira et al., “Comprehensive Multi-omics Analysis Reveals Mitochondrial Stress as a Central Biological Hub for Spaceflight Impact,” Cell, vol. 183, no. 5, pp. 1185-1201.e20, 2020.

[17] J. Kuligowski, Á. Sánchez-Illana, D. Sanjuán-Herráez, M. Vento, and G. Quintás, “Intra-batch effect correction in liquid chromatography-mass spectrometry using quality control samples and support vector regression (QC-SVRC),” Analyst, vol. 140, no. 22, pp. 7810–7817, 2015.

[18] A. Gil-De-La-Fuente et al., “CEU Mass Mediator 3.0: A Metabolite Annotation Tool,” J. Proteome Res., vol. 18, no. 2, pp. 797–802, 2019.

[19] X. W. Mao et al., “Spaceflight environment induces mitochondrial oxidative damage in ocular tissue,” Radiat. Res., vol. 180, no. 4, pp. 340–350, 2013.

[20] M. L. Lewis, J. L. Reynolds, L. A. Cubano, J. P. Hatton, B. D. Lawless, and E. H. Piepmeier, “Spaceflight alters microtubules and increases apoptosis in human lymphocytes (Jurkat),” FASEB J., vol. 12, no. 11, pp. 1007–1018, 1998.

[21] Y. Wang et al., “Effect of Prolonged Simulated Microgravity on Metabolic Proteins in Rat Hippocampus: Steps toward Safe Space Travel,” J. Proteome Res., vol. 15, no. 1, pp. 29–37, 2016.

[22] F. Ebnerasuly, Z. Hajebrahimi, S. M. Tabaie, and M. Darbouy, “Simulated microgravity condition alters the gene expression of some ECM and adhesion molecules in adipose derived stem cells,” Int. J. Mol. Cell. Med., vol. 7, no. 3, pp. 146–157, 2018.

[23] T. G. Hammond et al., “Gene expression in space,” Nat. Med., vol. 5, no. 4, pp. 1999–1999, 1999.

[24] A. Michaletti, M. Gioia, U. Tarantino, and L. Zolla, “Effects of microgravity on osteoblast mitochondria: A proteomic and metabolomics profile,” Sci. Rep., vol. 7, no. 1, pp. 1–12, 2017.

[25] H. P. Nguyen, P. H. Tran, K. S. Kim, and S. G. Yang, “The effects of real and simulated microgravity on cellular mitochondrial function,” npj Microgravity, vol. 7, no. 1, 2021.

[26] C. Chaimoff, P. Fishman, J. Hart, and M. J. Djaldetti, “Transformation of erythrocytes to spherocytes following incubation with malignant cells.,” Submicrosc Cytol., vol. 17, no. 3, pp. 465–8, 1985.

[27] X. Song et al., “Existence of circulating mitochondria in human and animal peripheral blood,” Int. J. Mol. Sci., vol. 21, no. 6, 2020.

[28] K. Göran Ronquist, “Extracellular vesicles and energy metabolism,” Clin. Chim. Acta, vol. 488, no. November 2018, pp. 116–121, 2019.

[29] S. Dinarelli et al., “Erythrocyte’s aging in microgravity highlights how environmental stimuli shape metabolism and morphology,” Scientific Reports, vol. 8, no. 1. 2018.

[30] C. Granchi, S. Bertini, M. Macchia, and F. Minutolo, “Inhibitors of Lactate Dehydrogenase Isoforms and their Therapeutic Potentials,” Curr. Med. Chem.,

vol. 17, no. 7, pp. 672–697, 2010.

[31] M. Suistomaa, E. Ruokonen, A. Kari, and J. Takala, “Time-pattern of lactate and lactate to pyruvate ratio in the the first 24 hours of intensive care emergency admissions,” Shock, vol. 14, no. 1, pp. 8–12, 2000.

[32] F. E. Garrett-Bakelman et al., “The NASA twins study: A multidimensional analysis of a year-long human spaceflight,” Science (80-.)., vol. 364, no. 6436, 2019.

[33] M. V Liberti and J. W. Locasale, “The Warburg Effect : How Does it Bene fi t Cancer Cells ?,” Trends Biochem. Sci., vol. 41, no. 3, pp. 211–218, 2016.

[34] M. Gallo, L. Sapio, A. Spina, D. Naviglio, A. Calogero, and S. Naviglio, “Lactic dehydrogenase and cancer: An overview,” Front. Biosci. - Landmark, vol. 20, no. 8, pp. 1234–1249, 2015.

[35] O. Warburg, “On the origin of cancer cells,” Science (80-.)., vol. 123, no. 3191, pp. 309–314, 1956.

[36] V. M. G. Heiden, L. C. Cantley, and C. B. Thompson, “Understanding the Warburg Effect: The Metabolic Requirements of Cell Proliferation,” Science (80-.)., vol. 324, no. 5930, pp. 3828–3828, 2009.

[37] J. Teixeira et al., “Extracellular acidification induces ROS- and mPTP-mediated death in HEK293 cells,” Redox Biol., vol. 15, no. November 2017, pp. 394–404, 2018.

[38] M. Packer, “Uric Acid Is a Biomarker of Oxidative Stress in the Failing Heart: Lessons Learned from Trials With Allopurinol and SGLT2 Inhibitors,” J. Card. Fail., vol. 26, no. 11, pp. 977–984, 2020.

[39] A. Arduini et al., “Effects of l-carnitine and its acetate and propionate esters on the molecular dynamics of human erythrocyte membrane,” BBA - Biomembr., vol. 1146, no. 2, pp. 229–235, 1993.

CONCLUSIONS

The aim of this PhD work was to investigate haematological alterations caused by microgravity conditions using metabolomics and multivariate analysis. The spatial anemia in astronauts has been noted since the earliest space missions, but the contributing pathophysiological mechanisms during space flight remained unclear and scarcely studied. Due to their high sensitivity and to their strong reproducibility in metabolomics analysis, for this study project we chose to use analytical platforms such as liquid chromatography coupled with mass-spectrometry and ion mobility, and capillary electrophoresis coupled with mass-spectrometry. Datasets were processed using multivariate statistic packages to fully understand the most significant metabolites implicated in haematological alterations. While three-dimensional SEM was used for the imaging analysis and a fine resolution of erythrocyte structures.

Human erythrocytes and human plasma samples were investigated under microgravity conditions. SEM and confocal microscopy, ROS, TAC, GSH, and MDA analysis, and lipid profile evaluation demonstrated that samples exposed to simulated microgravity conditions exhibited remarkable changes in red cell cytoskeletal architecture and membrane rigidity. Such alterations are known to enhance the programmed cells death process as previously reported.

To investigate the molecular mechanisms that induce a reduction in the number of erythrocytes during spaceflight, we performed a in dept study of the lipid profile of human erythrocytes under microgravity conditions. Thanks to the advancement of hyphenated techniques and mass analyzers we were able to identify biologically active complex lipids susceptible to microgravity, allowing new possible hypotheses that explain the anemia experienced by astronauts.

In more detail, lipidomic analysis of erythrocytes revealed a double mechanism that generates the reduction in the number of red blood cells. On the one hand, there is an increase in the levels of 20:4 PC determining a reduction of cellular proliferation. On the other hand, the increase in the levels of EtherOxPC 16:0_20:4 stimulates the immune response by attracting the C-reactive protein and macrophages and induces an increase of ROS production. This ROS accumulation, caused by microgravity,

inevitably induces mitochondrial damage and dysfunction as indicated by the accumulation of HexCer lipid species in clinorotated erythrocytes. This accumulation acts as a pro-apoptotic signal condemning the erythrocytes to death.

Alterations in mitochondrial activity have also been observed in circulating mitochondria present in human plasma. Indeed, through CE-MS analysis, we detected a significant increase of short and medium-chain acylcarnitines that are tightly correlated to a loss of mitochondrial integrity and resulting in incomplete β-oxidation of fatty acids. The plasma metabolomics profile indicates an evident dysregulation of mitochondrial homeostasis with defective respiratory chain, oxidative environment, and incomplete β-oxidation of fatty acids with consequent accumulation of carnitines. Moreover, since an ability of propionyl carnitine to affect the plasma membrane of erythrocytes and given the membrane damage observed through SEM analysis, further in vivo studies are needed to understand if the mitochondrial production of propionyl carnitine may contribute to the damage.

Certainly, the implications of this research work and the corresponding future developments are related to the basic investigation of the intrinsic mechanisms underlying the behaviour of different types of human cells in conditions of microgravity that will be able to provide a useful contribution both to the understanding and the potential prevention of the classic health risks associated with astronauts involved in deep space exploration scenarios.